

AD A116192

1.3
AD-F300 046

AD

CONTRACT REPORT ARBRL-CR-00481

GAS CHEMISTRY
EFFECTS ON GUN BARREL EROSION
A SHOCK TUBE GUN INVESTIGATION

C. C. Morphy
E. B. Fisher

June 1982



US ARMY ARMAMENT RESEARCH AND DEVELOPMENT COMMAND
BALLISTIC RESEARCH LABORATORY
ABERDEEN PROVING GROUND, MARYLAND

Approved for public release; distribution unlimited.

82 06 10 080

Destroy this report when it is no longer needed.
Do not return it to the originator.

Secondary distribution of this report by originating
or sponsoring activity is prohibited.

Additional copies of this report may be obtained
from the National Technical Information Service,
U.S. Department of Commerce, Springfield, Virginia
22161.

The findings in this report are not to be construed as
an official Department of the Army position, unless
so designated by other authorized documents.

*The use of trade names or manufacturers' names in this report
does not constitute endorsement of any commercial product.*

SECURITY CLASSIFICATION OF THIS PAGE (When Data Entered)

DD FORM 1473 EDITION OF 1 NOV 65 IS OBSOLETE

SECURITY CLASSIFICATION OF THIS PAGE (When Data F. Available)

UNCLASSIFIED

SECURITY CLASSIFICATION OF THIS PAGE(When Data Entered)

20. (Cont.)

compress mixtures of pure gases to simulate propellant gas flow conditions and cycle times experienced in large caliber guns.

Tests were conducted with mixture ratios of carbon monoxide and carbon dioxide that characterize the normal range of CO/CO₂ ratios found in propellant gas, i.e., 2.0 to 8.1. Progressive substitution of carbon monoxide for nitrogen in the mix quantified erosion as a function of increasing CO concentration or CO/CO₂ ratio. Subsequent tests were conducted with gas mixtures containing double the amount of carbon monoxide and carbon dioxide but with the same effective CO/CO₂ ratio, to measure erosion as a function of absolute reactant concentration for the two gas species.

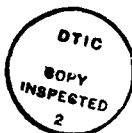
The basic chemical effect was observed to be a shift in the erosion threshold to less severe convective heating conditions in response to increasing the CO/CO₂ ratio above a value of 5.6. The magnitude of the shift appeared to be directly proportional to the absolute concentrations of the two reactant gases. Variation of both CO/CO₂ ratio and absolute amounts of the two gases resulted in distinct changes in specimen surface characteristics, both at near threshold and above threshold flow conditions.

UNCLASSIFIED

SECURITY CLASSIFICATION OF THIS PAGE(When Data Entered)

TABLE OF CONTENTS

| | Page |
|---|------|
| I. INTRODUCTION | 9 |
| Objective | 9 |
| Historical Perspective | 9 |
| Method of Research | 11 |
| II. EXPERIMENTAL PROCEDURES. | 15 |
| Test Criteria | 15 |
| Identification of propellant gas CO/CO ₂ mole ratios | 15 |
| Modeling propellant gas with pure CO and CO ₂ | 15 |
| Test Matrix Formulation | 16 |
| III. EXPERIMENTAL MATERIEL | 18 |
| Shock Tube Gun Facility | 18 |
| Construction | 18 |
| Operation | 20 |
| Test Specimen Design | 25 |
| Heat Transfer Instrumentation | 25 |
| IV. EXPERIMENTAL RESULTS | 28 |
| Gas Chemistry Test Data | 28 |
| Correlation of Erosion Data with Flow Conditions | 31 |
| Correlation of Erosion Data with CO/CO ₂ Ratio | 34 |
| Correlation of Erosion Data with CO ₂ Concentration | 34 |
| Correlation of Erosion Data with Heat Flux | 37 |
| Characterization of Test Specimen Surfaces | 42 |
| V. CONCLUSIONS | 59 |
| VI. REFERENCES | 61 |
| APPENDIX A - SHOCK TUBE GUN COMPUTER SIMULATION | 65 |
| APPENDIX B - ISENTROPIC EQUILIBRIUM COMBUSTION CODE | 93 |
| DISTRIBUTION LIST. | 99 |



A

LIST OF FIGURES

| Figure | | Page |
|--------|---|------|
| 1 | Equilibrium propellant gas CO/CO ₂ ratio versus pressure | 14 |
| 2 | Isentropes of test gas mixtures undergoing adiabatic compression | 15 |
| 3 | Projectile launch and capture components of the Shock Tube Gun | 19 |
| 4 | Piston, chamber and toggle restraint components of the Shock Tube Gun | 21 |
| 5 | Temperature response and total heat input curves for an STG thermocouple | 24 |
| 6 | Test specimen used in the Shock Tube Gun | 25 |
| 7 | In-wall thermocouple installed in the Shock Tube Gun test section | 26 |
| 8 | Peak test gas mixture pressure versus specimen mass loss | 32 |
| 9 | Peak test gas mixture temperature versus specimen mass loss | 33 |
| 10 | Isotherms of test gas mixtures containing 2.5% CO ₂ | 35 |
| 11 | Isothermal comparison of 2.5% CO ₂ and 5% CO ₂ mixtures | 36 |
| 12 | Convective hot-wall heat flux versus specimen mass loss | 40 |
| 13 | Surface characteristics of specimen no. 79 (test no. 116) after near negligible mass loss in a 5% CO/2.5% CO ₂ atmosphere at 256 MPa, 3380°K | 45 |
| 14 | Surface characteristics of specimen no. 77 (test no. 114) after 39.5 milligrams mass loss in a 5% CO/2.5% CO ₂ atmosphere at 322 MPa, 3590°K | 46 |
| 15 | Surface characteristics of specimen no. 85 (test no. 122) after near negligible mass loss in a 10% CO/5% CO ₂ atmosphere at 313 MPa, 3430°K | 47 |
| 16 | Surface characteristics of specimen no. 81 (test no. 118) after 82.0 milligrams mass loss in a 10% CO/5% CO ₂ atmosphere at 325 MPa, 3460°K | 48 |

LIST OF FIGURES (Cont'd)

| Figure | | Page |
|--------|--|------|
| 17 | Surface characteristics of specimen no. 74 (test no. 111) after near negligible mass loss in a 9% CO/2.5% CO ₂ atmosphere at 236 MPa, 3310°K | 49 |
| 18 | Surface characteristics of specimen no. 86 (test no. 123) after 67.9 milligrams mass loss in a 9% CO/2.5% CO ₂ atmosphere at 327 MPa, 3620°K | 50 |
| 19 | Surface characteristics of specimen no. 71 (test no. 108) after near negligible mass loss in a 14% CO/2.5% CO ₂ atmosphere at 203 MPa, 3170°K | 51 |
| 20 | Surface characteristics of specimen no. 87 (test no. 124) after 59.4 milligrams mass loss in a 14% CO/2.5% CO ₂ atmosphere at 321 MPa, 3600°K | 52 |
| 21 | Surface characteristics of specimen no. 67 (test no. 104) after near negligible mass loss in a 20.5% CO/2.5% CO ₂ atmosphere at 245 MPa, 3340°K | 53 |
| 22 | Surface characteristics of specimen no. 88 (test no. 125) after 87.2 milligrams mass loss in a 20.5% CO/2.5% CO ₂ atmosphere at 318 MPa, 3620°K | 54 |
| 23 | Surface characteristics of specimen no. 62 (test no. 99) after near negligible mass loss in a 40.5% CO/5 CO ₂ atmosphere at 261 MPa, 3250°K | 55 |
| 24 | Surface characteristics of specimen no. 63 (test no. 100) after 38.9 milligrams mass loss in a 40.5% CO/5% CO ₂ atmosphere at 293 MPa, 3360°K | 56 |
| 25 | Surface characteristics of specimen no. 66 (test no. 103) after near negligible mass loss in a 43% CO/2.5% CO ₂ atmosphere at 261 MPa, 3380°K | 57 |
| 26 | Surface characteristics of specimen no. 65 (test no. 102) after 37.7 milligrams mass loss in a 43% CO/2.5% CO ₂ atmosphere at 268 MPa, 3410°K | 58 |

LIST OF TABLES

| Table | | Page |
|-------|--|------|
| 1 | Shock Tube Gun Characteristics | 20 |
| 2 | Gas Chemistry Test Data | 29 |
| 3 | Characteristics of STG Test Specimen Flow Surfaces | 44 |

I. INTRODUCTION

Objective

The objective of this study is to investigate the contribution of a particular propellant gas chemistry to the overall wear in a gun tube.

As a continuation of two previous studies^{1,2} conducted at Calspan to research the pure carburizing and oxidizing regimes of ballistic chemistry, the present work attempts to characterize the erosion potential of gas mixtures that represent the narrow band of CO/CO₂ mole ratios, occupied by present day large caliber gun propellants. This band of CO/CO₂ ratio ranges from a value of 3, approximately the neutral point of chemical activity for the CO/CO₂ system, to about 19, the highest value calculated for an experimental gun propellant, a low temperature RDX (trimethylene trinitramine) compound, that was investigated during World War II.³

Historical Perspective

Historically, the connection of nitramine propellants and high CO/CO₂ ratios to enhanced gun tube wear probably dates from the World War II period. One NDRC study⁴ found that an RDX formulation was more erosive than a single base propellant (M1) with a comparably low flame temperature. The experiments were conducted with both an erosion combustor fitted with vent plugs and a caliber .50 barrel fixture.

Other research^{5,6} both during and after the war, found that pure gas mixtures of CO and CO₂ exhibited erosivity at below melting conditions

1. C.C. Morphy and E.B. Fisher, "The Role of Carburization in Gun Barrel Erosion and Cracking," ARRADCOM Contractor Report ARBRL-CR-00459, Calspan Corporation, Buffalo, New York, July 1981. (AD A102625)
2. E.B. Fisher and C.C. Morphy, "The Role of Oxygen in Gun Barrel Erosion and Cracking--A Shock Tube Gun Investigation," ARRADCOM Contractor Report ARBRL-CR-00427, Calspan Corporation, Buffalo, New York, April 1980. (AD A085720)
3. F.C. Kracek, "Properties of Powder Gas," Hypervelocity Guns and The Control of Gun Erosion, Summary Technical Report of Division 1, NDRC, Vol. 1, Washington, D.C., 1946, pp. 21-53.
4. J.N. Hobstetter, "Erosion of Gun Steel by Different Propellants," Hypervelocity Guns and The Control of Gun Erosion, Summary Technical Report of Division 1, NDRC, Vol. 1, Washington, D.C., 1946, pp. 308-328.
5. R.C. Evans, F.H. Horn, Z.M. Shapiro, and R.L. Wagner, "The Chemical Erosion of Steel by Hot Gases under Pressure," J. Physical and Colloidal Chemistry, Vol. 51, 1947, pp. 1404-1429.
6. J.C.W. Frazer, F.H. Horn, and R.C. Evans, "Vent Plug Erosion by the CO-CO₂ Gas System," NDRC Contractor Report A-310, Johns Hopkins University, Baltimore, Md., October 1944.

in an erosion combustor. Other conclusions from these studies; namely, that erosion was independent of CO_2 concentration as long as the CO/CO_2 ratio was greater than unity at equilibrium, and that various recognized carburizing catalysts such as hydrogen sulphide, ammonia and free hydrogen, when added to the test mixtures, greatly increased vent plug erosion, led to the further conclusion that carburization was playing an important role in thermochemical erosion of gun barrels. Several explanations of this phenomenon were put forth. Cracking of excess CO would enrich a gun tube's surface with carbon, producing a drop in solidus temperature of the steel, from 1720°K to perhaps 1400°K . The gun bore would, therefore, melt and be lost at a correspondingly lower gas temperature. Also, Frazer hypothesized the formation and highly exothermic decomposition of iron penta carbonyl early in the ballistic cycle, when tube surface temperatures were rising. The dissolution of $\text{Fe}(\text{CO})_5$ would augment the already increasing surface heat flux, resulting in critical tube temperatures being prematurely reached and held over a greater portion of the cycle time.

In recent years, the connection of nitramines and CO/CO_2 ratios to gun erosion has also been alluded to but in a slightly different context. Propellant formulations containing the aforementioned RDX and now, also, HMX (cyclotetramethylene tetranitramine) are more often compared to the double base (nitrocellulose-nitroglycerine) and triple base (NC-NG-nitroguanidine) propellants that they have to compete with for acceptance in modern, large caliber gun systems. The earlier comparison of low flame temperature propellants with varying impetus levels has given way to present day comparisons of high impetus propellants with different flame temperatures. Of course, the isochoric flame temperature is still a primary consideration when selecting a gun propellant since this property is directly linked to tube wear. Propellants, such as the nitramines, that possess both high impetus and low flame temperature would appear to have a clear advantage in properties. Unfortunately, the recent research in nitramines doesn't reflect that clear advantage.

Several laboratory experiments, utilizing a blow out gun^{7,8,9} have indicated that nitramines are no more erosive than double base propellants that were comparable in either flame temperature or impetus. Ballistic

7. R.W. Geene, J.R. Ward, T.L. Brosseau, A. Niiler, R. Kirkmire, and J.J. Rocchio, "Erosivity of a Nitramine Propellant," Technical Report ARBRL-TR-02094, ARRADCOM, Aberdeen Proving Ground, MD, August 1978. (AD A060590)
8. J.R. Ward and R.W. Geene, "Erosivity of a Nitramine Propellant with a Flame Temperature Comparable to M30 Propellant," Technical Report ARBRL-MR-02926, ARRADCOM, Aberdeen Proving Ground, MD, June 1979. (AD A074346)
9. R. Geene, B. Grollman, A. Niiler, A. Rye, and J.R. Ward, "Nitramine Propellant Erosivity-III," Technical Report ARBRL-TR-02278, ARRADCOM, Aberdeen Proving Ground, MD, December 1980. (AD A096878)

testing^{10,11} and tests performed with different vented erosion testers¹² have indicated, however, that nitramine appears more erosive than several conventional propellants. If nitramines have a distinct thermal advantage over hotter propellants, the conflicting results of contemporary studies would indicate that under certain conditions, nitramines are at an equally distinct, chemical or thermochemical disadvantage. Recognition of this chemical handicap and analyzing its possible origin are the purposes of this work.

Keeping in mind that the chemical difference between nitramine and conventional propellant gas is more than one of just CO/CO₂ mole ratios, the fact remains that it is a major difference. Double base propellants have low CO/CO₂ ratios and nitramines, like single base propellants have high CO/CO₂ ratios. This research attempts to isolate that parameter from the other thermochemical phenomena that contribute to the complex mechanism of gun barrel erosion, and perhaps, characterize the impact of CO/CO₂ ratio on the otherwise desirable attributes of present and future gun propellants.

Method of Research

Research is being performed by utilizing Calspan's Shock Tube Gun (STG) facility, which duplicates the thermodynamics of gun chamber combustion with a tube chamber incorporating a moving wall, i.e., the leading face of a gas driven piston. The gases compressed in the tube chamber by piston motion vent in a conventional manner by forcing a projectile down the adjoining gun barrel. During the venting cycle, the gases must pass through the nozzled flow channel of a gun-steel sample positioned in front of the barrel entrance. As a result, the channel wall of the sample experiences histories of pressure, temperature, and forced convective heating, similar to those of a gun barrel. Unlike the combustion system where propellant formulation dictates a set flame temperature and impetus, the STG permits independent variation of any or all conditions affecting ballistic histories; and unlike smaller ballistic compressors being utilized in similar research work, the STG can duplicate the pressure cycle time of most large caliber gun systems.

-
10. F.A. Vassallo, "A Report on The Erosivity of a Nitramine Propellant When Fired in a 105mm M68 Tube," ARRADCOM Contractor Report DAAK10-80-M-3150, Calspan Corporation, Buffalo, New York, February 1981.
 11. A.J. Bracuti, L. Bottei, J.A. Lannon, and L.H. Caveny, "Evaluation of Propellant Erosivity with Vented Erosion Apparatus," 1980 JANNAF Propulsion Meeting, Vol. I, CPIA, Johns Hopkins University, Laurel, MD, March 1980.
 12. F.A. Vassallo, "Thermal and Erosion Phenomenology in Medium Caliber Anti-Armor Automatic Cannons (MC-AAAC)," 1980 JANNAF Propulsion Meeting, Vol. I, Chemical Propulsion Information Agency, Johns Hopkins University, Laurel, MD, March 1980.

Several computer programs provide analytic support for the STG tests. One code models the STG gas compression cycle using a van der Waals equation of state. It computes gas pressure and temperature, convective heating, total heat input and in-wall temperatures of the test sample surface. This program is used mainly in a predictive mode to select gas composition and peak pressure for an actual test. A detailed description of the code can be found in Appendix A. Another code, described in Appendix B, accepts gas mixture and pressure data from tests conducted and computes equilibrium temperature and species concentration values along isentropes. This information can then be returned to the preceding program to improve its prediction of barrel heating and wear. STG testing and computer analysis, as performed in this program, are intended to expand present knowledge of wear and erosion phenomenology.

II. EXPERIMENTAL PROCEDURES

Test Criteria

As stated in the introduction, the primary objective of this study is to quantify the erosion potential of propellant gases in terms of equilibrium CO/CO₂ mole ratio at their respective flame temperatures. To accomplish this objective, two primary criteria of the test procedure must be met.

Identification of Propellant Gas CO/CO₂ Mole Ratios

The equilibrium CO/CO₂ mole ratios of a representative group of propellants, both conventional and experimental, are delineated over the realistic range of ballistic conditions. The mole ratios can be obtained by Blake Code calculation of individual species concentration as a function of pressure, temperature, and the equilibrium constants of all gas species that make up a given propellant gas. In this study, the combustion gas concentrations of six propellants are used to cover the realistic range of equilibrium CO/CO₂ mole ratios that exist at ballistic pressures. The propellants are illustrated in Figure 1. M8 and M5 are conventional double base propellants. M30 is triple-based. HFP and NT are nitramine based and M1 is a single base propellant.

Modeling Propellant Gas with Pure CO and CO₂

Within the range of CO/CO₂ ratios represented in Figure 1 by the six propellants, identical ratios of the two pure gases are used in STG tests to model each propellant. The absolute concentration of carbon monoxide and carbon dioxide combined would be about 50 mole percent of actual propellant gas. The present format of the STG allows a maximum CO-CO₂ concentration of about 45 mole percent of the mix, providing the absolute CO₂ concentration does not exceed about 5 mole percent. This limitation results from disparity in mass between the CO and CO₂ molecules. Increasing the CO₂ concentration lengthens cycle time, which is acceptable if cycle time is a test parameter, but can be unfavorable when attempting to compare tests of different propellant gas models. More importantly, increasing CO₂ concentration decreases the mix ratio of specific heats which results in pressure/temperature conditions that are not representative of the propellant gas being modeled. That is, in order to generate a realistic "flame temperature" in the STG, the peak test pressure would have to be unrealistically high. Figure 2 illustrates the pure gas isentropes generated by the Isentropic Equilibrium Combustion Code (described in Appendix B) during adiabatic compression in the STG. The 10 percent CO₂ isentropes is shown as a dashed line since it cannot be used in the present STG configuration for the reasons stated above. Also shown in Figure 2 are the six propellants whose gases are being modeled. Their nominal peak pressure/temperature conditions are indicated.

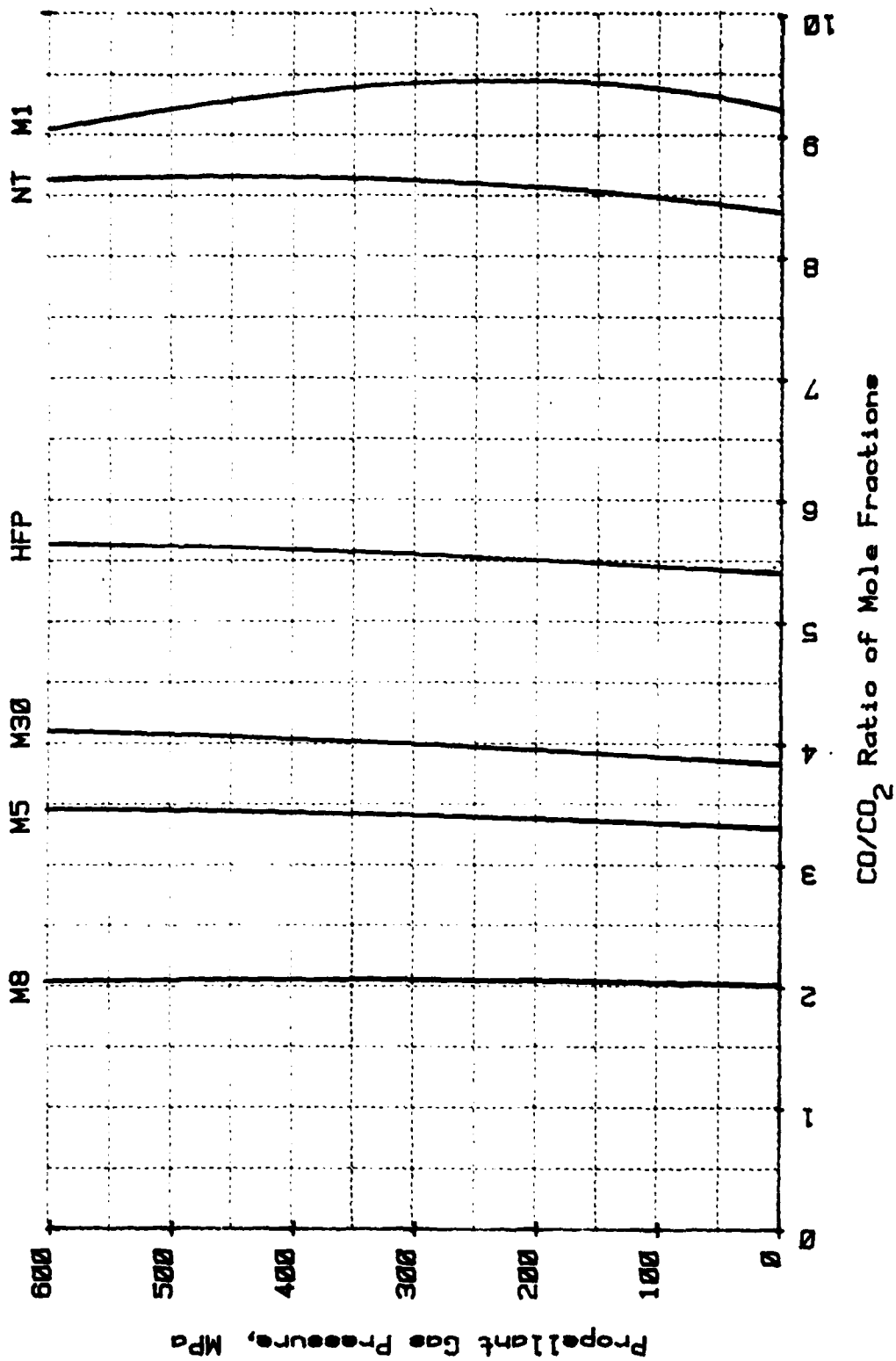


Figure 1. Equilibrium propellant gas CO/CO_2 ratio versus pressure

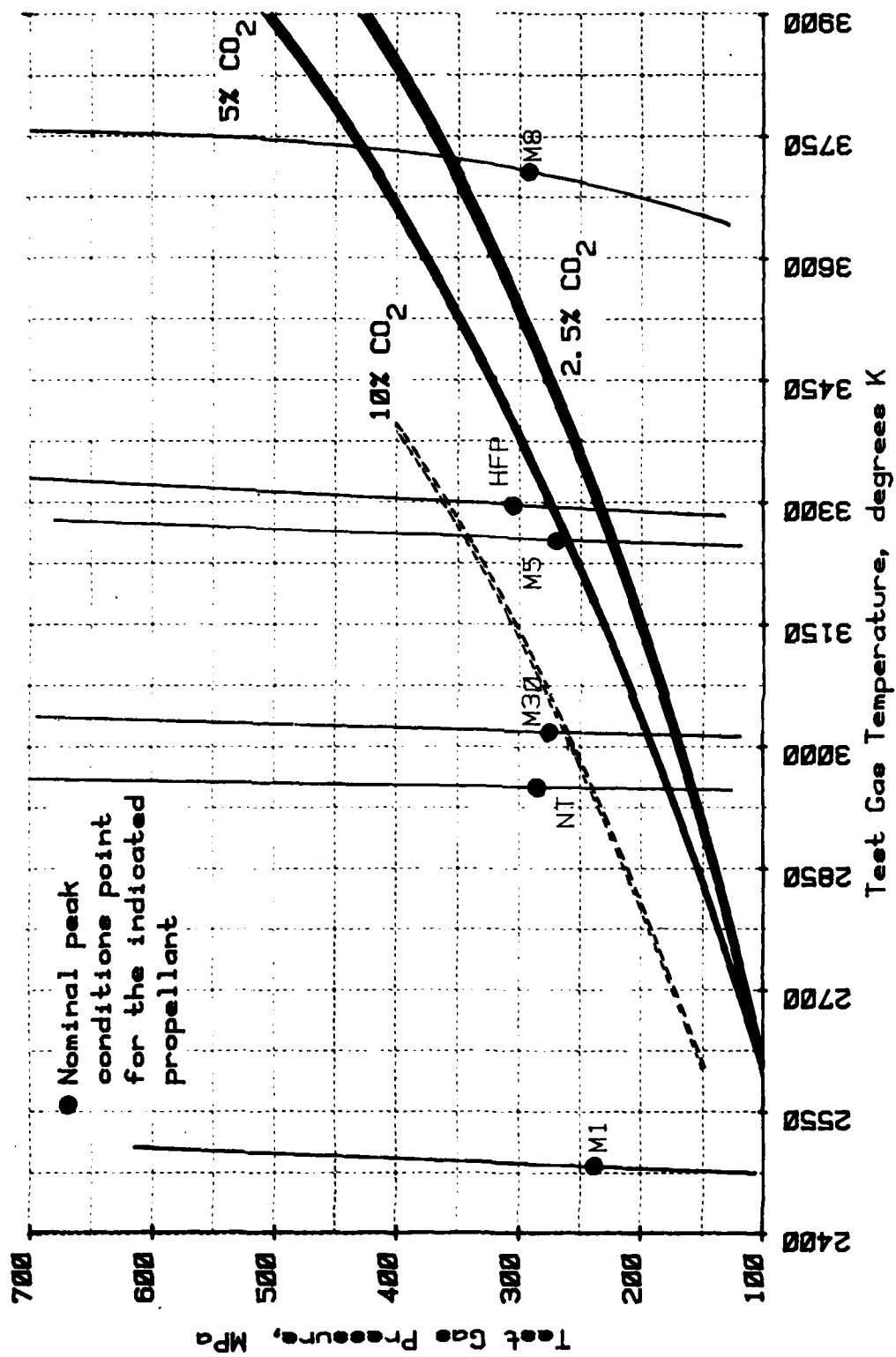


Figure 2. Isentropes of test gas mixtures undergoing adiabatic compression

Test Matrix Formulation

Successful STG modeling of known propellant gases should identify the ratio of carbon monoxide (carburizes steel when cracked and absorbed) to carbon dioxide (decarburizes steel when absorbed and dissociated) that will yield the minimum amount of erosion and the maximum wear life for a gun barrel at characteristic gas, and therefore, tube temperatures. Based on the above test criteria, the test matrix is formulated in the following ways:

1. Each test mixture used models the CO/CO₂ ratio of one or more known propellants at their respective flame temperatures, e.g., HFP (PPL-A-6380), a nitramine propellant (48.6 mole percent RDX) is represented by a 14% CO-2.5% CO₂ mixture in STG tests, producing a characteristic CO/CO₂ ratio of 5.6 at 300 MPa, 3300°K.
2. Each test series, utilizing the same CO/CO₂ ratio includes runs that represent the temperature conditions of all the propellants that the particular CO/CO₂ ratio models, e.g., a gas mixture of 9% CO-2.5% CO₂ with a CO/CO₂ ratio of 3.6 is tested at 3000°K (275 MPa) to model M30 (PPL-A-6372) and tested again at 3300°K (275 MPa) to model M5.
3. Each test series includes additional tests as required to delineate the threshold of erosion as a function of gas temperature for a particular gas mixture.
4. In comparing the results of tests incorporating different gas mixtures, it is beneficial to remove pressure and temperature as contributing variables. One method of accomplishing equalization of flow conditions is to maintain test gas mass at a constant level, without severely altering the ratio of specific heats.

The method of maintaining flow conditions that found application in the present program is the substitution of nitrogen for carbon monoxide, to effectively alter the CO/CO₂ ratio. Because N₂ and CO have near identical molecular weights, the total mass of the gas mixture remains constant. The limiting assumption is one of inert or near-inert nitrogen activity under test conditions.

5. There are two reasons for using two absolute CO₂ concentrations in the test matrix. First, the 5 percent CO₂ mixtures best model the majority of propellant gases shown. However, the 2.5 percent CO₂ mixture is needed for the highest CO/CO₂ mix ratio of 17.2 because of the 45.5 mole percent limitation on total CO and CO₂ in a test mixture. Second, in actual propellant gas, the CO₂ concentration has been shown to exceed a limiting value where an increase in CO₂ does not produce a like increase in erosion. However, a CO₂ concentration of 5 mole percent, or less, may fall below the limiting value for certain test conditions, where the CO₂ level directly affects the erosion potential of a gas mixture. If identical CO/CO₂ ratio mixtures with different absolute CO₂ concentrations, i.e., 2.5 percent

and 5 percent, are tested at similar flow conditions, the variation in erosion potential can be quantified in terms of a known change in CO₂ levels.

6. Surface conditions of the sample remain essentially frozen after a test, since the thermochemical mechanisms of interest proceed at a meaningful rate, only at elevated temperatures. Through the use of pure gases in STG testing, the room temperature activity of propellant gas residues on the steel surface is eliminated.

III. EXPERIMENTAL MATERIEL

Shock Tube Gun Facility

The Shock Tube Gun, as designed and developed by Calspan applies shock tube principles to the study of interior ballistics. The facility consists of a driver gas chamber, a driven tube containing a latchable flying piston, an instrumented gas collection chamber and an instrumented gun tube containing a projectile.

One unique design feature of the STG is the driven piston which, by its presence, affords physical isolation of the driver gas, normally nitrogen, and the chamber or test gas, which varies in composition with test objectives. The driven piston, by virtue of its mass in conjunction with the projectile's mass, also controls the compression history of the test gas, enabling the facility to duplicate the interior ballistic environment of various large caliber guns, up to and including an 8" howitzer.

Another key design feature of the STG is the test section contained within the gas collection chamber. It accepts specimens of various physical configurations equipped with in-wall thermocouples and/or surface heat flux meters, and holds them in place adjacent to the attached barrel. In effect, this design offers a replaceable, highly instrumented bore entrance to an otherwise conventional gun tube.

With suitable variation in test parameters, made possible by the design of the STG, including driver pressure, piston mass, test gas composition, specimen configuration, shot start capability and projectile mass, one may investigate any or all of the internal factors affecting ballistic phenomena, such as the gun barrel erosion and cracking, which the present study addresses.

Construction

Table 1 lists the present structural dimensions of the STG as used in this study, and dictated by adiabatic compression modeling and material availability.

As shown in Figure 3, the projectile launch components consist of the 191 mm driven tube, the instrumented, high pressure, test gas collection chamber or plenum and a 30 mm smooth-bore barrel. These are supported on a shock table which is free to move on tracks in the direction of piston motion, during the severe impulse loading caused by unbalanced chamber pressure due to test gas compression by the decelerating piston. This floating mount system minimizes shearing forces to the supporting base structure, but requires an adjustable pneumatic brake on the driven tube to absorb the axial loading on the launch components, primarily the driven tube itself.

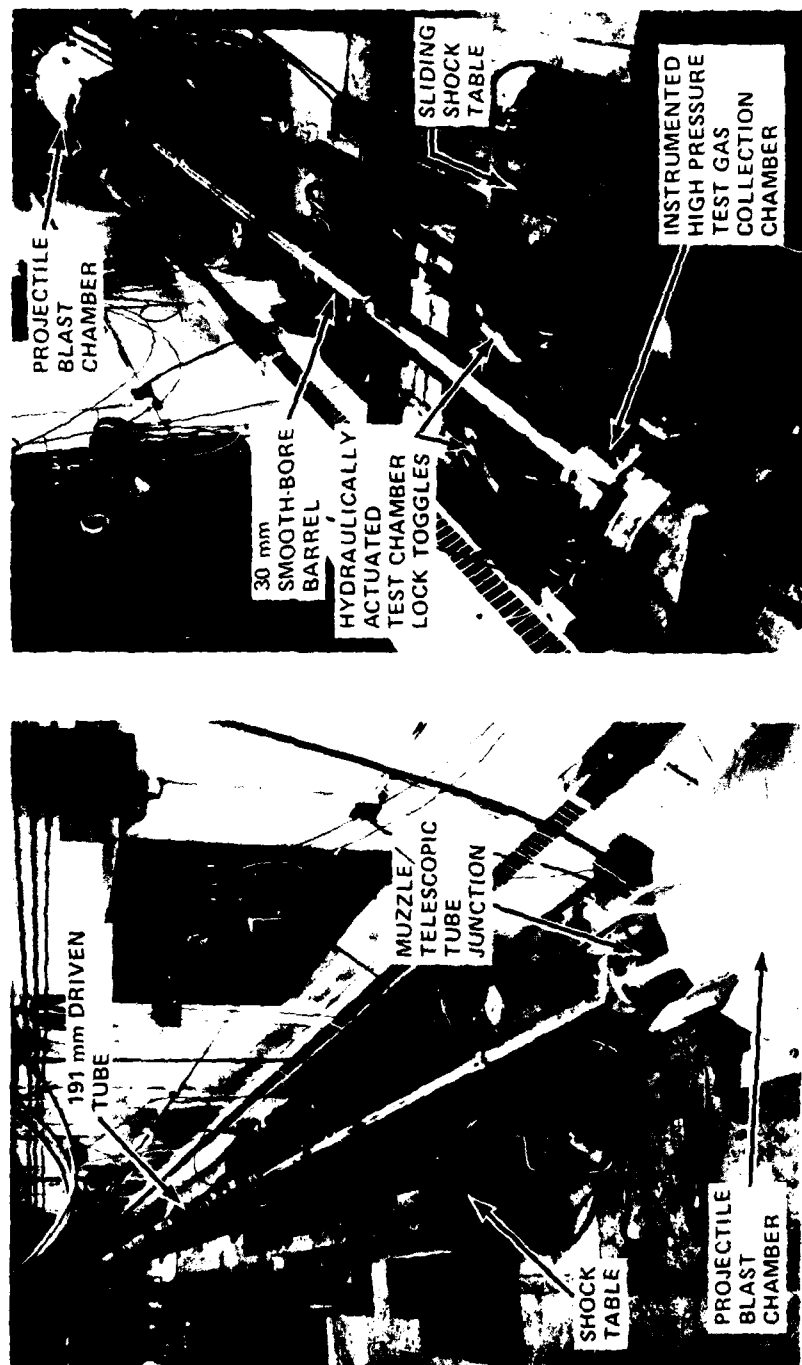


Figure 3. Projectile launch and capture components of the Shock Tube Gun

Table 1. Shock Tube Gun Characteristics

Configuration Data:

| | | |
|-------------------------------------|-----------------------|----------------------------|
| Driven Tube I.D. | 0.191 m | (7.5 in.) |
| Driven Tube Length | 24.6 m | (970 in.) |
| Piston Area | 0.0285 m ² | (44.179 in. ²) |
| Piston Mass | Up to 91.0 kg | (200 lbm) |
| Projectile Diameter | 30 mm | (1.181 in.) |
| Projectile Area | 706 mm ² | (1.095 in. ²) |
| Projectile Mass | Up to 0.91 kg | (2 lbm) |
| Driver Volume | 0.885 m ³ | (54,000 in. ³) |
| Chamber Volume | 2140 mm ³ | (130.8 in. ³) |
| Pressure - at release of projectile | Variable | |
| Barrel Length | 4.57 m | (180 in.) |

The projectile capture components consist of a telescoping tube coupled to the barrel muzzle, a projectile blast chamber, and a sand filled tube to decelerate and catch the projectile. The telescoping tube, the purpose of which is to permit independent motion of the shock tube and blast chamber, contains replaceable screens for measuring projectile velocity. The blast chamber reduces the noise and pressure levels as the projectile exits the barrel.

Figure 4 shows the chamber and toggle restraint system needed to contain the high chamber pressures and associated axial loads. Chamber pressures are sensed using piezoelectric transducers. The entrance region of the launch tube can accommodate pressure, heat flux, and erosion sensing devices.

The piston, which is used to compress the test gas, is made from 4340 steel and weighs 68 kg, including the latching block on its rear face which secures it at the upstream end of the driven tube, prior to release or "firing." Gas seal is maintained using "T" rings at the front and rear of the piston. Three brass wear rings or "bore riders" are used to prevent steel-to-steel contact between piston and tube. A buffer projection on the face of the piston and a complementary piston stop ring at the downstream end of the driven tube prevent direct impact of the piston into the test gas collection chamber in the event that the compressed test gas develops insufficient pressure or loses pressure prematurely due to chamber seal failure.

Operation

Operation of the STG to collect test data regarding ballistics, heating and erosion follows a fixed experimental pattern. Prior to a run being conducted, the facility is inspected for damage from the preceding test and needed repairs are performed. Components such as the driven tube,

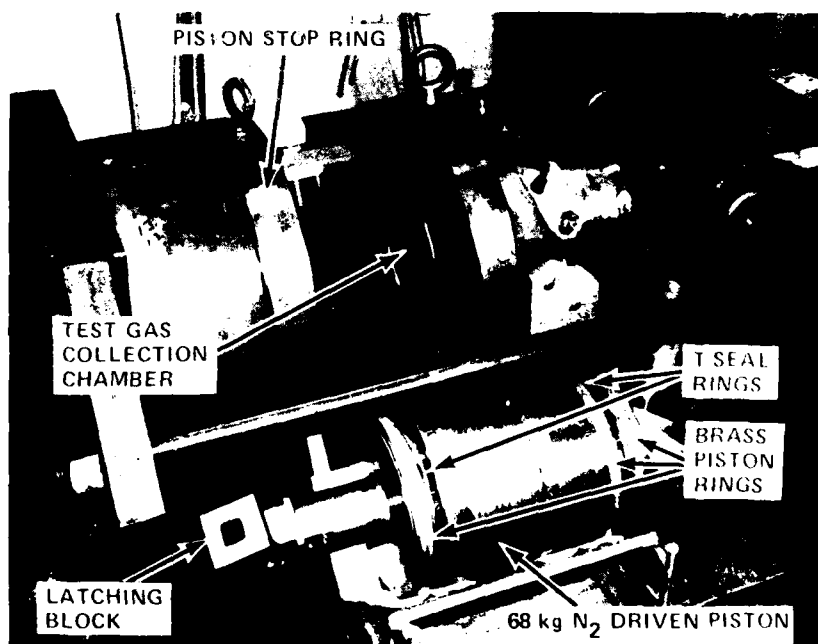
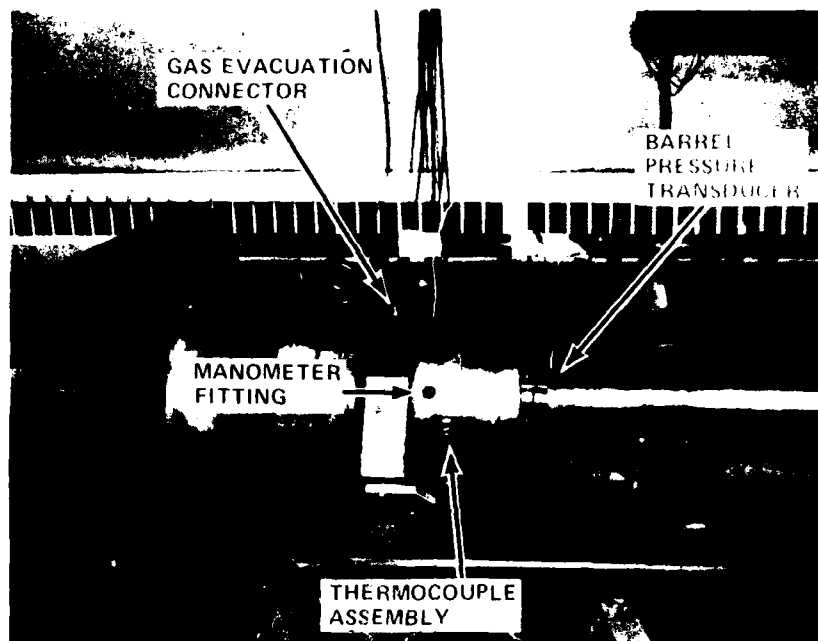


Figure 4. Piston, chamber, and toggle restraint components of the Shock Tube Gun

piston, and gas collection chamber which contact the test gas during a run are carefully cleaned to eliminate contaminants from their surfaces. All wearing surfaces, including piston "O" rings and bore riders, tube seals and stop ring buffers are replaced if their wear limits are reached. The piston is then inserted in the upstream end of the tube and latched to the driver release mechanism. A new projectile is inserted in the barrel.

The numbered specimen is weighed prior to testing using an analytical balance for initial mass, given a final cleaning with freon, and then installed in the sample holder within the gas collection chamber. M-11 mechanical pressure gauges are also installed in the chamber. Thermocouples are inserted through the chamber wall, positioned in the sample wall and then the chamber/barrel assembly is lowered into position and sealed to the downstream end of the driven tube with hydraulic toggles.

After installation of the projectile and specimen, the entire tube/chamber cavity is evacuated to a pressure of 2.0 mm Hg or less. If vacuum is maintained for a reasonable time, indicating seal integrity, the cavity is purged with argon, re-evacuated, again purged with argon, and evacuated for a third time. The cavity is then charged to the local atmospheric condition with the required partial pressures of the gases selected for the test mixture. These partial pressures are dependent upon the mix ratio desired.

Equations for establishing partial pressure settings are derived from the Dalton model of ideal gas mixtures, which assumes the following:

1. The moles of mixture, n , equals the sum of the moles of the component gases, $n_A + n_N + n_{CO} + n_{CO_2}$, where A, N, CO and CO_2 are subscripts referring to argon, nitrogen, carbon monoxide, and carbon dioxide, respectively.
2. Each component gas in the mixture occupies the entire mixture volume, V , which in this case is the volume of the driven tube.
3. The temperature, T , of the components before and after mixing remains constant.
4. The mixture pressure, P , in this case, 1 atmosphere, is reasonably low, to assure near ideal gas behavior.

$$\begin{array}{ll} \text{For the components: } P_A V = n_A \bar{R}T & P_{CO} V = n_{CO} \bar{R}T \\ P_N V = n_N \bar{R}T & P_{CO_2} V = n_{CO_2} \bar{R}T \end{array}$$

$$\text{For the mixture: } PV = n\bar{R}T$$

Since V/\overline{RT} is a constant in all the equations:

$$\frac{P_A}{n_A} = \frac{P_N}{n_N} = \frac{P_{CO}}{n_{CO}} = \frac{P_{CO_2}}{n_{CO_2}} = \frac{P}{n}$$

Rewriting:

$$\frac{P_A}{P} = \frac{n_A}{n} \quad \frac{P_{CO}}{P} = \frac{n_{CO}}{n}$$

$$\frac{P_N}{P} = \frac{n_N}{n} \quad \frac{P_{CO_2}}{P} = \frac{n_{CO_2}}{n}$$

That is, for each component of a mixture of ideal gases, the mole fraction and the ratio of the partial pressure to the total pressure are equal.

Upon completion of test gas charging, the mixture is given time to equilibrate in the driven tube while the required instrumentation including pressure transducers and thermocouples are connected to suitable recording devices and checked for correct operation. The piezoelectric pressure output is recorded by a Nicolet Explorer III digital oscilloscope and stored for future analysis on the scope's integral disk memory. The thermocouple output is recorded through an analog to digital converter by a Rockwell AIM 65 microprocessor, programmed to print out time versus both temperature and total heat input for both data channels. Figure 5 is an example of plotted data taken from the AIM printer.

If the instrumentation checks out satisfactorily, the nitrogen tank farm valve is opened, the tube air brake is charged, the driver is pressurized to the desired level for the experiment, recording devices are activated and the piston is released.

After exhausting residual driver pressure, the air brake is bled, and the chamber/barrel assembly is decoupled from the tube. The specimen is carefully removed, inspected, weighed and measured diametrically at four axial locations. Hard copy is made of all test data for further reduction and analysis.

Test Specimen Design

The primary objective of this study is to determine if certain propellant gas conditions enhance barrel erosion and cracking. To correlate the test data, the specimens used are made nearly identical in shape and composition, i.e., a 4340 steel cylinder, 38.1 mm in length, 31.75 mm in diameter, and bored concentrically to 12.7 mm, to create a sonic flow

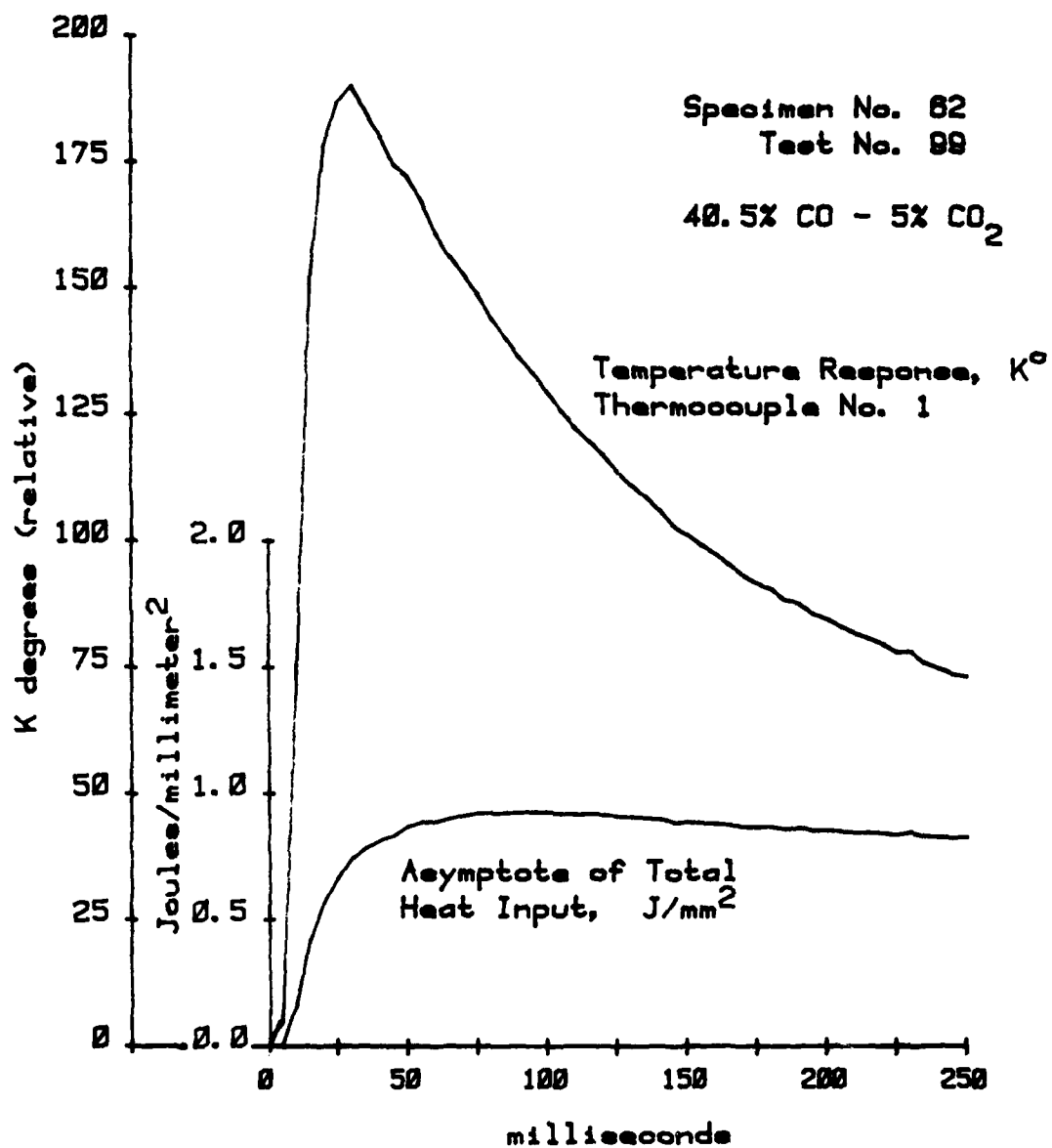


Figure 5. Temperature response and total heat input curves for an STG thermocouple

condition during the tests. The flow channel inlet is radiused to reduce turbulence and to increase heat flux over a larger portion of the flow channel surface. The samples are small enough to fit in the specimen stage of Calspan's Scanning Electron Microscope (SEM) such that bore surface examinations can be conducted without using replicas. Conversely, the samples are large enough to register finite changes in weight and bore diameter, resulting from test conditions. Mass changes are measured in tenths of a milligram on an analytical balance. Diametral recession is measured to within 10^{-4} mm at four specific axial locations, as shown in Figure 6. Also shown in the figure are the ports for in-wall thermocouples which are used to determine the integrated heat input. Dimensions on the figure are given in millimeters.

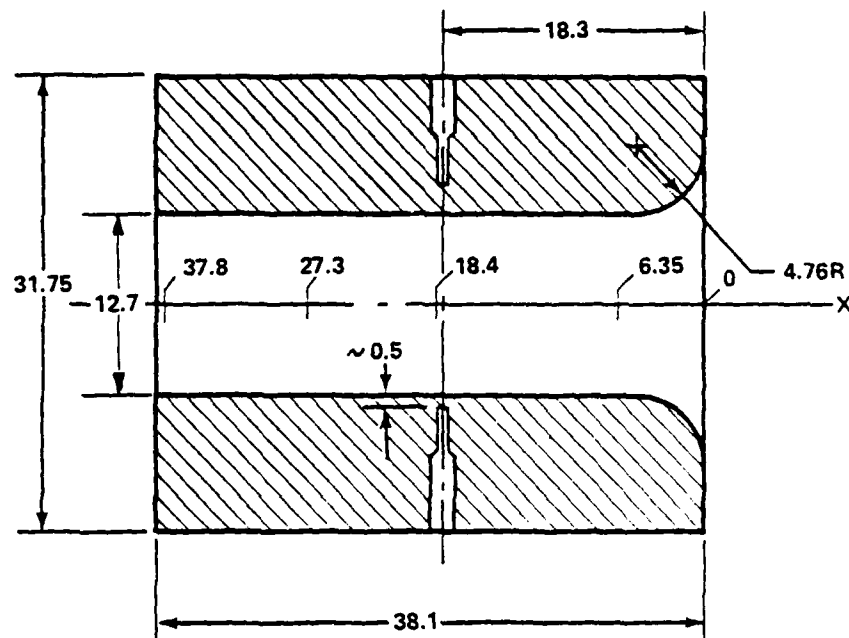
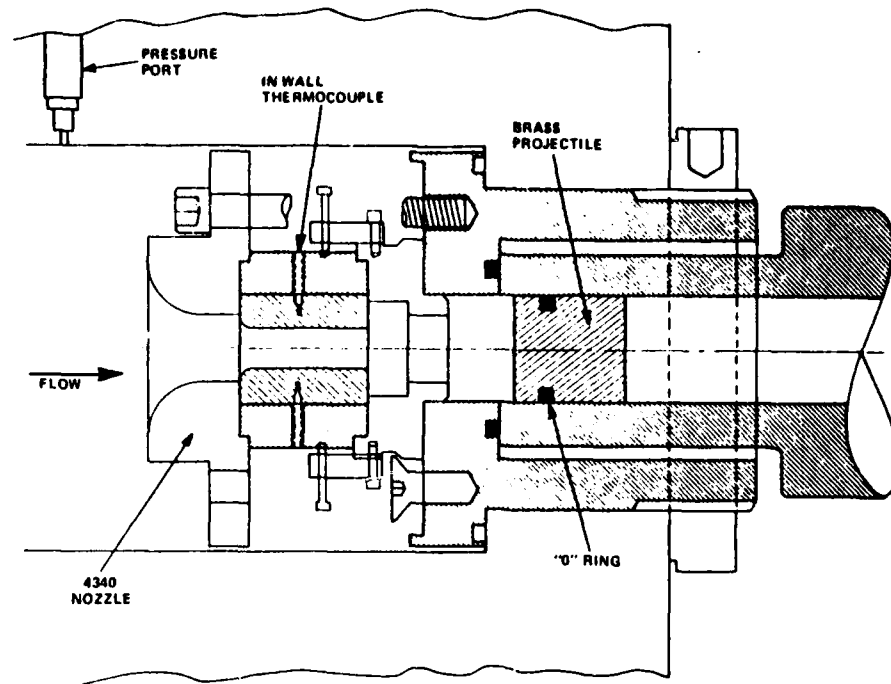


Figure 6. Test specimen used in the Shock Tube Gun

Heat Transfer Instrumentation

A primary measurement of the study is the amount of bore heating associated with each test. For this measurement, two in-wall thermocouples are installed in each sample, at distances approximately 0.5 mm from the bore surface. The method of installation is shown in Figure 7. Each of



SHOCK TUBE GUN TEST SECTION

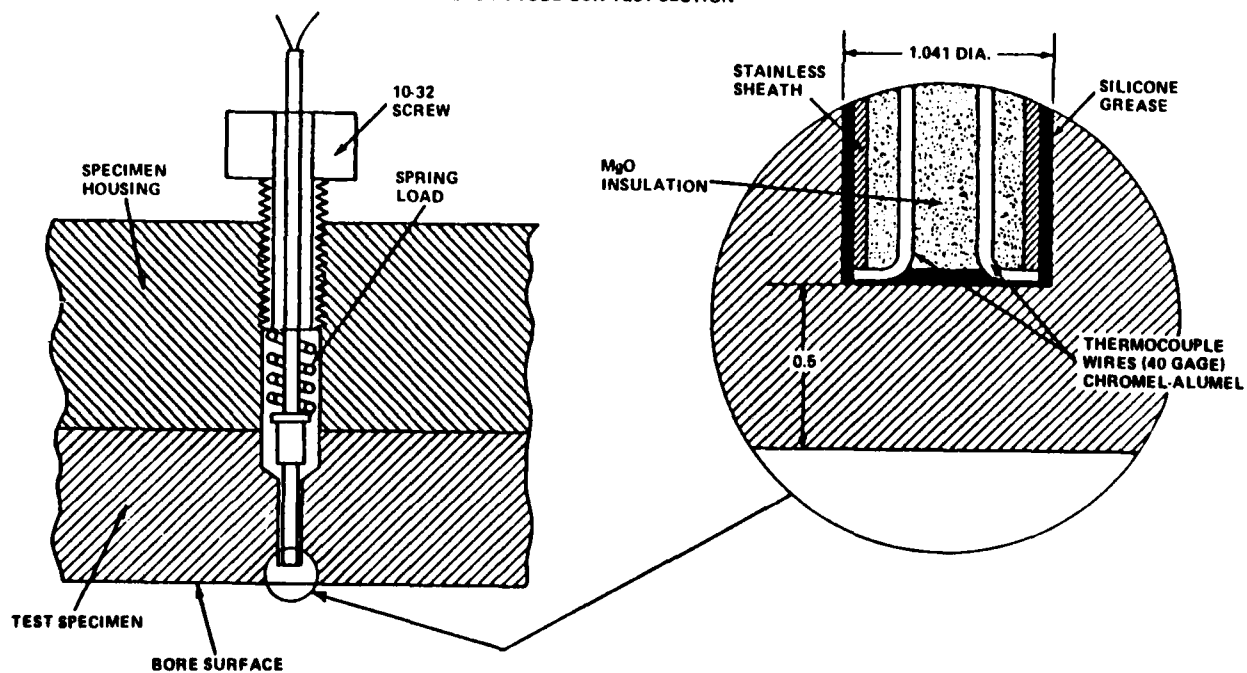


Figure 7. In-wall thermocouple installed in the Shock Tube Gun test section

these thermocouples independently may be used to determine net heating to the bore. Total heat input is calculated from the in-wall thermocouple's output by use of methods developed and reported by Calspan.¹⁵ Briefly, conversion of thermocouple output (millivolts vs. time) to total net heat input per unit area is accomplished by using the relationship:

$$Q(t) = \Delta T(t) \sqrt{\pi k c \rho t} \quad (1)$$

where $Q(t)$ is the net bore heat input

$\Delta T(t)$ is the measured change in in-wall temperature as a function of time

k is the thermal conductivity

c is the heat capacity per unit volume

t is the time after start of heating.

Data reduction procedure consists of calculating $Q(t)$ using Equation (1) at successive time intervals to produce a curve of $Q(t)$ vs. t which becomes asymptotic to the true heat input. To compute the correct asymptote, time zero for the start of heating must be established accurately on the thermocouple trace. It was concluded in a previous STG study², that correctly shaped asymptotes were most consistently produced by placing time zero at the intersection of the trace baseline and the average slope of the initial heat pulse's leading edge.

Corrected values for Heat Input are taken from end points on the $Q(t)$ vs. t curves that have been divided by a correction factor to account for the heat flux being dispersed over an increasing surface area as it passes through the test specimen's radial wall. This correction factor, $\eta(r)$, based on geometric considerations,¹⁵ is calculated from the relation

$$\eta(r) = 1 - 0.52e^{-5.71r} \quad (2)$$

For the test specimen bore radius of 6.35 mm, $\eta(r) = .87$

15. F.A. Vassallo, "Mathematical Models and Computer Routines Used in Evaluation of Caseless Ammunition Heat Transfer," Calspan Report GM-2948-2-1, Calspan Corporation, Buffalo, New York, June 1971.

IV. EXPERIMENTAL RESULTS

Gas Chemistry Test Data

Seven groups of tests were conducted to quantify the thermochemical erosion of 4340 steel specimens. The primary variable among these groups was CO/CO₂ mole ratio with values of 2.0, 3.6, 5.6, 8.1, and 17.2 being represented. CO/CO₂ ratios of 2.0 and 8.1 were each represented by two test groups containing 2.5 and 5.0 mole percent CO₂. Absolute CO₂ concentration, as explained earlier, was the secondary variable among test groups although groups with CO/CO₂ mole ratios of 3.6, 5.6, and 17.2 contained 2.5 percent CO₂ only.

The results of all STG tests conducted for this program are presented chronologically in Table 2. Upon preliminary inspection, it appears that Table 2 contains many more than seven test gas groups. However, the last five series containing anywhere from one to three test shots are continuations of the earlier groups, and the first test, i.e., 95, which uses the 45.5 percent CO "carburizing" gas mixture of the previous program¹ was merely intended as a shakedown run for the STG facility and for the new instrumentation being employed in this study.

The first test group, consisting of tests 96 through 100 and tests 130 and 131 employed a 40.5 percent CO-5 percent CO₂ mixture with an effective CO/CO₂ ratio of 8.1. This test group models NT (PPL-A-6396), a nitramine propellant containing 44.8 mole percent RDX.

The second test group, including tests 101 through 103, and 127 through 129, doubled the effective CO/CO₂ ratio of the previous group to 17.2 by halving the CO₂ concentration. The 43 percent CO-2.5 percent CO₂ mixture did not model the gas chemistry of any known propellant in the normal flame temperature regime, but these tests did provide erosion data at a finite CO/CO₂ ratio that falls between the "neutral activity" point and the full-carburizing level of the previous program,¹ throughout the temperature/pressure range of interest.

The third group, made up of tests 104 through 106 along with tests 125 and 126, returned to a CO/CO₂ mole ratio of 8.1 while keeping the CO₂ concentration at 2.5 percent. This was accomplished by substituting 22.5 mole percent N₂ for a like amount of CO. With respect to the first test group, the molecular concentrations of CO and CO₂ were both halved.

The fourth group of runs, tests 107 through 109 and 124 continued the process of lowering the CO/CO₂ ratio (to 5.6) by replacing more CO with N₂. This 14 percent CO-2.5 percent CO₂ mixture in the STG represents the gas evolved from another nitramine propellant, HFP (PPL-A-6380) which contains 48.6 mole percent RDX.

Table 2. Gas chemistry test data

| Test No. | Spec. No. | Active* Constituent (%) | CO/CO ₂ Ratio (Normal) | Peak Press. (MPa) | Peak Temp. (°K) | Mass** Loss (mg) | A (mm) | B (mm) | C (mm) | D (mm) |
|----------|-----------|---|-----------------------------------|-------------------|-----------------|------------------|--------|--------|--------|--------|
| 95 | 58 | 45.5CO | | 220 | 5360 | 0 | 0 | 0 | 0 | 0 |
| 96 | 59 | | | 219 | 5100 | (1.2) | (.003) | (.003) | 0 | 0 |
| 97 | 60 | | | 239 | 5170 | (0.5) | (.003) | (.005) | (.001) | (.020) |
| 98 | 61 | 40.5CO-5CO ₂ | 8.1 | 236 | 5160 | (1.0) | (.003) | (.005) | (.010) | (.003) |
| 99 | 62 | | | 261 | 5250 | (2.1) | (.003) | (.003) | (.003) | (.013) |
| 100 | 63 | | | 293 | 5360 | 38.9 | .018 | (.005) | (.008) | (.013) |
| 101 | 64 | | | 232 | 5270 | 5.7 | .003 | (.008) | (.010) | (.003) |
| 102 | 65 | 43CO-2.5CO ₂ | 17.2 | 268 | 5410 | 37.7 | (.008) | (.008) | (.017) | (.019) |
| 103 | 66 | | | 261 | 5380 | 0.5 | (.017) | (.024) | (.008) | (.009) |
| 104 | 67 | | | 245 | 5340 | (1.4) | 0 | (.001) | (.003) | (.025) |
| 105 | 68 | 20.5CO-2.5CO ₂ -22.5N ₂ | 8.1 | 237 | 5310 | 1.7 | (.020) | 0 | (.013) | (.032) |
| 106 | 69 | | | 200 | 5150 | 1.3 | (.004) | (.011) | (.008) | 0 |
| 107 | 70 | | | 250 | 5280 | 13.0 | (.003) | 0 | 0 | (.010) |
| 108 | 71 | 14CO-2.5CO ₂ -29N ₂ | 5.6 | 203 | 5170 | 0.1 | .003 | (.005) | 0 | (.001) |
| 109 | 72 | | | 229 | 5270 | 1.9 | (.003) | (.006) | (.004) | (.048) |
| 110 | 73 | | | 275 | 5440 | 8.5 | .004 | (.003) | (.008) | 0 |
| 111 | 74 | 9CO-2.5CO ₂ -34N ₂ | 3.6 | 256 | 5310 | (0.7) | (.008) | (.005) | 0 | (.006) |
| 112 | 75 | | | 262 | 5400 | 10.5 | 0 | (.003) | (.004) | (.004) |
| 113 | 76 | | | 269 | 5420 | 1.8 | (.005) | 0 | 0 | 0 |
| 114 | 77 | | | 522 | 5590 | 59.5 | .055 | (.004) | (.009) | 0 |
| 115 | 78 | 5CO-2.5CO ₂ -38N ₂ | 2.0 | 270 | 5450 | 0.5 | (.006) | (.005) | (.004) | (.001) |
| 116 | 79 | | | 256 | 5380 | (2.5) | .003 | .001 | 0 | (.001) |
| 117 | 80 | | | 545 | 5660 | 118.5 | .052 | .008 | 0 | (.009) |

*The remaining 54.5% of the test gas mixture is argon.

**Parenthesis indicate mass gain and/or diametral recession.

Table 2. (cont)

| Test No. | Spec. No. | Active* Constituent (%) | CO/CO ₂ Ratio (Normal) | Peak Press. (MPa) | Peak Temp. (°K) | Mass** Loss (mg) | Diametral Recession** | | | |
|----------|-----------|---|-----------------------------------|-------------------|-----------------|------------------|-----------------------|--------|--------|--------|
| | | | | | | | A (mm) | B (mm) | C (mm) | D (mm) |
| 118 | 81 | 10CO-5CO ₂ -30.5N ₂ | 2.0 | 325 | 3460 | 82.0 | .025 | (.005) | (.004) | (.006) |
| 119 | 82 | | | 356 | 3540 | 28.0 | .013 | (.003) | (.008) | (.003) |
| 120 | 84 | | | 153 | 2750 | 2.4 | .013 | .023 | .010 | .023 |
| 121 | 83 | | | 331 | 3480 | 19.3 | .008 | (.004) | (.003) | (.005) |
| 122 | 85 | | | 313 | 3430 | 5.4 | (.008) | (.005) | (.003) | (.004) |
| 123 | 86 | 9CO-2.5CO ₂ -34N ₂ | 3.6 | 327 | 3620 | 67.9 | .048 | (.001) | (.009) | (.001) |
| 124 | 87 | 14CO-2.5CO ₂ -29N ₂ | 5.6 | 321 | 3600 | 59.4 | .039 | .004 | (.009) | (.008) |
| 125 | 88 | 20.5CO-2.5CO ₂ -22.5N ₂ | 8.1 | 318 | 3620 | 87.2 | .037 | .003 | .003 | (.011) |
| 126 | 89 | | | 350 | 3690 | 224.1 | .064 | .028 | .018 | (.014) |
| 127 | 90 | 43CO-2.5CO ₂ | 17.2 | 130 | 2770 | (0.6) | (.003) | (.006) | (.004) | (.003) |
| 128 | 91 | | | 93 | 2510 | (0.6) | (.005) | (.010) | (.004) | (.013) |
| 129 | 92 | | | 370 | 3740 | 120.0 | .047 | .019 | .010 | .011 |
| 130 | 93 | 40.5CO-5CO ₂ | 8.1 | 219 | 3100 | 2.0 | (.001) | (.001) | (.001) | (.005) |
| 131 | 94 | | | 157 | 2820 | 0.0 | (.001) | (.001) | .001 | (.006) |

*The remaining 54.5% of the test gas mixture is argon.

**Parenthesis indicate mass gain and/or diametral recession.

The process of approaching the theoretical neutral point of chemical activity was completed by the fifth (tests 110-112, 123) and sixth (tests 113 through 117) groups which further lowered the CO/CO_2 to 5.0 and 2.0, respectively, while maintaining the CO_2 concentration at 2.5 percent. These groups represent the equilibrium CO/CO_2 ratios of most conventional double and triple-based propellants.

The seventh test groups, consisting of runs 118 through 122 duplicates its predecessor's CO/CO_2 ratio of 2.0 but at double the CO_2 content, i.e., 5 mole percent.

In addition to listing the active constituents of each test gas mixture, Table 2 also itemizes peak STG chamber pressure, the associated peak temperature from the isentropic equilibrium combustion code (Appendix B), mass lost or gained by a test specimen during its test run and the complimentary diametral changes in the specimen's flow channel.

Correlation of Erosion Data with Flow Conditions

The flow conditions for any particular test in this program are, to a large degree, set by the initial conditions of the test. Peak test gas pressure is a function of the STG driver pressure and the mass of the test gas mixture. The mass is a constant throughout a group of tests employing the same test gas mixture and a conscious effort was made to minimize mass change between test groups by utilizing the $\text{CO}-\text{N}_2$ exchange method to effectively alter the CO/CO_2 ratio while maintaining near constant mixture mass. Mass change was unavoidable when switching CO_2 concentration level but because CO_2 mole percents were always low; either 2.5 or 5.0, the change in total mixture mass was limited to about 1.1 percent.

Figure 8 illustrates the relationship between peak test gas mixture pressure and specimen mass loss. Also included on the figure are erosion curves for oxidizing, carburizing, and inert (nitrogen) mixtures used in the two previous programs.^{1,2} While initially it may appear that this program's mixtures were less active than those of the previous studies, the combination of CO and CO_2 in one mixture produced equilibrium ratios of specific heat in the range of 1.37 to 1.40, which were measurably "colder" than values calculated for the inert and 45.5 percent CO mixtures, typically 1.41 or higher. It was therefore necessary to run the present tests at comparatively higher gas pressure in order to generate the same gas temperatures of interest that were sought in the previous programs. Figure 8 has been included to point out the apparent weakness of simple pressure/erosion correlations.

Figure 9 illustrates the relationship of specimen mass loss to the peak test gas mixture temperature. Because the specimen wall temperature, at which the erosion takes place, is more closely linked to the gas temperature than to the gas pressure, Figure 9 is a better correlation of a flow condition with a surface reaction than is Figure 8. As was expected, most of

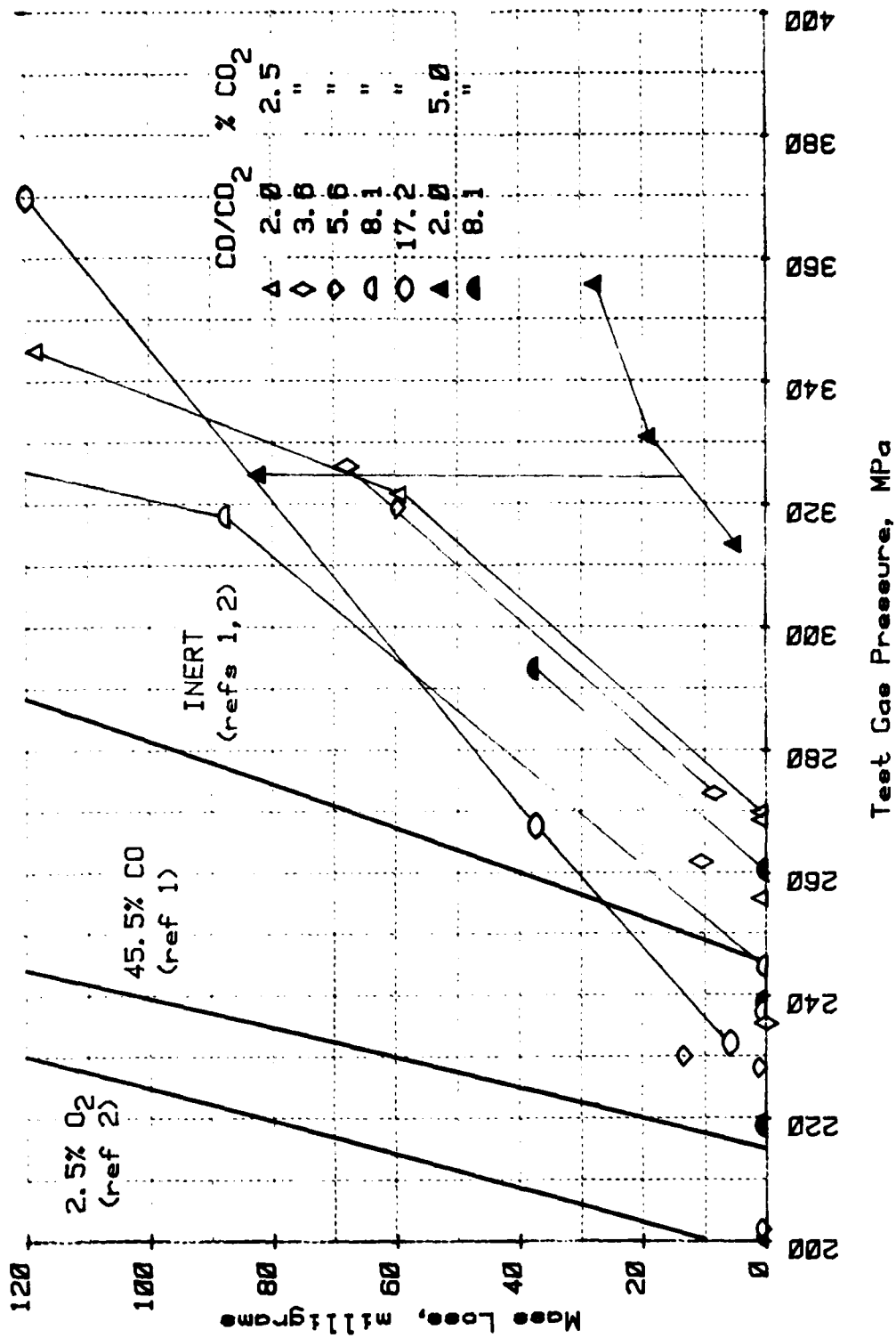


Figure 8. Peak test gas mixture pressure versus specimen mass loss

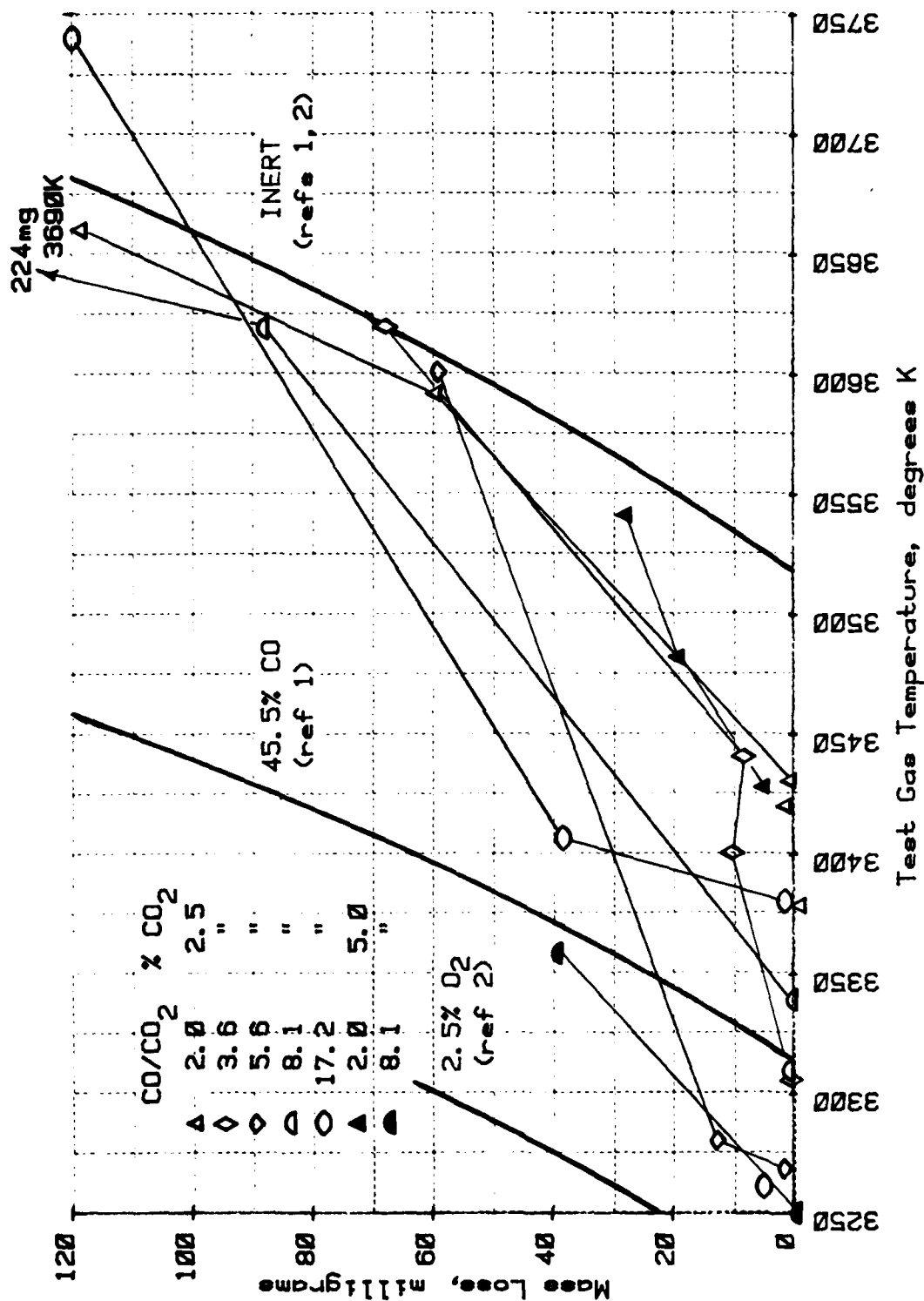


Figure 9. Peak test gas mixture temperature versus specimen mass loss

the CO/CO₂ mixtures fell between the inert and full carburizing curves, previously established.^{1,2} Notable exceptions are the 8.1 CO/CO₂, 5 percent CO₂ point (dark hemicycle) at the 40 mg level and the 17.2 CO/CO₂, 2.5 percent point (hollow ellipse) at the 120 mg level. The former lies very near to the 45.5 percent CO curve and may have fallen to the right of it if more tests using this mixture could have been performed. Alternately, this mixture also represents the best compromise of potentials of any used in the program to produce both low temperature carburization and high temperature oxidation. The latter point, mentioned above, appears to be substantially to the right of where it was expected to fall, i.e., just to the right of the 45.5 percent CO curve. Again, further testing would probably have clarified this discrepancy.

To summarize, the erosion potential of CO/CO₂ mixtures in relation to flow conditions appears to be buffered by the opposing chemical affinities of the two molecules. CO/CO₂ mixture ratios of from 2.0 to 5.6 produced similar levels of erosion, despite any change in CO₂ concentration. These mixture ratios represent most of the conventional double base and triple base propellants. A CO/CO₂ mixture ratio of 8.1 appeared to be more sensitive to its absolute CO₂ mole percent content. This mixture ratio is representative of the gas produced by nitramine base propellants.

Correlation of Erosion Data with CO/CO₂ Ratio

An attempt was made to better understand the flow conditions/erosion data of the previous figures from the standpoint of CO/CO₂ ratio alone. Figure 10 represents the isotherms for the test data in terms of mass loss and their respective CO/CO₂ ratios. Only data from tests using the primary CO₂ concentration, i.e., 2.5 mole percent, are shown.

It is apparent that overall erosion potential of the test mixtures does not vary substantially with CO/CO₂ ratio, nor with temperature other than in a purely thermal way. However, the 5.6 CO/CO₂ mole ratio mixture is the least susceptible to increasing temperature, in terms of its erosiveness. Ironically, this mixture was used to model HFP, a nitramine propellant, whose normal flame temperature is too low to take advantage of this high temperature/low erosion characteristic.

Correlation of Erosion Data with CO₂ Concentration

Two of the STG test gas mixtures had duplicates, in terms of CO/CO₂ ratio, but with double the amounts of CO and CO₂. That is, a 5 percent CO-2.5 percent CO₂ mixture and a 10 percent CO-5 percent CO₂ mixture both had a ratio of 2.0. Similarly, a 20.5 percent CO-2.5 percent CO₂ mixture and a 40.5 percent CO-5 percent CO₂ mixture both had a ratio of 8.1. To delineate the effects of temperature and CO₂ or CO concentration with erosivity, data from these four test groups were plotted as functions of CO/CO₂ ratio and mass loss on Figure 11.

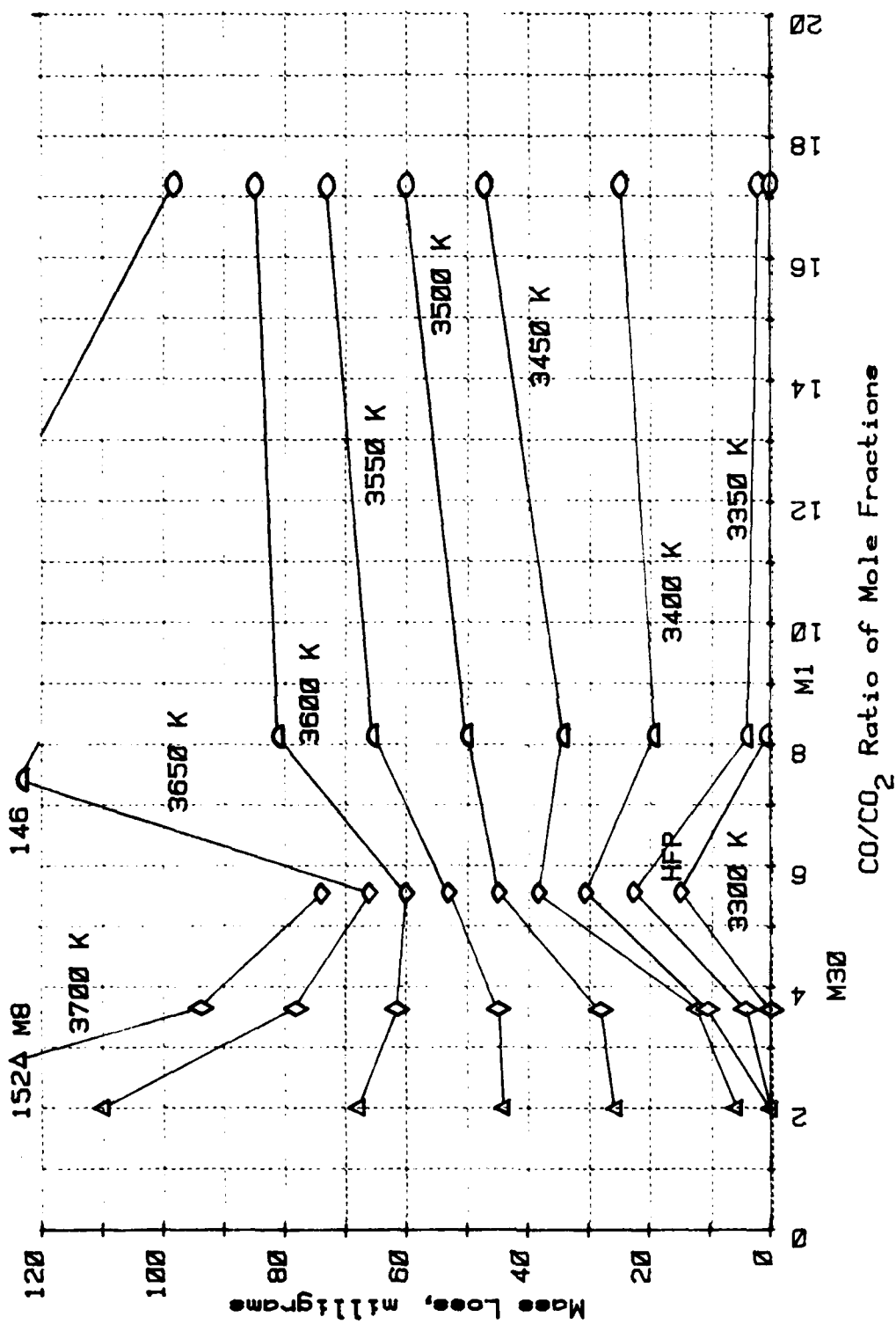


Figure 10. Isotherms of test gas mixtures containing 2.5% CO₂

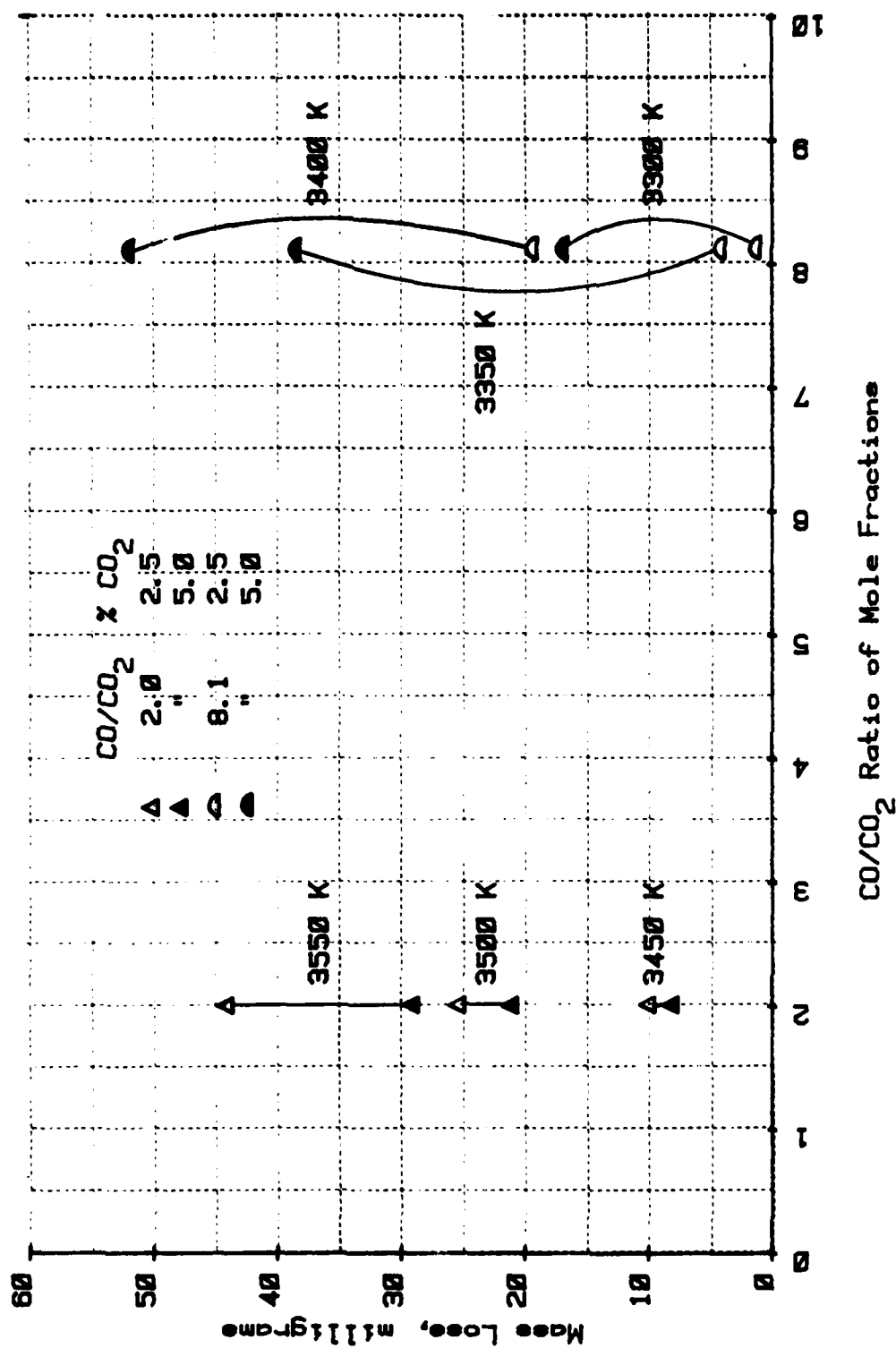


Figure 11. Isothermal comparison of 2.5% CO₂ and 5% CO₂ mixtures

Immediately evident is the inversion in erosivity as a function of absolute CO-CO₂ concentration for the two different CO/CO₂ ratio groups. Increasing CO-CO₂ concentration for the 2.0 CO/CO₂ mixture results in a relative decrease in erosion. Conversely, increasing CO-CO₂ concentration for the 8.1 CO/CO₂ mixture results in a relative increase in erosion. This would indicate that a CO/CO₂ ratio of 2.0 lies to the oxidizing side of the neutral activity point since a 2 to 1, CO to CO₂ reduction results in increased erosion, and that the 8.1 CO/CO₂ ratio lies to the carburizing side of the neutral point since an 8 to 1, CO to CO₂ reduction results in decreased erosion. This finding is in agreement with metallurgical data which places the neutral point of activity at a CO/CO₂ ratio of about 5.

The ratio of specific heats for the 2:1 mixtures was 1.57 and for the 8:1 mixtures, 1.39. To a small degree, this explains the greater overall erosion at lower temperature and pressure for the higher CO/CO₂ ratio mixtures as shown on Figure 11. Their higher total concentration of the two active gases would also be a contributing factor to increased erosion by the high CO/CO₂ ratio mixtures. Additionally, the decreasing disparity in erosiveness with decreasing temperature between mixtures with the same CO/CO₂ ratio but different CO₂ concentrations is a limiting effect of STG action or cycle time (4 to 6 milliseconds) on the erosion threshold of any particular gas mixture tested.

What is most noteworthy is that none of the three factors mentioned: higher ratio of specific heats, higher absolute CO-CO₂ content, and limited STG cycle time in relation to that of any large caliber gun, explain away the fact that at 3450K the 2.0 CO/CO₂ ratio mixture had fallen close to its erosion threshold as dictated by the STG flow conditions but that the 8.1 CO/CO₂ ratio mixture had not reached a similar state at 3500K under similar conditions.

The importance of this finding lies in its application to guns of varying calibers and action times. Despite the fact that the tests conducted with the STG in this program were unable to show the exact combination of temperature and cycle time that would pinpoint the critical CO/CO₂ propellant gas ratio in large caliber gun erosion, the data presented does indicate a trend towards increasing chemical activity with increasing CO/CO₂ ratios at comparatively longer action times and lower temperatures. This finding is in agreement with previous studies, where pure gas mixtures or propellant gases with high CO/CO₂ ratios proved no more erosive than low CO/CO₂ ratio gases when tested in combustion fixtures with short cycle times of 1 to 4 milliseconds, but produced greater erosion when tested in full scale gun fixtures with normal cycle times of over 8 milliseconds.

Correlation of Erosion Data with Heat Flux

Gasdynamic barrel erosion is the result of heat transfer to a melting surface, i.e., a hot-wall heat flux. Hot-wall heat flux, in this instance,

is defined as convective heating by the gas stream of a surface at the melting temperature of steel. The flow parameters of gas density, velocity and temperature are included in this heat flux calculation. Therefore, this quantity may be a better means for correlating erosion data than either pressure or temperature because the hot-wall heat flux includes effects of both. The previous Shock Tube Gun data correlations with temperature or pressure were realistic because temperature is a function of the pressure in a ballistic compressor during the adiabatic compression of similar gas compositions. However, for different gas compositions the temperature can change independently of the pressure. By using a quantity such as hot-wall heat flux, these independent changes of temperature and pressure can be taken into account.

To perform the heat flux calculation, flow conditions for each test were computed, using a combination of two computer programs and the experimentally measured peak pressures. The STG cycle model (Appendix A) was used to create the proper pressure profile. Also included in this particular code is a representation of the flow through the test sample and the calculation of the convective heat flux using the empirical equation for turbulent flow over a flat plate. The gas conditions of temperature, density and velocity are evaluated in this code. The local hot wall heat flux is computed and a running summation of the heat input to the wall is evaluated. The computed total heat input was compared with the experimentally determined value for the input gas mixture. A factor was applied to the heat flux calculation to bring the total heat input into agreement with the experimentally determined value. In this manner, the instantaneous value of convective heating, as determined by the flow conditions and exclusive of chemical heating, is believed to be reasonably correct.

The gas temperature, as determined by the STG model in its current state of development, is only an approximate calculation. A more accurate temperature calculation is provided by the equilibrium combustion code that is described briefly in Appendix B. The code computes an isentropic compression of gases beginning with an arbitrary mixture. In addition to determining the temperature and pressure, the concentration of the various chemical species formed during the equilibrium combustion process are also determined.

An approximate technique was used to correct the heat flux calculated by the STG model to the more accurate temperature conditions of the equilibrium combustion code. The heat flux to a surface is equal to the product of a coefficient and the temperature difference between the gas and the surface,

$$q = h (T_o - T_w). \quad (3)$$

For the heat flux to a flat plate in turbulent flow, the coefficient is functionally proportional to the gas density, velocity and viscosity,

$$h \sim (\rho u)^{0.8} \mu^{0.2} \quad (4)$$

These gas parameters can be expressed in terms of temperature as follows:

$\rho \sim T^{-1}$ through the ideal gas equation of state
 $u \sim T^{0.5}$ through the energy equation,
 and $\mu \sim T^{0.5}$ from molecular transport theory.

Thus, the approximate dependence of h on the gas temperature is

$$h \sim (T^{-1} \cdot T^{0.5})^{0.8} (T^{0.5})^{0.2} = T^{-.5} \quad (5)$$

The convective hot wall heat flux computed by the STG code is

$$q_s \sim T_{gs}^{-0.5} (T_{gs} - T_{ws}) \quad (6)$$

where T_{gs} and T_{ws} are the respective peak values for gas and surface temperatures. Similarly, the convective heat flux to a melting steel surface is

$$q_{hw} \sim T_{ge}^{-0.5} (T_{ge} - T_{wm}) \quad (7)$$

where T_{ge} is the gas temperature calculated by the equilibrium combustion code and T_{wm} is the solidus temperature of 4340 steel, 1720°K. The corrected value for the heat flux, q_{hw} , is

$$q_{hw} = q_s \frac{T_{ge}^{-0.5} (T_{ge} - T_{wm})}{T_{gs}^{-0.5} (T_{gs} - T_{ws})} \quad (8)$$

This represents an approximate value of convective heat flux to a melting surface.

The correlation of data from the present program with previously obtained mass loss data^{1,2} in terms of hot-wall heat flux, is shown in Figure 12. The data from the two previous programs show the shift in erosion threshold caused by insertion of one percent oxygen in the test gas in one case, ten percent CO₂ in another case, and 45.5 percent CO in a third case; all with respect to the inert case where pure nitrogen was the primary test gas. It should be noted that in the previous programs as well as the current one, the test gas was composed of at least 54.5 percent argon in order to alter the ratio of specific heats to obtain the desired gas temperature.

In reference 1, it was noted that a ratio of carbon monoxide to carbon dioxide (CO/CO₂) of 3 was the approximate neutral point where a gas might be expected to behave like an inert gas. On Figure 12, when the CO/CO₂ ratio was 2, 3.6, or 5.6, most of the data points fell along a curve slightly to the right of the previously-obtained inert curve. Therefore the gas conditions represented by these data points more or less coincide with those of inert gases. It is noted that most energetic single-base, double-base, and

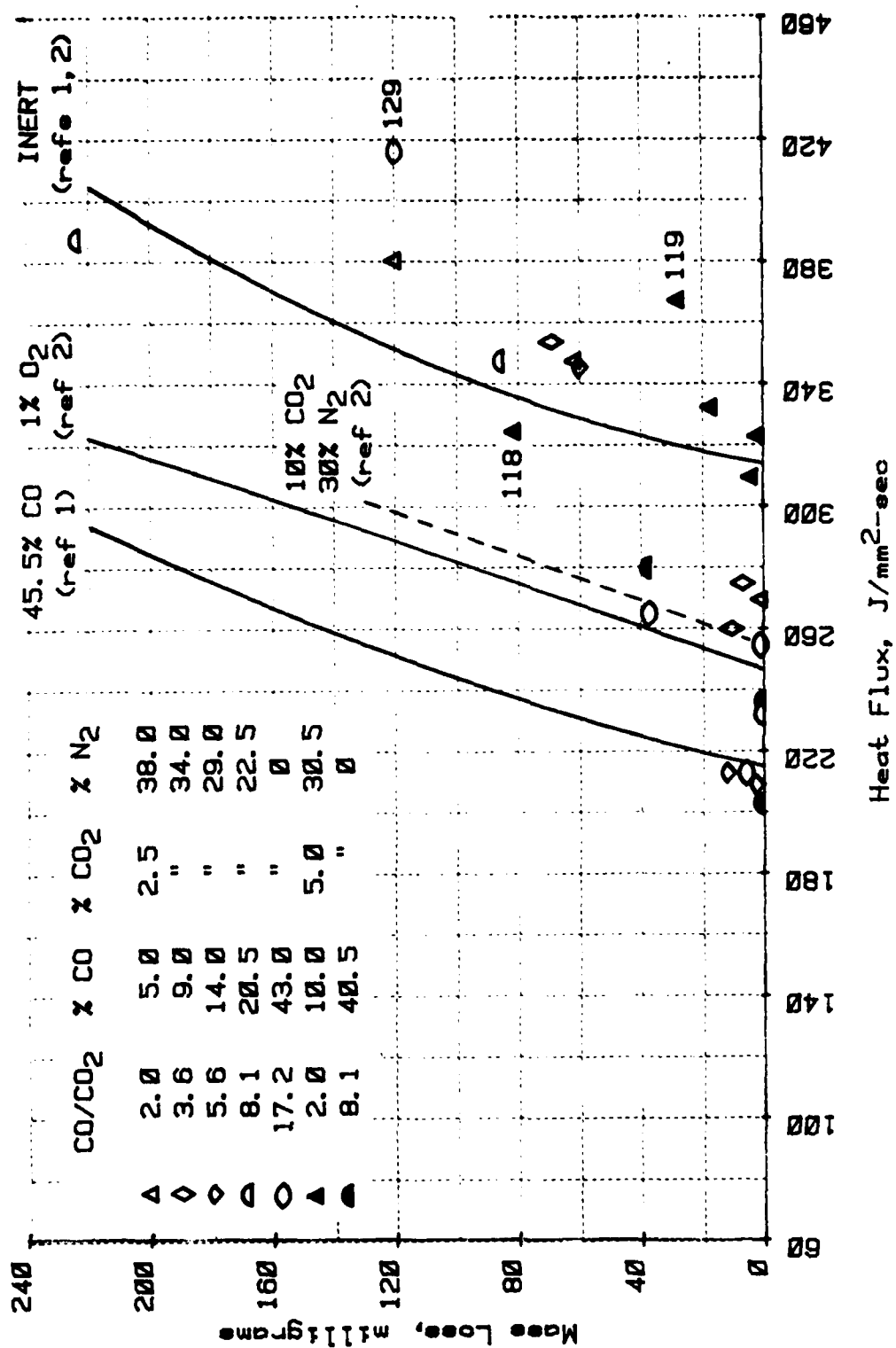


Figure 12. Convective hot-wall heat flux versus specimen mass loss

triple-base gun propellants fall in this region. Two points obtained during Runs 118 and 119 with a CO/CO_2 ratio of 2.0, do not fall on this curve. The mass loss for Run 118, as indicated on the figure, is somewhat higher than expected and Run 119 is somewhat lower. The reasons for these excursions are currently unexplained and additional testing is required to obtain the true mass loss functions for this test gas mixture. It should also be noted that erosion between 0 and 10 milligrams lies in the noise region on the figure and only erosion levels in excess of that level should be considered significant.

The higher concentrations of CO, as indicated by the open and closed hemicyclic symbols and the open ellipse-like symbol, clearly indicate greater erosion for these points than for the other test gas mixtures at the same heating level. The uppermost symbols at 270 and 280 $\text{J}/\text{mm}^2\text{-sec}$ of heat flux show the erosion threshold is essentially midway between that of the 45.5 percent CO and the inert composition. It is noted that these points contain 40.5 and 43 percent CO with 5 and 2.5 percent, respectively, of CO_2 .

The data obtained during Run 129 was presumably an outlier since data obtained at lesser conditions previously have exhibited significantly higher erosion. At present this low value is unexplained but it can't be ignored. This particular point is pivotal in that it clouds some conclusions that might otherwise be drawn from the data of this program. The mass loss from that sample might be expected to be three times the level measured if it were to be in agreement with the other ellipse shaped point at a heat flux of 270 $\text{J}/\text{mm}^2\text{-sec}$. Clearly, additional data at this high heating point should be taken in order to verify or refute the results of this run.

Other data taken at a CO/CO_2 ratio of 8.1 but with 20.5 percent CO lie slightly to the left of the inert curve, showing less influence of the higher CO/CO_2 ratio than the tests with a higher concentration of CO.

The correlation of the test gas data with convective hot wall heat flux indicate the following trends.

1. The test with gas mixtures containing both low levels of CO and CO_2 , and a low value of CO/CO_2 ratio (5.6 to 2), behaved quite similarly to previously-obtained inert data. An attempt to polish the surface of the test specimen during this program might well explain the small shift from the previously obtained inert gas curve (N_2 and Ar).
2. Higher levels of CO/CO_2 ratio and percentage content of CO and CO_2 were observed to shift the erosion threshold to lower values of convective heating.
3. The amount by which the erosion threshold was shifted appears to depend upon both the CO/CO_2 ratio and on the percentage content of CO and CO_2 in the test gas, although none of the data obtained on this program where CO_2 was incorporated in the gas mixture approached the level of erosion obtained previously when 45.5 percent CO was tested alone with argon. The fact that

increasing the amount of CO in high CO/CO₂ ratio gases appears to decrease the level of heating at which the erosion threshold occurs seems to indicate a diffusion controlled reaction where the magnitude of the reaction is governed by the amount of reactants diffusing through the surface. That is, as the percentage of the non-equilibrated reactants increase, the amount of reaction increases correspondingly.

Characterization of Test Specimen Surfaces

The Scanning Electron Microscope was used to help characterize the surface features of each test specimen used in this program. The samples were first sawed in half along their flow axes, ultrasonically cleaned, degaussed, and then photomicrographs of a representative area near the inlet, center, and exit of each specimen's flow surface were made. Table 3 lists the surface characteristics in addition to pertinent test data for a series of specimens that represents the seven gas mixture groups tested, both at near threshold and above threshold conditions. The photomicrographs of the fourteen specimens tabulated are shown in Figures 13 through 26.

As can be seen in the odd numbered figures, near threshold flow conditions have minimal effect on the surface features of the 4340 steel specimens, irregardless of the gas mixture used. Erosion is confined to the leading edges of larger machine marks that are most exposed to convective flow and least capable of dissipating heat other than through fusion. The major part of each flow surface looks smooth and untested at all of the locations photographed.

The even numbered figures illustrate the contrasting surface features of seven test specimens which experienced similar finite levels of erosion at above threshold conditions. The surface characteristics appear to be dependent on flow channel location; i.e., localized flow factors such as turbulence level or boundary layer thickness, and local heat flux, that effect the amount of melt and how it is deposited, or if it is deposited on the altered surface of the steel.

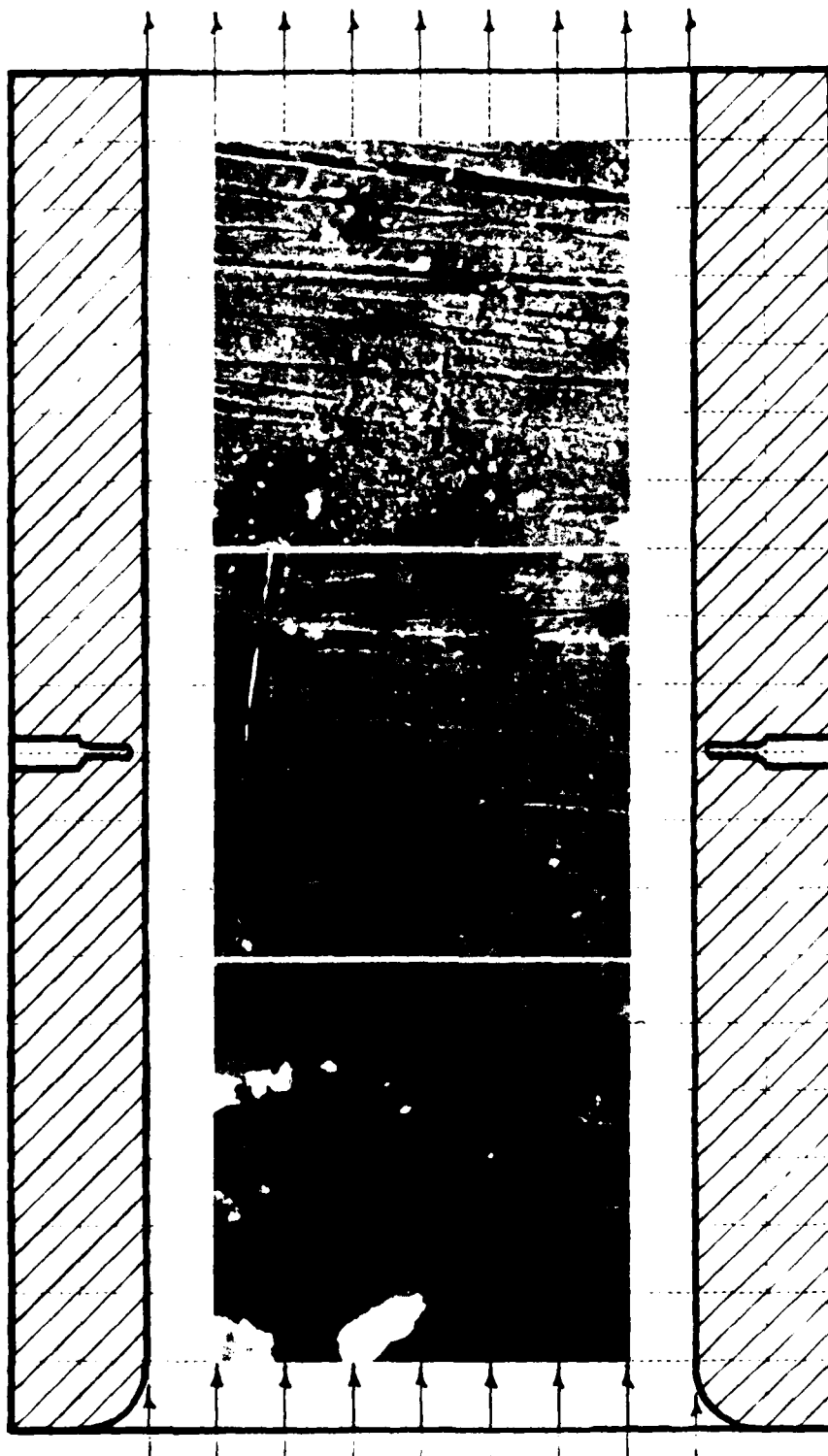
The changes in flow surface appearance seem also to depend on the chemistry of the gas that a particular specimen was exposed to when tested. This finding is corroborated by comparing the photomicrographs of the present test specimens with those from the two previous reports.^{1,2} For example, in the "inlet" photographs on Figures 14 and 16, there is evidence of the clustered beading that was evident on sample surfaces eroded by oxygen and carbon dioxide gas mixtures used in the oxidation study.² The beading may be granular corrosion; the preferential oxidation of alpha iron. Figures 14 and 16 represent the two test groups with the lowest CO/CO₂ ratio and therefore the greatest potential for oxidation-type reactions.

In another comparison of present and previous test specimen surfaces, the "pebbling" alluded to in Table 3, is prevalent on the "inert" gas

specimens used in the carburization study. This pebbling is thought to be intergranular corrosion, i.e., the preferential erosion of carbides at the steel's grain boundaries where they are concentrated. "Pebbling" is most prominent when no oxygen, either free or complexed, is present in the test atmosphere and the amount of pebbling appears to decrease and then vanish as either the CO/CO₂ ratio increases or the CO₂ concentration increases, or both. In short, "pebbling" is not a characteristic feature produced by either oxidizing atmospheres or those gases containing more than about 20 mole percent carbon monoxide, which can be referred to as carburizing. In the latter case, the CO levels are probably high enough so that the eutectic carbides within the pearlitic structure of the grain are eroded in addition to the intergranular carbides. This may explain the dendritic formations seen on sample surfaces that were exposed to CO concentrations of greater than 40 mole percent, both in this program and the previous carburization study. Another feature shared by high CO exposure samples of these two programs is the "potato eye" or whorl formations found on the downstream surfaces of these specimens. No explanation of this unique surface characteristic is given at this time.

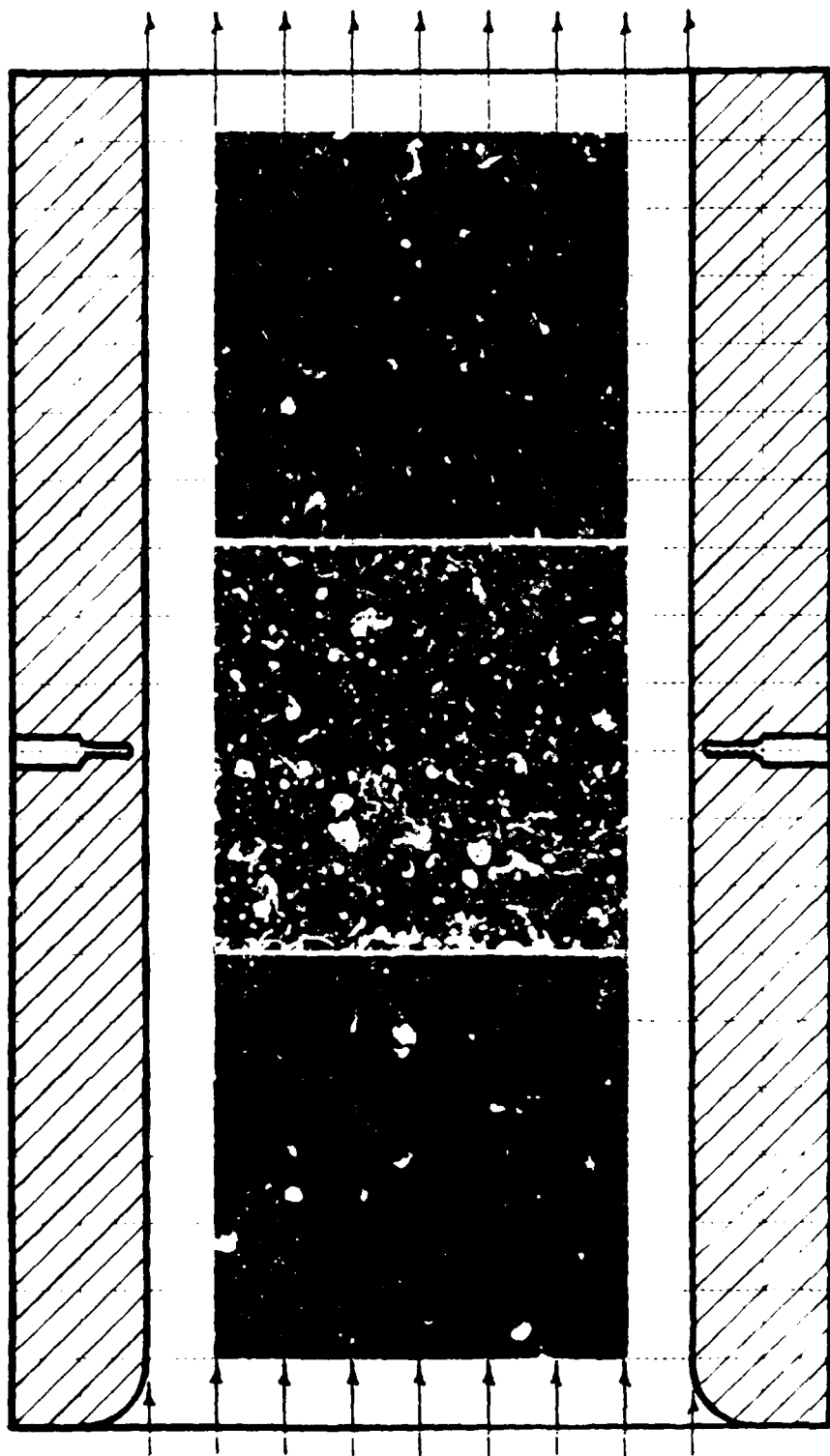
Table 3. Characteristics of STG Test Specimen Flow Surfaces

| Test No. | Spec. No. | CO ₂ (%) | CO/CO ₂ Ratio | Erosion (mg) | Inlet | Test Specimen Surface Characteristics | | Exit |
|----------|-----------|---------------------|--------------------------|--------------|--|---|---|------|
| 116 | 79 | 2.5 | 2.0 | -0 | Finest machine marks gone -very thin scale formation | Bulged machine marks -slight erosion | Bulged machine marks -minimal deposits | |
| 114 | 77 | 2.5 | 2.0 | 59.5 | Pebbled with a mixture of fine and coarse grains | Pebbling with a few cracks partly obscured by crust | Uniformly pebbled-intergranular flow striations | |
| 122 | 85 | 5.0 | 2.0 | -0 | Fine machine marks present very slight pebbling | Minimal erosion | Minimal erosion | |
| 118 | 81 | 5.0 | 2.0 | 82.0 | Distinct pebbling-melt streamers | Resolidified melt no pebbling observable | Minimal machine marks slight pebbling and melt | |
| 111 | 74 | 2.5 | 3.6 | -0 | No erosion-looks untested | No erosion-looks untested | Minimal machine marks slight erosion | |
| 123 | 86 | 2.5 | 3.6 | 67.9 | Minimal pebbling-fine grain structure | Distinct pebbling | Background pebbling partly covered with melt | |
| 108 | 71 | 2.5 | 5.6 | -0 | No erosion-looks untested | No erosion-looks untested | Minimal local erosion some melt deposits | |
| 124 | 87 | 2.5 | 5.6 | 59.4 | Minimal pebbling | Minimal pebbling | Minimal pebbling some melt deposits | |
| 104 | 67 | 2.5 | 8.1 | -0 | Finest machine marks gone very thin scale formation | Most machine marks present minimal melt | Most machine marks present minimal melt | |
| 125 | 88 | 2.5 | 8.1 | 87.2 | Machine marks gone very slight pebbling | Noticeable pebbling some melt | Pebbling-minimal melt -melt deposits | |
| 99 | 62 | 5.0 | 8.1 | -0 | No pebbling melt at machine marks | No erosion looks untested | Minimal erosion | |
| 100 | 63 | 5.0 | 8.1 | 38.9 | Smooth-dendritic marks some melt deposits | Pronounced dendrites some cracks-no pebbling | Pronounced dendrites no pebbling | |
| 103 | 66 | 2.5 | 17.2 | -0 | No erosion looks untested | Minimal erosion | Minimal erosion | |
| 102 | 65 | 2.5 | 17.2 | 37.7 | Smooth-no pebbling some melt deposits | Smooth-dendritic turbulent waves of melt | Turbulent waves of melt no pebbling | |



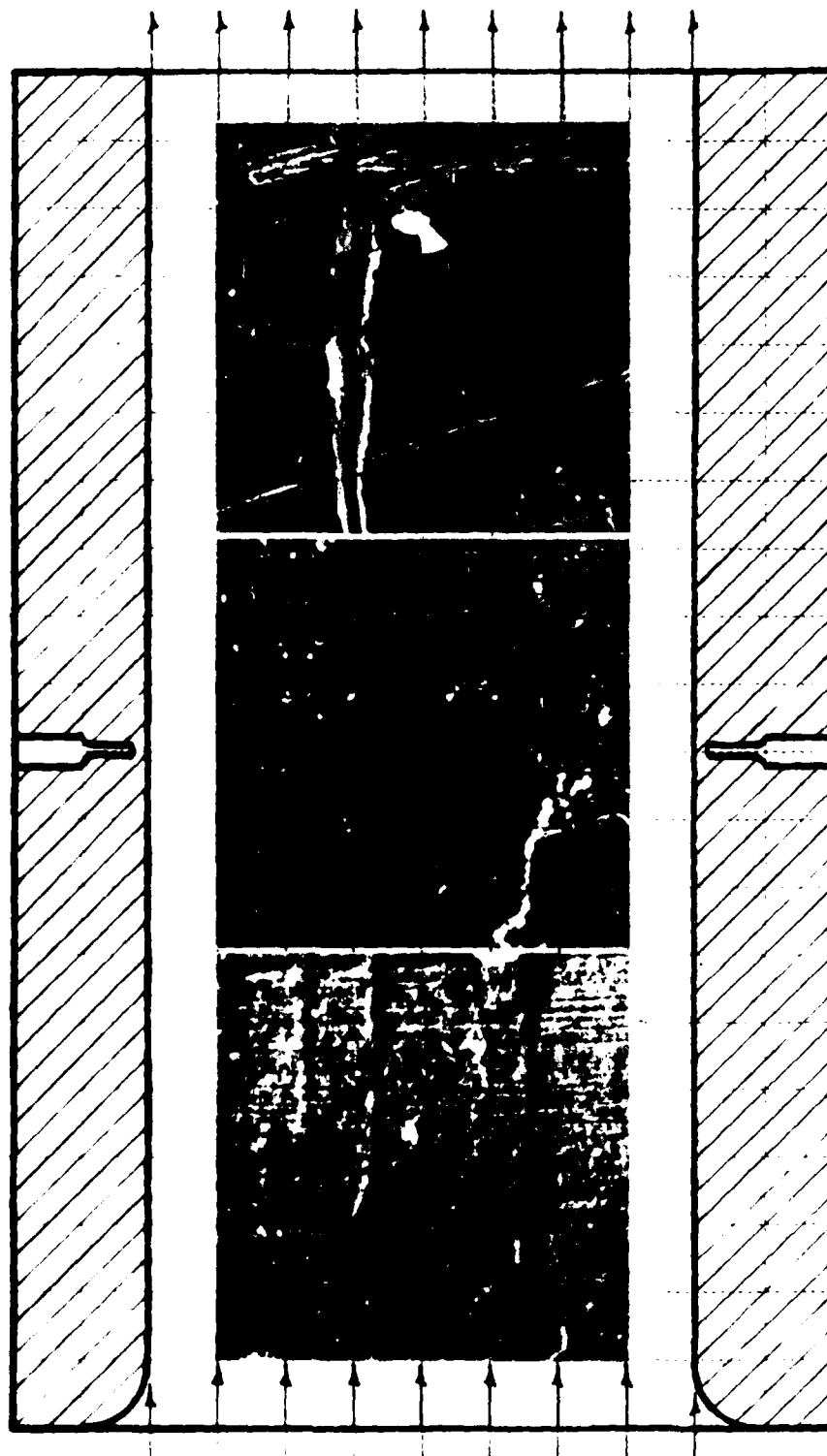
SEM PHOTOMICROGRAPHS (1000X) OF THE 4340 STEEL SPECIMEN'S FLOW SURFACE

Figure 13. Surface characteristics of specimen no. 79 (test no. 116) after near negligible mass loss in a 5% CO / 2.5% CO₂ atmosphere at 256 MPa, 3380°K



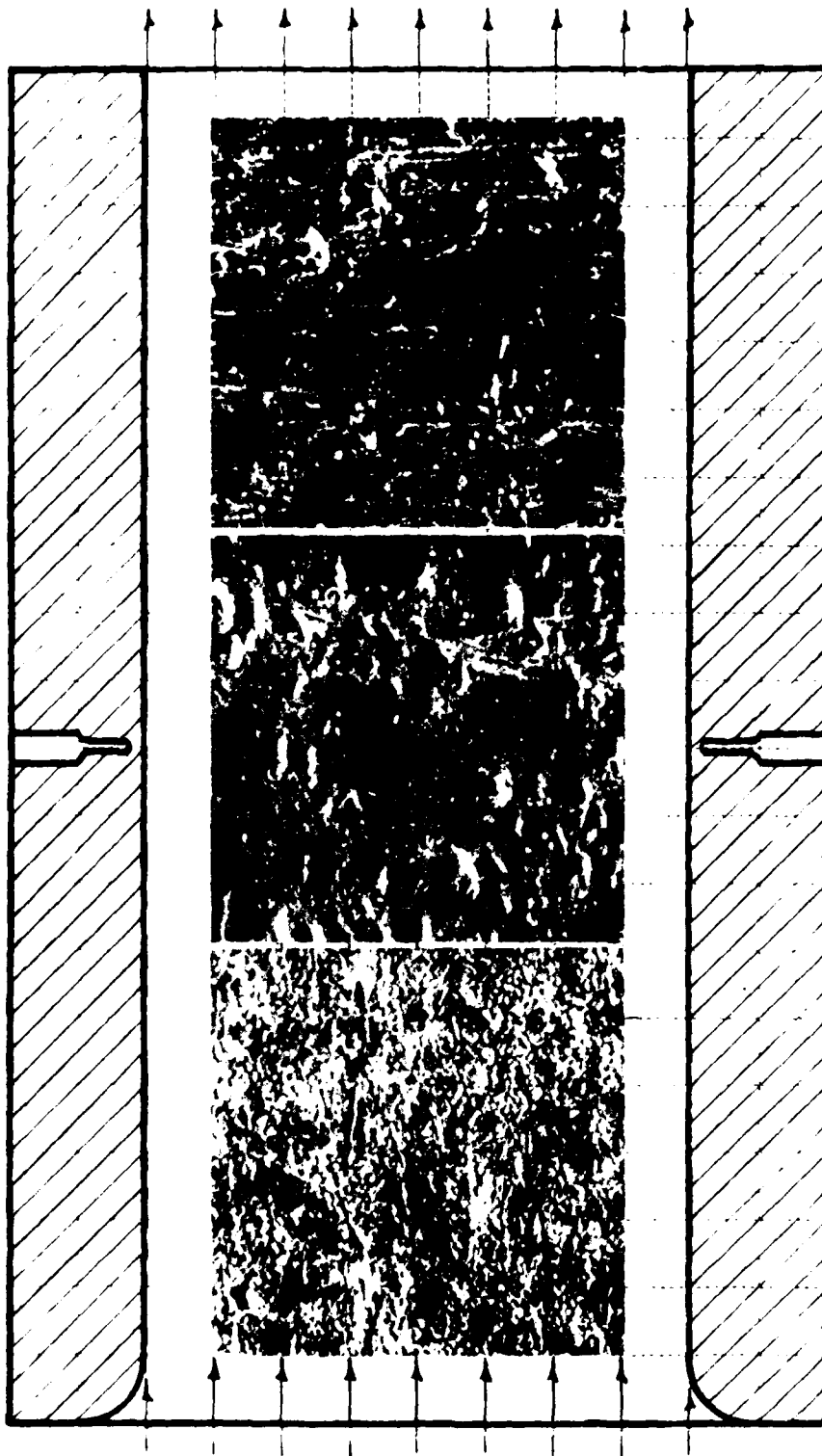
SEM PHOTOMICROGRAPHS (1000X) OF THE 4340 STEEL SPECIMEN'S FLOW SURFACE

Figure 14. Surface characteristics of specimen no. 77 (test no. 114) after 59.5 milligram mass loss in a 5% CO / 2.5% CO₂ atmosphere at 322 MPa, 3590°K



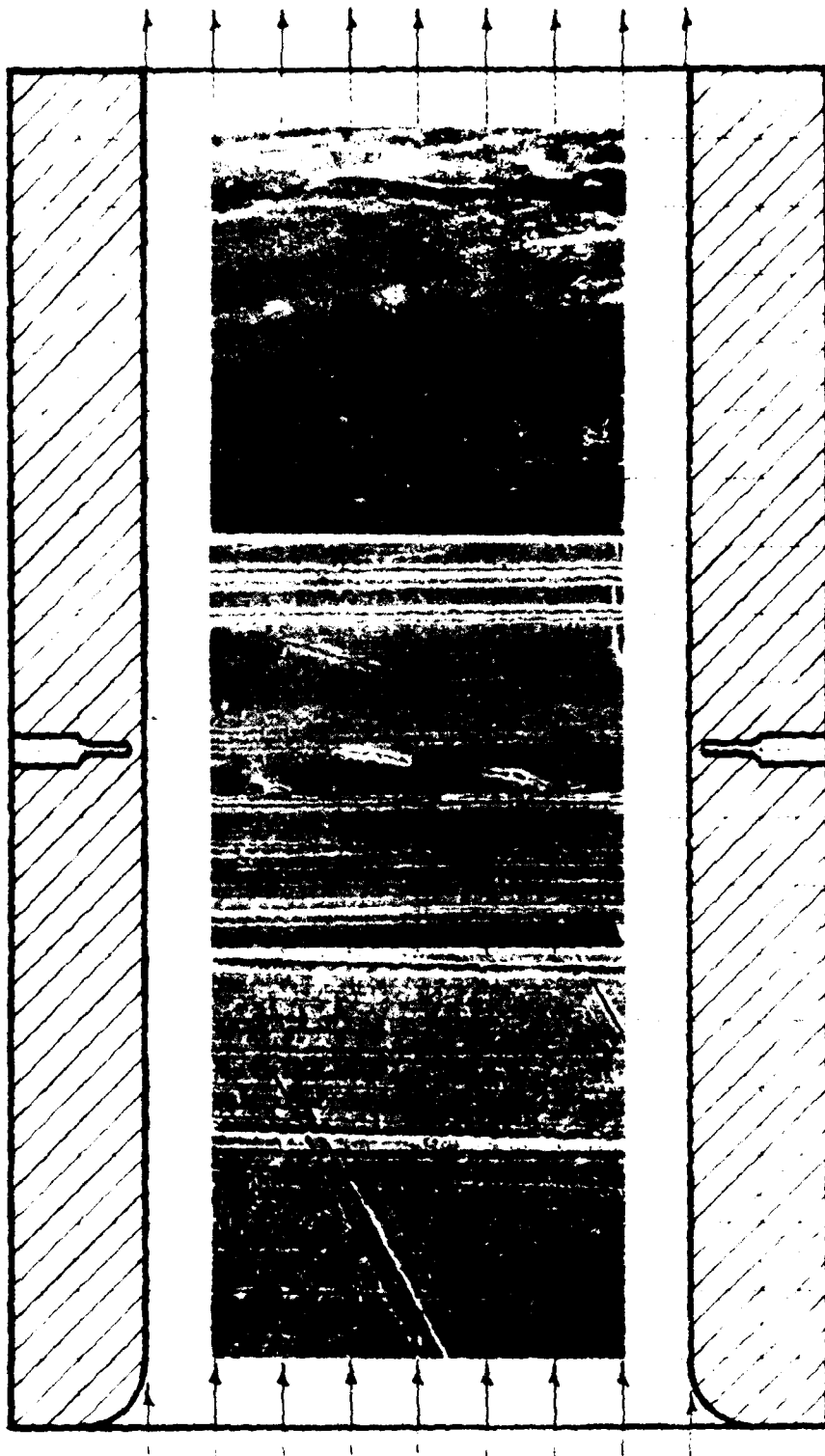
SEM PHOTOMICROGRAPHS (1000X) OF THE 4340 STEEL SPECIMEN'S FLOW SURFACE

Figure 15. Surface characteristics of specimen no. 85 (test .122) after near negligible mass loss in a 10% CO / 5% CO₂ atmosphere at 313 MPa, 3430°K



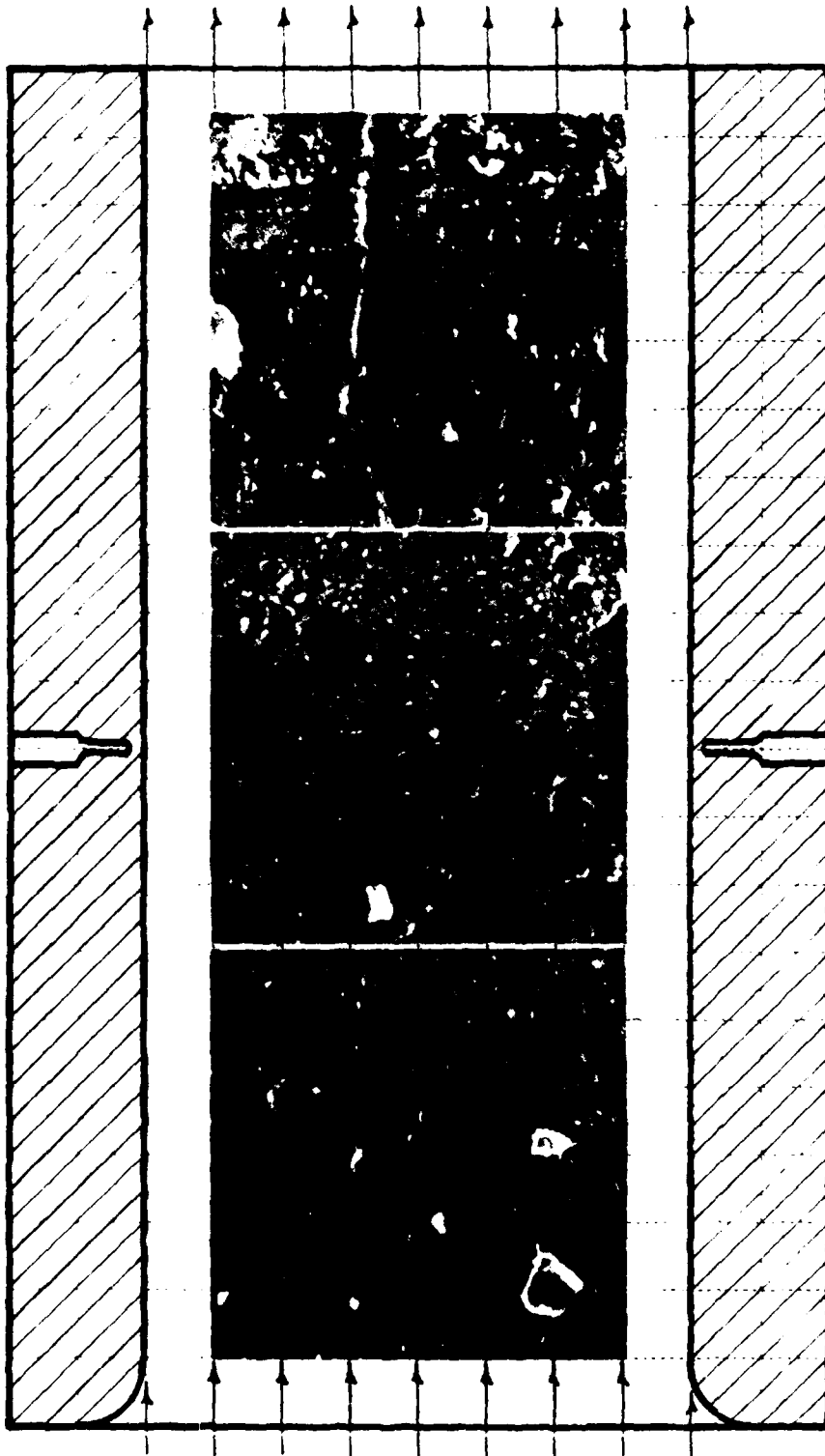
SEM PHOTOMICROGRAPHS (1000X) OF THE 4340 STEEL SPECIMEN'S FLOW SURFACE

Figure 16. Surface characteristics of specimen no.81 (test no.118) after 82.0 milligram mass loss in a 10% CO / 5% CO₂ atmosphere at 325 MPa, 3460°K



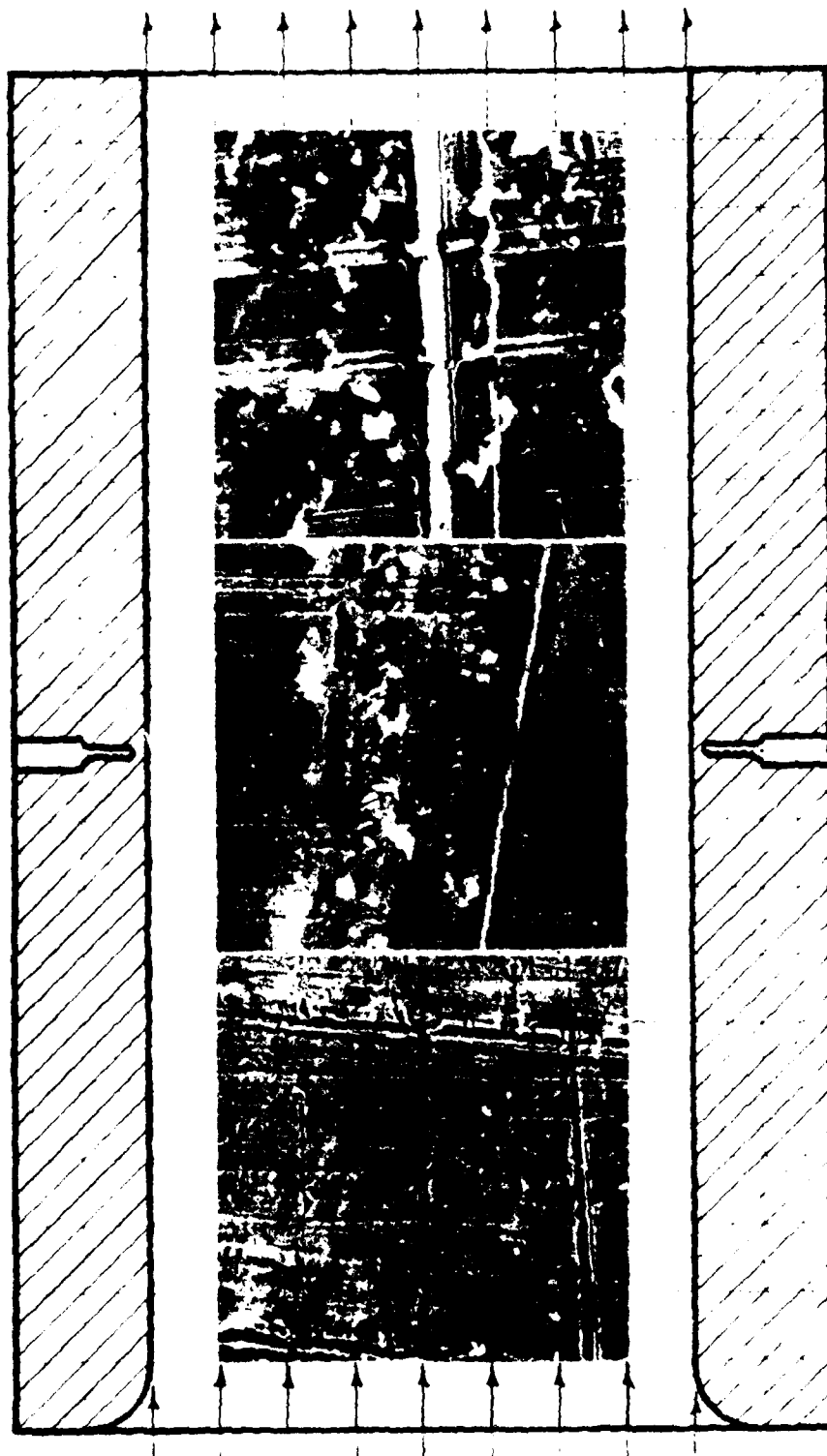
SEM PHOTOMICROGRAPHS (1000X) OF THE 4340 STEEL SPECIMEN'S FLOW SURFACE

Figure 17. Surface characteristics of specimen no. 74 (test no. 111) after near negligible mass loss in a 9% CO / 2.5% CO₂ atmosphere at 236 MPa, 3310°K



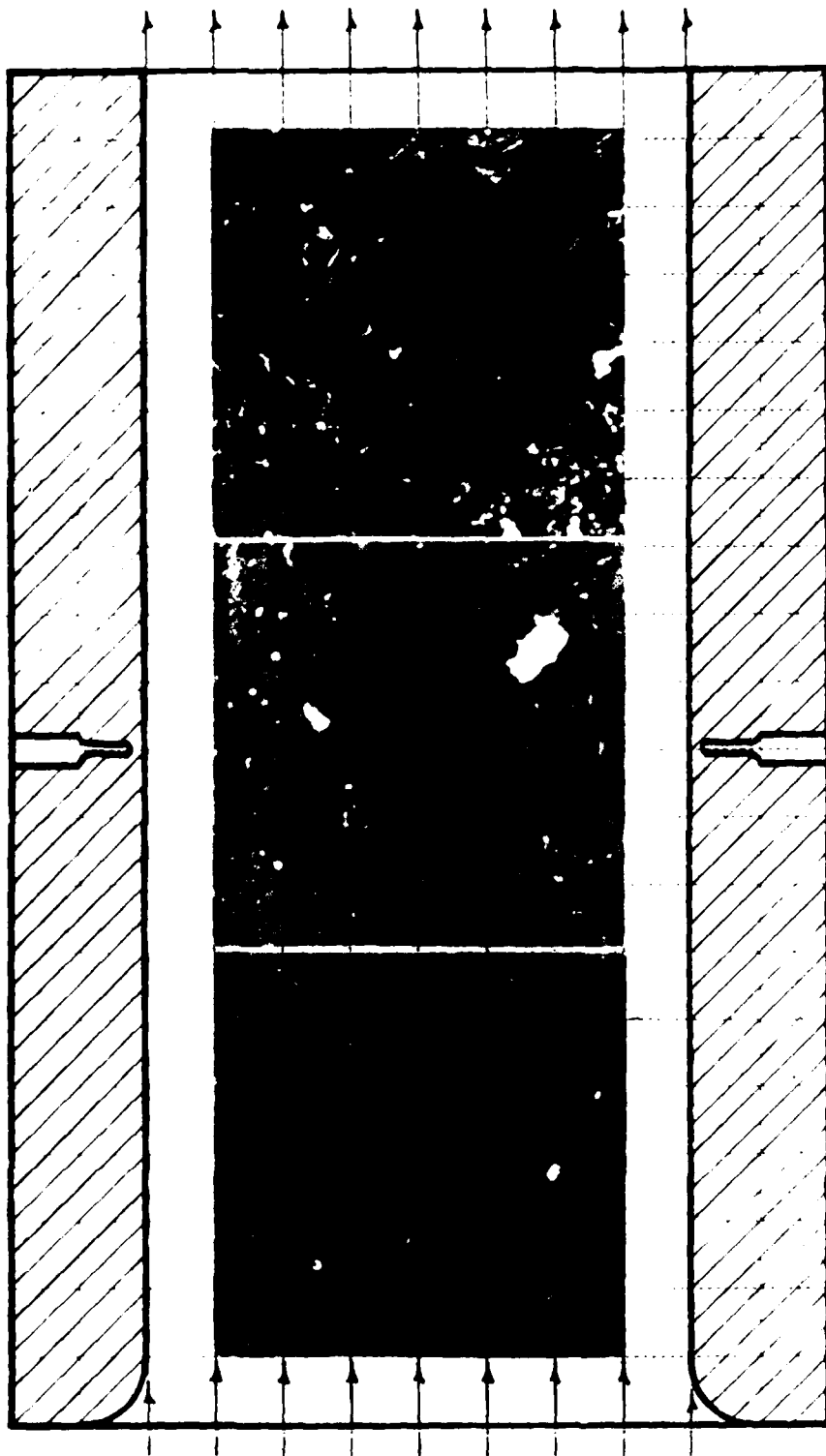
SEM PHOTOMICROGRAPHS (1000X) OF THE 4340 STEEL SPECIMEN'S FLOW SURFACE

Figure 18. Surface characteristics of specimen no. 86 (test no. 123) after 67.9 milligramme mass loss in a 9% CO / 2.5% CO₂ atmosphere at 327 MPa, 3620°K



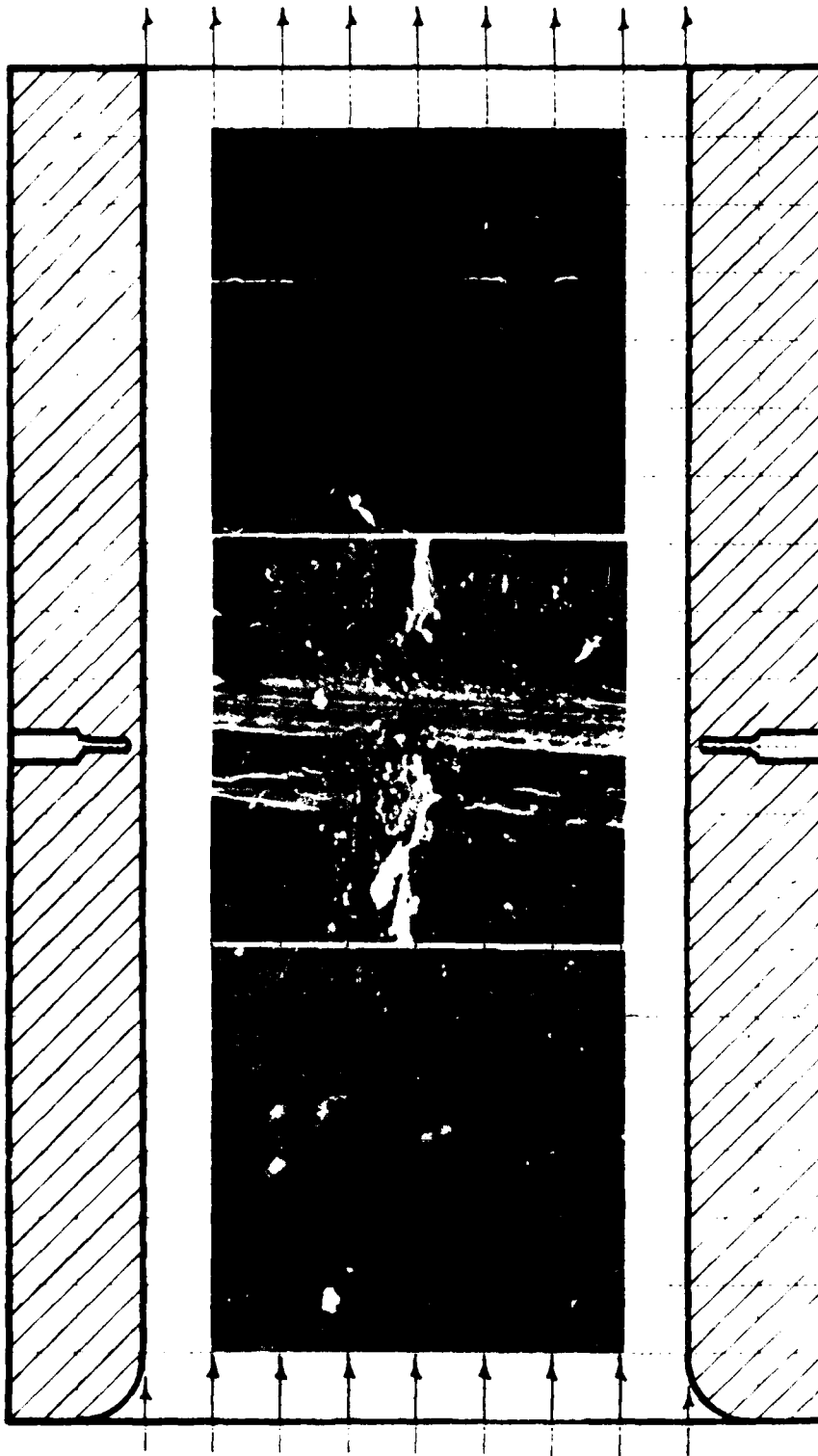
SEM PHOTOMICROGRAPHS (1000X) OF THE 4340 STEEL SPECIMEN'S FLOW SURFACE

Figure 19. Surface characteristics of specimen no. 71 (test no. 108) after near negligible mass loss in a 14% CO / 2.5% CO₂ atmosphere at 203 MPa, 317B°K



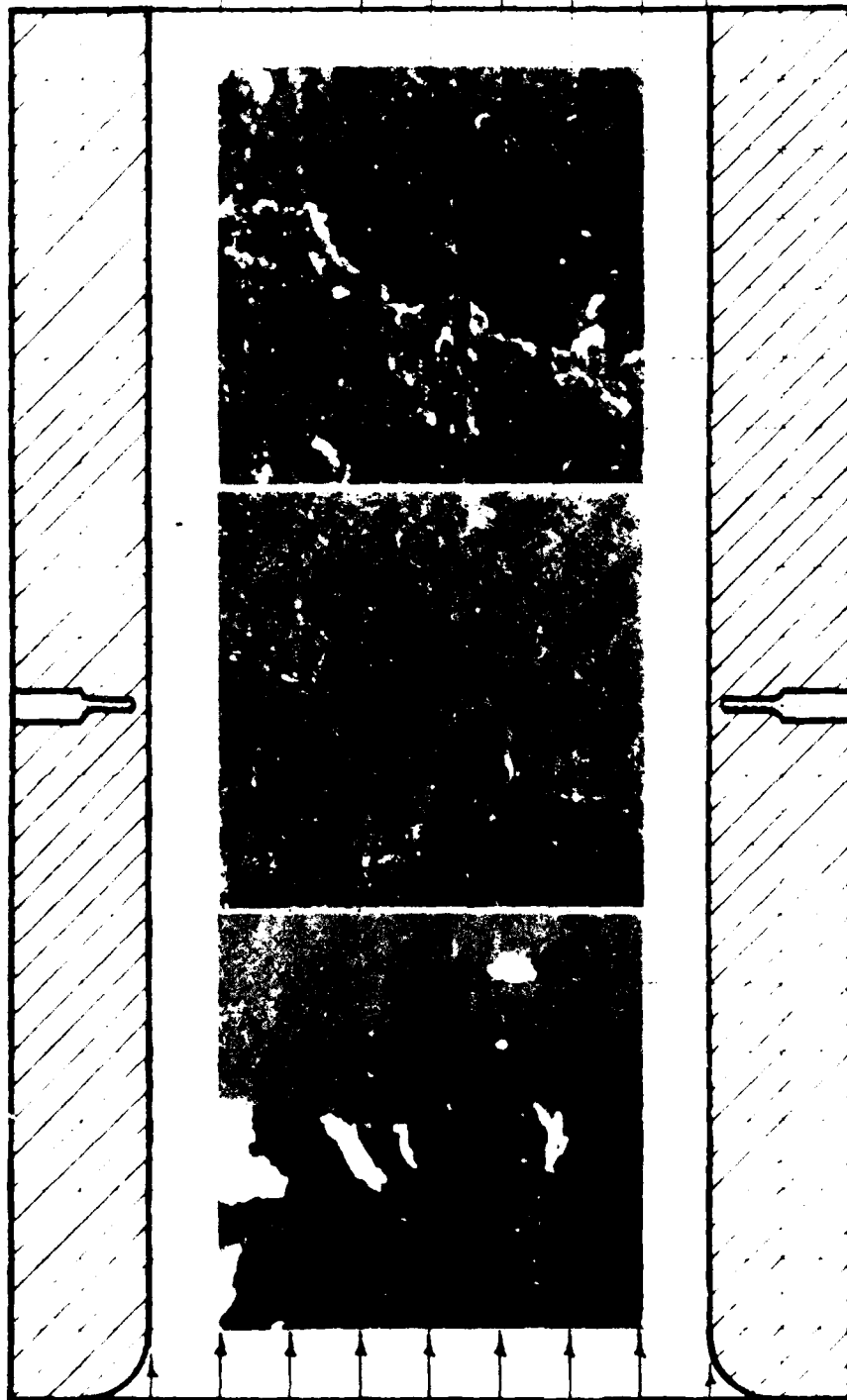
SEM PHOTOMICROGRAPHS (1000X) OF THE 4340 STEEL SPECIMEN'S FLOW SURFACE

Figure 20. Surface characteristics of specimen no. 87 (test no. 124) after 59.4 milligrams mass loss in a 14% CO / 2.5% CO₂ atmosphere at 321 MPa, 3600°K



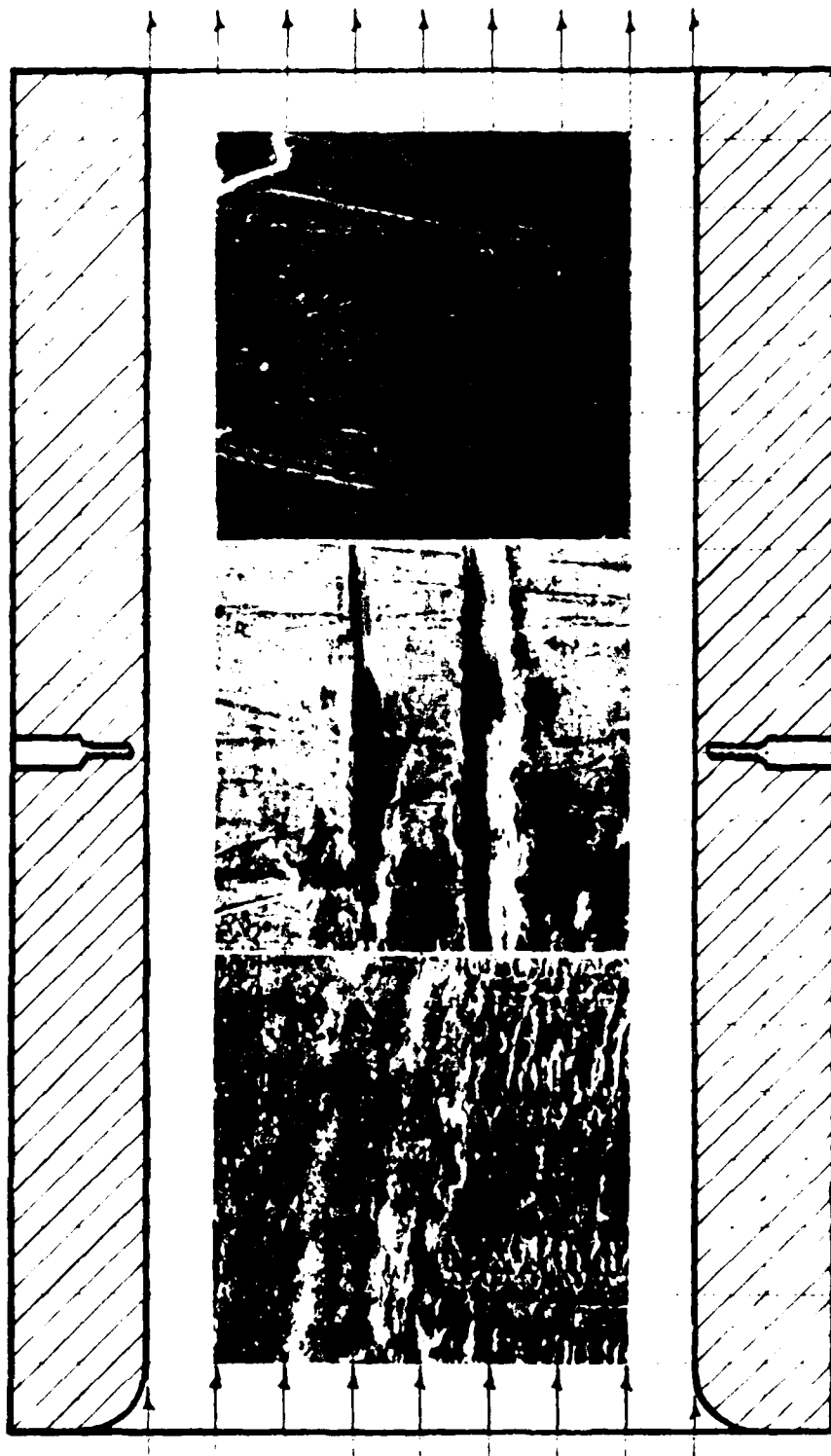
SEM PHOTOMICROGRAPHS (1000X) OF THE 4340 STEEL SPECIMEN'S FLOW SURFACE

Figure 21. Surface characteristics of specimen no. 67 (test no. 104) after near negligible mass loss in a 20.5% CO / 2.5% CO₂ atmosphere at 245 MPa, 3340°K



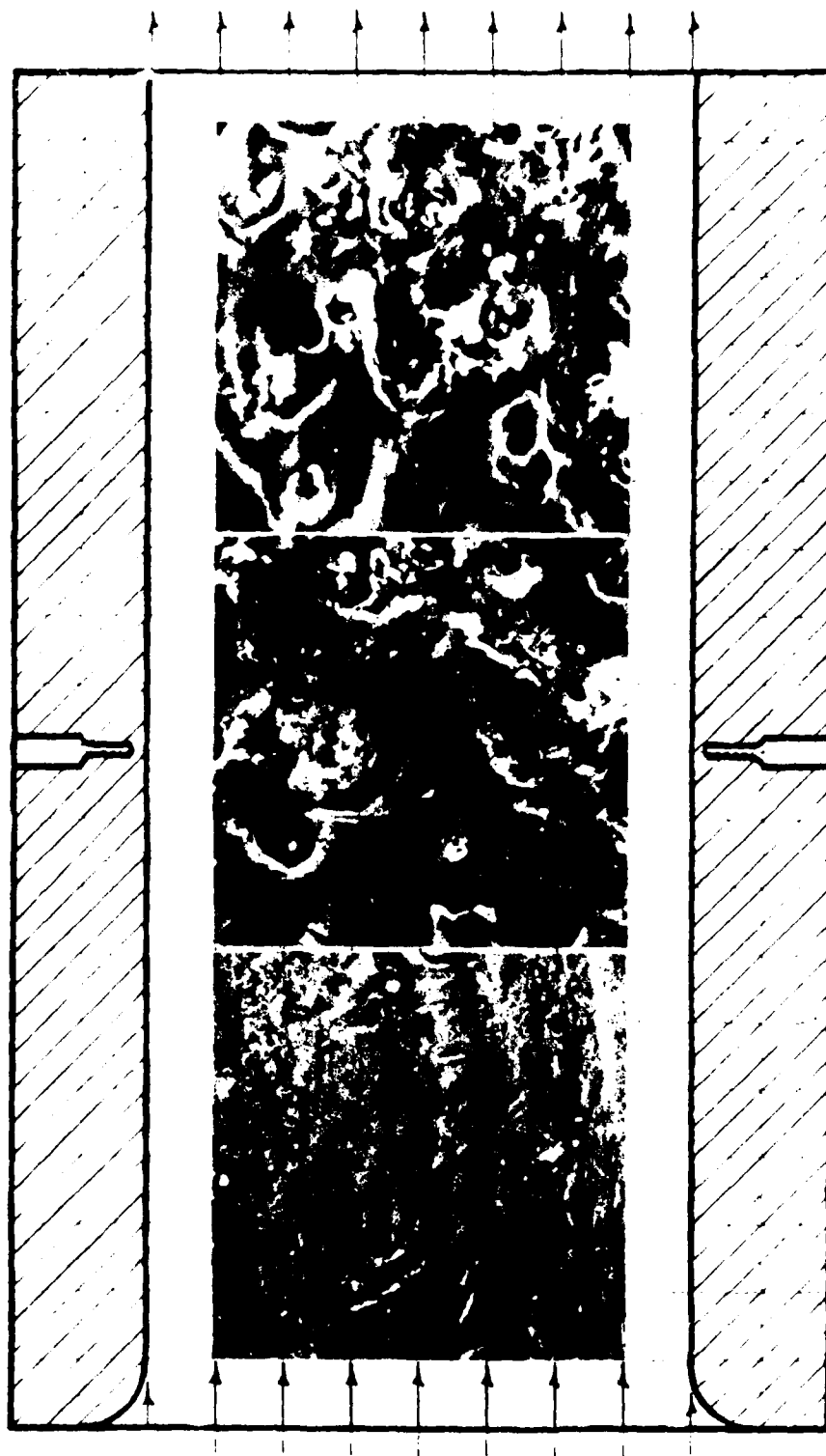
SEM PHOTOMICROGRAPHS (1000X) OF THE 4340 STEEL SPECIMEN'S FLOW SURFACE

Figure 22. Surface characteristics of specimen no. 88 (test no. 125) after 87.2 milligram mass loss in a 20.5% CO / 2.5% CO₂ atmosphere at 318 MPa, 3620°K



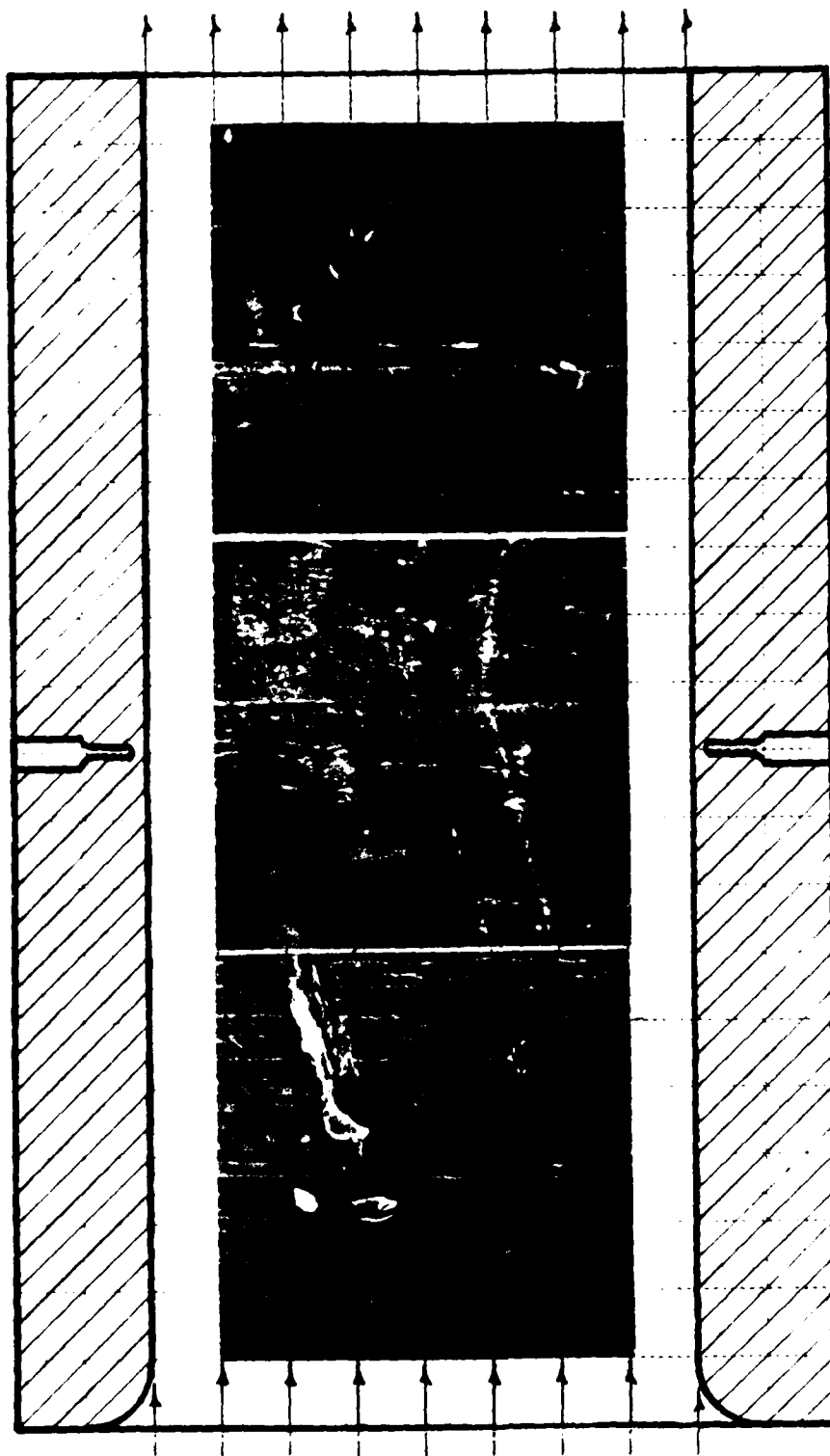
SEM PHOTOMICROGRAPHS (1000X) OF THE 4340 STEEL SPECIMEN'S FLOW SURFACE

Figure 23. Surface characteristics of specimen no. 62 (test no. 99) after near negligible mass loss in a 40.5% CO₂ / 5% CO atmosphere at 261 MPa, 3250°K



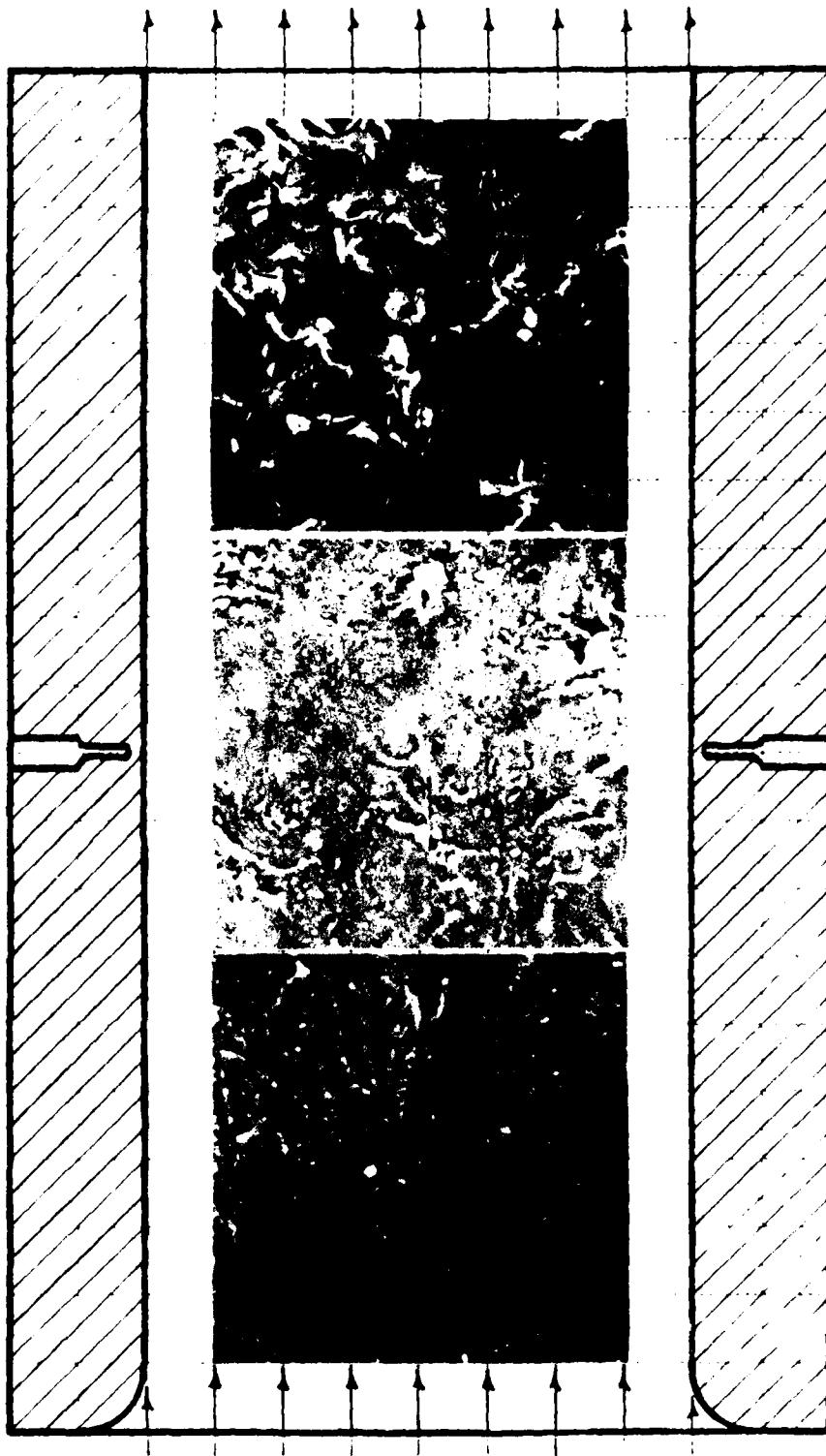
SEM PHOTOMICROGRAPHS (1000X) OF THE 4340 STEEL SPECIMEN'S FLOW SURFACE

Figure 24. Surface characteristics of specimen no. 63 (test no. 100) after 38.9 milligrams mass loss in a 40.5% CO / 5% CO₂ atmosphere at 293 MPa, 3360°K



SEM PHOTOMICROGRAPHS (1000X) OF THE 4340 STEEL SPECIMEN'S FLOW SURFACE

Figure 25. Surface characteristics of specimen no. 66 (test no. 103) after near negligible mass loss in a 43% CO / 2.5% CO₂ atmosphere at 261 MPa, 3380°K



SEM PHOTOMICROGRAPHS (1000X) OF THE 4340 STEEL SPECIMEN'S FLOW SURFACE

Figure 26. Surface characteristics of specimen no. 65 (test no. 102) after 37.7 milligramme mass loss in a 43% CO / 2.5% CO₂ atmosphere at 268 MPa, 3410°K

V. CONCLUSIONS

The objective of this program has been to investigate the potential of various concentrations and concentration ratios of carbon monoxide and carbon dioxide, which make up nearly half of all propellant gases, to erode 4340 gun barrel steel. As such, the program deals exclusively with CO-CO₂ equilibrium, sometimes referred to as the "soot" equation. It does not study the "water-gas" reaction equilibrium, nor the presence of catalytic trace compounds, nor unique barrel material properties; all of which effect the CO-CO₂ activity in the complete gun erosion system. The overall conclusion from this and previous studies would, therefore, have to be that much more research needs to be carried out, particularly in regard to the unstudied mechanisms cited above, in order to complete the gun erosion picture.

In regard to the present program which dealt with erosion of 4340 steel in varying CO/CO₂ atmospheres, the following conclusions were reached.

1. CO/CO₂ ratios of 2.0 to 5.6 exhibit minimal erosion above the previously established "inert" level and minimal dependency on CO or CO₂ concentration for their erosion potential which is indicative of time dependent reactions. There is some indication that, of the three CO/CO₂ mole ratios used in this program and lying in the 2.0 to 5.6 range, the 5.6 CO/CO₂ ratio is the least susceptible to increasing erosiveness with increasing temperature. This indication implies that 5.6 most closely approaches the theoretical neutral activity value of all CO/CO₂ ratios investigated.
2. CO/CO₂ ratios of 8.1 and 17.2 shifted the erosion threshold to less severe flow conditions than those of the lower CO/CO₂ ratio and previous "inert" cases. These higher CO/CO₂ ratios were also more influenced by the absolute concentrations of the two gases, in terms of enhancing their erosion potential.

VI. REFERENCES

1. C.C. Morphy and E.B. Fisher, "The Role of Carburization in Gun Barrel Erosion and Cracking," ARRADCOM Contractor Report ARBRL-CR-00459, Calspan Corporation, Buffalo, New York, July 1981. (AD A102625)
2. E.B. Fisher and C.C. Morphy, "The Role of Oxygen in Gun Barrel Erosion and Cracking--A Shock Tube Gun Investigation," ARRADCOM Contractor Report ARBRL-CR-00427, Calspan Corporation, Buffalo, New York, April 1980. (AD A085720)
3. F.C. Kracek, "Properties of Powder Gas," Hypervelocity Guns and The Control of Gun Erosion, Summary Technical Report of Division 1, NDRC, Vol. 1, Washington, D.C., 1946, pp. 21-53.
4. J.N. Hobstetter, "Erosion of Gun Steel by Different Propellants," Hypervelocity Guns and The Control of Gun Erosion, Summary Technical Report of Division 1, NDRC, Vol. 1, Washington, D.C., 1946, pp. 508-528.
5. R.C. Evans, F.H. Horn, E.M. Shapiro, and R.L. Wagner, "The Chemical Erosion of Steel by Hot Gases under Pressure," J. Physical and Colloidal Chemistry, Vol. 51, 1947, pp. 1404-1429.
6. J.C.W. Frazer, F.H. Horn, and R.C. Evans, "Vent Plug Erosion by the CO-CO₂ Gas System," NDRC Contractor Report A-310, Johns Hopkins University, Baltimore, MD, October 1944.
7. R.W. Geene, J.R. Ward, T.L. Brosseau, A. Niiler, R. Kirkmire, and J.J. Rocchio, "Erosivity of a Nitramin Propellant," Technical Report ARBRL-TR-02094, ARRADCOM, Aberdeen Proving Ground, MD, August 1978. (AD A060590)
8. J.R. Ward and R.W. Geene, "Erosivity of a Nitramine Propellant with a Flame Temperature Comparable to M30 Propellant," Technical Report ARBRL-MR-02926, ARRADCOM, Aberdeen Proving Ground, MD, June 1979. (AD A074546)
9. R. Geene, B. Grollman, A. Niiler, A. Rye, and J.R. Ward, "Nitramine Propellant Erosivity-III," Technical Report ARBRL-TR-02278, ARRADCOM, Aberdeen Proving Ground, MD, December 1980. (AD A096878)
10. F.A. Vassallo, "A Report On the Erosivity of a Nitramine Propellant When Fired in a 105mm M68 Gun Tube," ARRADCOM Contractor Report DAAK10-80-M-3150, Calspan Corporation, Buffalo, New York, February 1981.
11. A.J. Bracuti, L. Bottei, J.A. Lannon, and L.H. Caveny, "Evaluation of Propellant Erosivity with Vented Erosion Apparatus," 1980 JANNAF Propulsion Meeting, Vol. I, CPIA, Johns Hopkins University, Laurel, MD, March 1980.
12. F.A. Vassallo, "Thermal and Erosion Phenomenology in Medium Caliber Anti-Armor Automatic Cannons (MC-AAAC)," 1980 JANNAF Propulsion Meeting, Vol. 1, Chemical Propulsion Information Agency, Johns Hopkins University, Laurel, MD, March 1980.

13. F.A. Vassallo, "Mathematical Models and Computer Routines Used in Evaluation of Caseless Ammunition Heat Transfer," Calspan Report GM-2948-Z-1, Calspan Corporation, Buffalo, New York, June 1971.

APPENDIX A

SHOCK TUBE GUN COMPUTER SIMULATION

APPENDIX A
SHOCK TUBE GUN COMPUTER SIMULATION

Model Description

The mathematical model described in this Appendix simulates the operation of the Shock Tube Gun. The simulation provides a complete description of the entire cycle of the Shock Tube Gun, beginning with release and subsequent acceleration of the piston by the high pressure driver gas. As the piston is accelerated through the driven tube, the simulation computes the increase in pressure and temperature of the test gas. In addition, the simulation evaluates the total temperature, pressure and density in the test gas collection chamber or plenum, and computes the flow through the test specimen. The heat flux to the specimen, the resulting temperature history at a location on the surface of the specimen and the temperature distribution in the specimen normal to the surface are also calculated. Finally, the simulation calculates the travel of a projectile through the barrel.

The objective of this code is to provide a means for calculating test conditions for the purpose of establishing the initial driver pressure and gas mixture. Differences in the ballistic cycle of the Shock Tube Gun due to gas composition are reflected through differences in pressure and total heat input. A primary use of the code is to help distinguish between erosion due to melting and that due to chemical effects. This is done through computation of the convective heating to the sample without chemistry which provides a means for comparing tests within a test matrix on an equal basis with respect to the inherent flow heating of the test gas. Thus, excess material removal from one gas mixture in comparison to another is likely due to chemical effects. This, in turn, allows estimates to be made of the effective heat input due to chemical effects. This can be done by comparing the heat input at the onset of erosion, or at points of equal erosion between inert and chemically active gases.

The major assumption applied with formulating the code was that of quasi-steady operation. That is, pressure waves and other unsteady aspects of the event are not calculated. The pressure is assumed to be constant throughout the driver system and throughout the driven tube at any instant of time during the compression cycle. The individual gas constituents are assumed to be mixed uniformly. Furthermore, the parameters used by the van der Waals equation of state for an imperfect gas and the temperature dependency of specific heat are assumed to be satisfied by linear averaging, according to mole fraction.

The other limiting assumption that is currently employed in this code is that of a frozen gas composition; i.e., the initial gas composition is assumed to be maintained throughout the ballistic cycle. This assumption influences the resulting temperature and pressures to some extent in cases where chemical reactions and dissociation become important.

Piston Motion

The piston motion is evaluated by applying a force balance on the piston. The accelerating force is applied by the high-pressure nitrogen driver, 500 to 700 psi, on the upstream side of the piston. The driven gas on the downstream side of the piston is initially at atmospheric pressure. It is assumed that no gas leaks past the piston. This is essentially verified, at least initially, by the ability to evacuate the driven gas chamber. The nitrogen gas is represented by the ideal gas equation of state. The driver conditions are calculated from conservation of energy principles which are used to continually evaluate the amount of energy that is being transferred from the gas to the piston. As cited previously, this calculation is quasi-steady in that the unsteady expansion aspects are not considered and the pressure is assumed to be constant throughout the driver system.

The driver gas (nitrogen) properties are assumed to be constant over the range of temperature and pressure encountered during the compression cycle and are specified by:

Equation of state gas constant, $R = 55.0 \text{ ft/lbf/lbm}^\circ\text{R}$

Specific heat at constant volume, $c_v = 0.177 \text{ Btu/lbm}^\circ\text{R}$

Specific heat at constant pressure, $c_p = 0.248$, and

Ratio of specific heats, $\gamma = 1.4$

The assumption of a perfect seal at the piston infers the existence of constant gas mass in the driver system during the cycle so that

$$p_D = \frac{m_D R T}{V} \quad (\text{A-1})$$

where R and m are constants, the driver volume, V , is expressed in terms of piston travel and the initial volume by

$$V = V_0 + A_T X_p \quad (\text{A-2})$$

where A_T is the driver tube bore area.

Gas temperature is expressed in terms of internal energy where

$$E = c_v m_D T \quad (\text{A-3})$$

and the energy change resulting from work expended through piston motion is

$$\Delta E = p_D A_T \Delta x_o / 778. = c_v m_D \Delta T \quad (\text{A-4})$$

The driver gas is initially at room temperature and it is assumed that the small temperature decrease during the cycle is not influenced by heat transfer.

Piston motion is evaluated by applying a force balance across the piston, taking into account the frictional drag.

$$F = A_t(p_D - p_T) - D \quad (A-5)$$

where p_D and p_T are the respective pressures of the driver and test gases, and D is the frictional drag of the piston which is expressed in terms of piston velocity by

$$D = kV_p \quad (A-6)$$

Piston acceleration, velocity and travel are then evaluated.

$$a_p = \frac{F}{M} \quad (A-7)$$

$$\Delta V_p = a_p \Delta t \quad (A-8)$$

$$\Delta x_p = \frac{a_p \Delta t^2}{2} + v_o \Delta t \quad (A-9)$$

Test Gas Compression

The compression of the test gas occurs as a result of piston motion. Energy that is added by virtue of the compression is calculated from the conservation of energy equation. The work done by the piston on the test gas during this compression is one term in this conservation of energy equation. Other terms include heat loss to the wall of the tube, which becomes important as the gas temperature rises. The other important equation is conservation of mass. The test chamber is not a closed chamber but contains an exhaust port at the downstream end where the test sample is located. Test gas is allowed to flow from the test chamber through the test sample. Therefore, the mass in the system is not constant by virtue of mass and energy flow from the driven tube and plenum chamber through the test sample. Terms in the conservation of energy and mass equations reflect this mass and energy loss.

The equation of state that applies to the test gas is the van der Waals equation which includes terms to express the nonlinear relationship between pressure, density and temperature. The terms for this equation are determined, as mentioned previously, by a linear averaging of the mole fraction of the test gas constituents.

The test gas specific heat is also assumed to be for non-perfect gas and is expressed in terms of a linear function of the gas temperature. The coefficients in this expression are also linear averages of the mole fraction of the test gas compositions. The test gas specific heat is expressed

in terms of a secant function in which the product of the specific heat and the temperature yield the internal energy. This is different from the normal expression of specific heat, a tangent function, whereby the product integral of specific heat and temperature yield the internal energy. The technique used here provides a rather simple yet effective means for evaluating the internal energy in a finite difference scheme with many time steps.

The van der Waals equation of state for the test gas:

$$p = \frac{RT}{v - \beta} + \frac{\alpha}{v^2} \quad (A-10)$$

where $\frac{\alpha_i}{\beta_i} = \frac{27}{8} RT_{ci}$ and $\frac{\alpha_i}{\beta_i^2} = 27p_{ci}$

v is the specific volume, and T_{ci} and p_{ci} are the critical temperature and pressure for the i th gas constituent. α and β are the average quantities based on the mole fraction of the i th constituent.

The specific heat at constant volume is

$$c_v = ((c_{v0} + \sum_i X_{gi} c_{vTi} (T - 460)^{e_i})T - \frac{\alpha p}{778}) \frac{1}{T_i} \quad (A-11)$$

where c_{v0} and c_{vTi} are the intercept and slope of the temperature-dependent specific heat, X_{gi} is the mole fraction of the i th constituent, and e_i is the temperature exponent in the curve-fitting relationship which includes temperature and high density effects.

The test chamber mass balance is given by

$$m_T = m_{T0} - \Delta m \quad (A-12)$$

where Δm is the mass flow through the test sample. Initially this flow is assumed to be negligible and the test chamber and barrel volumes are lumped together. When the projectile velocity exceeds 100 ft/sec, the calculation of flow through the test sample is initiated. This computation involves determination whether sonic or subsonic flow conditions exist within the test sample. The sonic static pressure is given by

$$p^* = p_1 \left(1 + \frac{\gamma - 1}{2}\right)^{-\gamma/(\gamma - 1)} \quad (A-13)$$

where p_1 is the test chamber pressure.

If p^* is greater than the barrel pressure, p_2 , (downstream from the test sample) then sonic conditions exist and

$$\Delta m = p^* A_{12} \left(\frac{g}{RT^*} \right)^{1/2} \Delta t \quad (A-14)$$

where A_{12} is the test sample flow area, T^* is the sonic static temperature, and Δt is the computation time interval.

If subsonic conditions exist,

$$\Delta m = 8.02 A_{12} \left((p_1 - p_2) \frac{c_1}{RT_1} \right)^{1/2} \Delta t \quad (A-15)$$

which is the equation for flow through a venturi in terms of the upstream and downstream line pressures.

The change in internal energy in the chamber over the calculation time interval is given by

$$\Delta E_1 = \frac{p_1 A_1 \Delta x}{778} - c_v \Delta m T_1 \quad (A-16)$$

which represents the compression work due to the piston and the loss in enthalpy due to flow through the test sample. Heat transfer losses in the driven tube and chamber are not included in this analysis at present. The gas chamber temperature is defined by

$$T_1 = E_1 / c_v m_1 \quad (A-17)$$

where E_1 is the current value of internal energy.

Test Sample Flow

The test sample contains a straight cylindrical channel with a radiused entrance. The flow through the channel is computed by either sonic or subsonic conditions depending on the pressure at the inlet and outlet to the sample. Code calculations provide the static flow conditions of pressure, temperature, and density in addition to the flow velocity over the channel surface of the sample. These conditions are in turn used in an equation that expresses turbulent heat flux to a flat plate. The heat flux is computed and then summed to yield a current level of total heat input. The heat flux to the surface is also applied to an unsteady heat conduction routine in which the surface temperature and the temperature distribution in the test sample are evaluated. These calculations are all performed within the same time step of the overall finite difference calculation.

The technique used to calculate heat flux to the test sample surface requires the flow velocity, density, and viscosity. The density and viscosity are evaluated on the basis of a reference temperature that takes into account the temperature profile resulting from the boundary layer velocity distribution and the sample surface temperature.

Free stream velocity is defined as

$$U_e = [5 \times 10^4 \gamma c_v (T_1 - T_e)]^{1/2} \quad (A-18)$$

where T_e , the free stream static temperature is

$$T_e = T_1 [1 + (\frac{\gamma - 1}{2}) M^2]^{-1}$$

and M , the Mach number of flow through the test sample is given by

$$M = \left(\left[\left(\frac{p_1}{p_s} \right)^{\frac{\gamma - 1}{\gamma}} - 1 \right] \frac{2}{\gamma - 1} \right)^{1/2} \quad (A-19)$$

where p_s equals the sonic static pressure if $M = 1$, or the downstream pressure, p_2 , if the flow is subsonic.

Density and viscosity are, respectively, given as

$$\rho_{ref} = p_s (\beta p_s + R T_{ref})^{-1} \quad (A-20)$$

$$\mu = 7 \times 10^{-7} T_{ref}^{1.5} (T_{ref} + 198)^{-1}$$

where T_{ref} , a reference temperature is defined as

$$T_{ref} = (T_e + T_{SAMP})/2 + 4.4 \times 10^{-6} \frac{U_e^2}{c_v \gamma} \quad (A-21)$$

and T_{SAMP} is the test sample surface temperature.

Turbulent flat plate heat flux at the location of the in-wall thermocouple then equals

$$Q = 0.052 (\rho_{ref} U_e)^{0.8} \mu^{0.2} c_v \gamma (T_1 - T_{SAMP}) \quad (A-22)$$

The sample surface temperature, T_{SAMP} , is determined from the one-dimensional unsteady state heat conduction equation,

$$\frac{\partial T}{\partial t} = \alpha \frac{\partial^2 T}{\partial x^2} \quad (A-23)$$

with the surface boundary condition,

$$Q = k \frac{dT}{dx} \quad (A-24)$$

for $x = 0$, where Q is the heat flux to the sample surface. This equation does not consider the effects of cylindrical geometry.

A finite difference technique using a geometrical node grid spacing was incorporated into the Calspan code to solve the unsteady heat conduction equation. The general finite difference relationship is given by

$$\frac{\Delta T_i}{\Delta t} = \frac{2\alpha}{(F+1)\Delta x_{i-1}^2} \left(T_{i-1} - \frac{F+1}{F} T_i + \frac{1}{F} T_{i+1} \right) \quad (A-25)$$

where α is the thermal diffusivity

T is the temperature rise

t is the time interval

Δx_{i-1} is the thickness of the $i-1$ grid

F is the geometrical multiplier with the thickness of the i th grid being F times that of the $i-1$ grid.

The exposed surface boundary condition is satisfied by first determining a fictitious temperature in free space,

$$T_0 = 2q \frac{\Delta x_1}{k} + T_2 \quad (A-26)$$

This temperature is then used to establish the surface temperature rise by

$$\frac{\Delta T_1}{\Delta t} = \frac{\alpha}{\Delta x_1^2} (T_0 - 2T_1 + T_2) \quad (A-27)$$

Barrel Flow and Projectile Motion

The flow through the barrel is expressed as an input of mass and energy to the volume between the test sample and the projectile. As mass and energy are accumulated, this is expressed in terms of pressure and temperature, which in turn provides the accelerating force for the projectile. In this calculation, the quasi-steady assumption of the previous calculation is relaxed by allowing pressure acting on the base of the projectile to be modified according to the Mach number of flow at the base of the projectile. In this way, the unsteady expansion effects of flow through the barrel is taken into account. The equation of state and the basic energy and mass conservation equations are the same as those for the test gas in the driven tube.

Projectile motion is calculated by an approximate technique that involves determination of the flow Mach number at the projectile base.

$$M = V_p [(\gamma - 1) H_{2\infty}]^{-1/2} \quad (A-28)$$

where V_p is the projectile velocity, and $H_{2\infty}$, the static enthalpy at the projectile base, is defined as

$$H_{2\infty} = 2.5 \times 10^4 H_2 - \frac{V_p^2}{2}$$

and H_2 , the specific enthalpy, is given as

$$H_2 = \frac{E_2 \gamma}{M_g}$$

where M_g is the mass of the gas contained in the barrel.

By assuming adiabatic flow and ideal gas behavior, the isentropic relations may be used to obtain the local static pressure at the projectile base,

$$p_{2\infty} = p_{20} \left(1 + \frac{\gamma - 1}{2} M^2\right)^{-\gamma/(\gamma - 1)} \quad (A-29)$$

where p_{20} is the local "reservoir" pressure, i.e. the static pressure of the barrel origin.

Projectile acceleration, a_p , may then be expressed as

$$a_p = 32.17(p_{2\infty} - p_r)/W_p$$

where p_r is the projectile's local resistance to motion, and W_p is the projectile mass.

Changes in projectile velocity, ΔV_p , and displacement, ΔX_p , can be written as

$$\Delta V_p = a_p \Delta t \text{ and } \Delta X_p = V_p \Delta t + a_p \frac{\Delta t^2}{2} \quad (A-30)$$

STG Model Printout

A sample printout of the STG program follows. Definitions of "Initial Condition" variables are given in the program printout. However, some explanation of the "Tabulated Output" variables is required.

| | |
|--------------|---|
| TIME | Time after piston release - seconds Time is initially zero and increases to a maximum value either when the projectile exits the barrel or when it equals a limiting value, i.e., TFP. |
| PCH | Driver gas pressure - MPa (psi) PCH is a prescribed maximum at TIME zero and decreases as the driver gas displaces the unlatched piston. |
| VOL1 | Test gas volume included from piston face to test specimen inlet - $m^3(ft^3)$. VOL1 is initially the entire volume of the driven tube but decreases to the volume of the test gas collection chamber when the piston has been fully displaced. |
| P1,T1,M1 | Test gas pressure, temperature and mass associated with VOL1, measured in MPa (psi), $^{\circ}K (^{\circ}R)$, and kg (lb), respectively. |
| VOL2 | Test gas volume included from test specimen inlet to projectile base - $m^3(ft^3)$. VOL2 has a minimum value of the test specimen bore volume at TIME zero and increases with projectile displacement to include the entire barrel volume. |
| P2,T2,M2 | Test gas pressure, temperature and mass associated with VOL2, measured in MPa (psi), $^{\circ}K (^{\circ}R)$, and kg (lb), respectively. |
| VELP, XP | Piston velocity and displacement - m/sec (ft/sec), m (ft). |
| VPROJ, XPROJ | Projectile velocity and displacement - m/sec (ft/sec), m (ft). |
| WORK | Work performed by driver gas on the driven piston, and by test gas on the projectile. During piston rebound, the program also computed negative work done on the piston by the test gas - J (ft-lbf). |
| UE | Test gas free stream velocity - m/sec (ft/sec). |
| QFLUX | Test sample surface heat flux - $J/mm^2\text{-sec}$ ($Btu/ft^2\text{-sec}$). |
| QTOT | Total integrated heat input to test sample surface - J/mm^2 (Btu/ft^2). |
| TSAMP | Test sample surface temperature - $^{\circ}K (^{\circ}R)$. TSAMP(1) is the computed temperature on the test sample surface. TSAMP(2) through TSAMP(9) are subsurface temperatures computed at depths printed in the nonlinear DELX array, which is amended when the time increment DELT is changed. |

```
C
C
C LIST OF CONSTANTS AND VARIABLES USED IN THIS SHOCK TUBE GUN PROGRAM
C
C DRIVER GAS PARAMETERS
C PCH      INITIAL DRIVER PRESSURE - PSI
C VOLO     INITIAL VOLUME OF PROPELLING GAS - FT**3
C TO       INITIAL PROPELLING GAS TEMPERATURE - DEG R
C CVDVR    DRIVER GAS SPECIFIC HEAT - BTU/LBM-DEG R
C RDVR     DRIVER GAS CONSTANT - FT-LBF/LBM-DEG R
C
C PISTON PARAMETERS
C AT       PISTON AREA - FT**2
C KP1      DRAG RATE CONSTANT - LBF/FT
C VELP     INITIAL PISTON VELOCITY - FT/SEC
C WSHLL    PISTON WEIGHT - LBM
C SHELVR   PISTON MASS DURING RETURN - LBM
C XPMAX    MAX PISTON DISPLACEMENT - FT
C
C TEST GAS PARAMETERS
C P20      INITIAL TEST GAS PRESSURE - PSI
C T20      INITIAL TEST GAS TEMPERATURE - DEG R
C R2       TEST GAS CONSTANT - FT-LBF/LBM-DEG R
C CV2      SPECIFIC HEAT OF TEST GAS- BTU/LBM-DEG R
C CVT2     TEST GAS SPECIFIC HEAT
C CVEXP    CURVE-FITTING EXPONENT
C ALFA2    VANDERWAAL CONSTANT
C BETA2    VANDERWAAL CONSTANT
C GAM2     TEST GAS RATIO OF SPECIFIC HEATS
C
C TEST VOLUME PARAMETERS
C A2       TEST VOLUME AREA - FT**2
C DOR12    DIAMETER OF TEST VOLUME EXIT - IN
C CD2      FLOW COEFF. OF TEST VOLUME EXIT
C VOL1F    FINAL OR MINIMUM TEST GAS VOLUME OF DRIVEN TUBE - FT**3
C VOL20    INITIAL OR MINIMUM TEST GAS VOLUME OF BARREL - FT**3
C
C PROJECTILE PARAMETERS
C BARL     BARREL LENGTH - FT
C BORED     BORE DIAMETER - IN
C PSTART   PRESSURE ABOVE WHICH PROJECTILE IS ALLOWED TO MOVE - PSI
C RESO     Y-INTERCEPT OF PROJECTILE RESISTANCE FUNCTION - LBM
C RESS     SLOPE OF PROJECTILE RESISTANCE FUNCTION - LBM/FT
C RESC     CONSTANT RESISTANCE TERM AFTER FUNCTION L.T. RESC - LBM
C VPROJ    INITIAL PROJECTILE VELOCITY - FT/SEC
C WPROJ    PROJECTILE WEIGHT - LBM
C XPROJ    INITIAL PROJECTILE DISPLACEMENT - FT
C
C TIME PARAMETERS
C DELT     TIME INCREMENT - SEC
C PRCI     NUMBER OF TIMES BETWEEN PRINT INTERVALS
C TFO      LIMITING TIME - SEC
C
C
C
```



```

0001      READ (5,101) NUMBER
0002      DO 99 NM=1,NUMBER
0003      DIMENSION RG(9),CVG(9),CVTG(9),CVEXPG(9),ALFAG(9),BETAG(9),XG(9)
0004      DIMENSION G1(9),G2(9),G3(9),G4(9),G5(9)
0005      DIMENSION TNEW(40),TSAMP(40),DELX(40),DXNEW(40),DTEMP(40)
0006      REAL*4 M2,M20,M1,KP1
0007      JJ=1
0008      KK=1
0009      NN=0
0010      QFLUX=0.0
0011      UE=0.0
0012      R2=0.0
0013      CV2=0.0
0014      CVT2=0.0
0015      CVEXP=1.0
0016      ALFA2=0.0
0017      BETA2=0.0
0018      GAM2=1.0
0019      P20=14.7
0020      T20=530.0
0021      XPROJ=0.0
0022      VELP=0.0
0023      VPROJ=0.0

C
C READ IN CONSTANTS AND VARIABLES.
0024      READ (5,100) PCH,VOLO,T0,CVDVR,RDVR
0025      READ (5,100) AT,KP1,WSHELL,SHELLRV,XPMAX
0026      READ (5,100) A2,DOR12,CD2,VOL1F,VOL20
0027      READ (5,100) BARL,BORED,PSTART,RES0,RESS,RESC,WPROJ
0028      READ (5,100) DELT,PRCI,TFO,FACTOR
0029      READ (5,101) NG
0030      WRITE (6,103) NM
0031      WRITE (6,104)
0032      DO 3 ID=1,NG
0033      READ (5,102) XG(ID),G1(ID),G2(ID),G3(ID),G4(ID),G5(ID),RG(ID),CVG(
+ID),CVTG(ID),CVEXPG(ID),ALFAG(ID),BETAG(ID)
0034      WRITE (6,105) XG(ID),G1(ID),G2(ID),G3(ID),G4(ID),G5(ID)
0035      R2 = R2 + XG(ID)*RG(ID)
0036      CV2 = CV2 + XG(ID)*CVG(ID)
0037      GAM2 = GAM2 + XG(ID)*(RG(ID)/(778.*CVG(ID)))
0038      ALFA2 = ALFA2 + XG(ID)*ALFAG(ID)
0039      BETA2 = BETA2 + XG(ID)*BETAG(ID)
0040      3 CONTINUE
0041      BORED = BORED/12.
0042      BORID = BORED*12.
0043      ABORE = 0.785*BORED**2
0044      CV=CVDVR
0045      DELT0=DELT
0046      DOR12 = DOR12/12.
0047      DORID = DOR12*12.
0048      A12=0.7854*DOR12**2
0049      IPRC=IFIX(PRCI)
0050      IPRINT=0
0051      PCH=PCH*144.
0052      PCHP=PCH/144.
0053      P20=P20*144.
0054      PP=P20/144.
0055      PARTIM = 0.

```

```

0056      PSTART=PSTART*144.
0057      PSTARP=PSTART/144.
0058      QTOT=0.0
0059      RGAS=RDVR
0060      CP=RGAS/778.+CV
0061      GAM=CP/CV
0062      GM = PCH/(RGAS*T0)*VOLO
0063      E=GM*(CP-RGAS/778.)*T0
0064      TIME = 0.
0065      VMAX=XPMAX*AT
0066      XP=XPMAX

C
C  INITIAL CONDITIONS - UPSTREAM - FROM PISTON FACE TO TEST SAMPLE
0067      P1=P20
0068      VOL1=VOL1F+XP*A2
0069      T1=T20
0070      M1=P1*VOL1/R2/T1
0071      CVT2=0.0
0072      DO 1 J=1,NG
0073      CVT2=CVT2+XG(J)*CVTG(J)*(T1-460.0)**CVEXPG(J)
0074      1 CONTINUE
0075      E1=M1*(CV2+CVT2)*T1
0076      RHO1=M1/VOL1
0077      VV1=1.0/RHO1

C
C  INITIAL CONDITIONS - DOWNSTREAM - FROM TEST SAMPLE TO PROJECTILE BASE
0078      P2=P20
0079      VOL2=VOL20+XPROJ*ABORE
0080      T2=T20
0081      M2=P2*VOL2/R2/T2
0082      CVT2=0.0
0083      DO 2 J=1,NG
0084      CVT2=CVT2+XG(J)*CVTG(J)*(T2-460.0)**CVEXPG(J)
0085      2 CONTINUE
0086      E2=M2*(CV2+CVT2)*T2
0087      RHO2=M2/VOL2
0088      VV2=1./RHO2

C
C  PRINT OUT INITIAL CONDITIONS.
0089      WRITE (6,110)
0090      WRITE(6,120)PP,PCHP,AT,T20,T0,KP1,R2,RDVR,WSHELL,CV2,CVDVR,SHELLRV,
+CVT2,VOLO,XPMAX,CVEXP,PSTARP,ALFA2,BARL,BETA2,A2,BORID,GAM2,
+DORID,CD2,RES0,DELT,VOL1F,RESS,PRCI,VOL20,RESC,TFO,WPROJ

C
C  INITIALIZE CONDITIONS FOR UNSTEADY HEAT CONDUCTION.
0091      DEPTH = 0.5/12.0
0092      XK = 19.3/3600.
0093      ALPHA = XK/57.6
0094      F=1.3
0095      DELX0=SQRT(ALPHA*DELT/0.25)
0096      SUMX=DELX0
0097      DELX(1)=DELX0
0098      DO 6 I=1,40
0099      TSAMP(I)=T0
0100      TNEW(I)=T0
0101      6 CONTINUE
0102      DO 7 I=1,39
0103      DELX(I+1)=DELX(I)*F

```

```

0104      IF(SUMX.GE.DEPTH) GO TO 7
0105      SUMX=SUMX+DELX(I)
0106      KTEMP = I
0107      7 CONTINUE
0108      CONST1=ALPHA*2.0/(1.0+F)
0109      CONST2=(1.0+F)/F
0110      CONST3=1.0/F
0111      TZIP=QFLUX*2.0*DELX(1)/XK+TSAMP(2)
0112      10 CONTINUE
0113      T=T0
0114      RGAS=57.4+.333E-5*PCH
0115      CV=0.175+.183E-4*T
0116      CP=RGAS/778.+CV
0117      GAM=CP/CV

C
C  COMPUTE THE DYNAMICS AND THERMODYNAMICS OF PISTON MOTION.
0118      IF(VELP.LT.-0.1) WSHLL=SHELLRV
0119      24 XD=XPMAX-XP
0120      DRAG=KP1*ABS(VELP)
0121      FOVM=((PCH*AT-P1*A2)-DRAG)/WSHELL*32.17
0122      26 DVELP = FOVM * DELT
0123      28 VELP =VELP +DVELP
0124      IF(XP.LE.0.00001.AND.VELP.GT.0.0) VELP=0.0
0125      DXP=DELT*(VELP+FOVM*DELT/2.)
0126      XP=XP-DXP
0127      IF(XP.LE..00001) GO TO 99
0128      WORK = PCH * AT * DXP/778.
0129      E = E - WORK
0130      30 VOL=VOL0+AT*XD
0131      RHOCH = GM/VOL
0132      T = E/((CP-RGAS/778.)*GM)
0133      PCH = RHOCH*RGAS*T

C
C  COMPUTE TEST GAS PROPERTIES.
0134      CVTX=0.0
0135      CVTY=0.0
0136      DO 31 J=1,NG
0137      CVTX=CVTX+(XG(J)*CVTG(J)*((T2-460.)**CVEXPG(J)))
0138      CVTY=CVTY+(XG(J)*CVTG(J)*((T1-460.)**CVEXPG(J)))
0139      31 CONTINUE
0140      CVY=((CV2+CVTY)*T1-ALFA2*RHO1/778.0)/T1
0141      CVX=((CV2+CVTX)*T2-ALFA2*RHO2/778.0)/T2
0142      RESIST = RES0 + RESS * XPROJ
0143      32 IF(RESIST.LT.RESC) RESIST=RESC
0144      H2=E2*GAM2/M2
0145      H2INF=25000.*H2-VPROJ**2/2.
0146      XM2INF=VPROJ/SQRT((GAM2-1.0)*H2INF)
0147      FM=(1.0+(GAM2-1.0)/2.0*XM2INF**2)**(-GAM2/(GAM2-1.0))
0148      DELP=P2*(1.0-FM)/(1.0+FM)
0149      33 P20=P2+DELP
0150      P2INF=P2-DELP
0151      PFORCE = A*ORE * (P2INF-RESIST)
0152      IF(PFORCE.LT.0.0) PFORCE=0.0
0153      IF(P2.LT.PSTART) PFORCE=0.0
0154      APROJ = PFORCE/WPROJ*32.17
0155      DXPROJ = VPROJ * DELT + APROJ * DELT**2/2.
0156      35 XPROJ = XPROJ + DXPROJ
0157      IF(XPROJ.GE.BARL) GO TO 99

```

```

0158      VPROJ = VPROJ + APROJ* DELT
0159      VOL1=VOL1F+XP*A2
0160      VOL2=VOL20+XPROJ*ABORE
0161      36 PIAVE=P1
0162         XM1=M1
0163         XM2=M2
0164         IPASS=0
0165         P1SAV=P1
0166         P2SAV=P2
0167      37 CONTINUE
0168         IPASS=IPASS+1
0169         PSTAR=P1*(1.0+(GAM2-1.0)/2.0)**(-GAM2/(GAM2-1.0))
0170         TTOT=T1
0171         PS=PSTAR
0172         PTOT=P1
0173         IF(P20.GT.P1) GO TO 47
0174         IF(PSTAR.GE.P20) GO TO 38
0175         PS=P20
0176         DELTM1=8.02*A12*SQRT((P1-P20)*P1/R2/T1)*DELT
0177         GO TO 49
0178      38 TSTAR=T1*2.0/(GAM2+1.0)
0179         DELTM1=PSTAR*A12*SQRT(GAM2*32.2/R2/TSTAR)*DELT
0180         GO TO 49
0181      47 CONTINUE
0182         PSTAR=PSTAR*P20/P1
0183         TTOT=T2
0184         PS=PSTAR
0185         PTOT=P20
0186         IF(PSTAR.GE.P1) GO TO 48
0187         PS=P1
0188         DELTM1=-8.02*A12*SQRT((P20-P1)*P20/R2/T2)*DELT
0189         GO TO 49
0190      48 TSTAR=T2*2.0/(GAM2+1.0)
0191         DELTM1=-PSTAR*A12*SQRT(GAM2*32.2/R2/TSTAR)*DELT
0192      49 CONTINUE
0193         XM1=M1-DELTMI
0194         XM2=M2+DELTMI
0195         RHO1=XM1/VOL1
0196         RHO2=XM2/VOL2
0197         VV1=1.0/RHO1
0198         VV2=1./RHO2
0199         WORK=-ABORT*DXPROJ*P2INF/778.0-P2/233.*XPROJ*3.1416*BORED*DELT
0200         IF(VPROJ.LT.100.) GO TO 58

C
0201      DELH=CVV*DELTMI*T1*GAM2
0202      50 IF(DELTMI.LT.0.0) DELH= CVX*DELTMI*T2*GAM2
0203      EX=E2+WORK+DELH
0204      T2=EX/CVX/XM2
0205      PX=(R2*T2)/(VV2-BETA2)+ALFA2/VV2**2
0206      P2=(PX+P2SAV)/2.0
0207      EY=E1-DELH+PIAVE/778.0*A2*DXP
0208      T1=EY/CVY/XM1
0209      PY=(R2*T1)/(VV1-BETA2)+ALFA2/VV1**2
0210      P1=(PY+P1SAV)/2.0
0211      54 DELP1=PY-P1
0212      PIAVE=P1+DELP1/2.0
0213      P20=P2+DELP1
0214      55 IF(IPASS.LT.3) GO TO 37

```

```

0215      E1=EY
0216      E2=EX
0217      P1=PY
0218      P2=PX
0219      M1=XM1
0220      M2=XM2
0221      XMOR=SQRT(((PTOT/PS)**((GAM2-1.0)/GAM2)-1.0)*2.0/(GAM2-1.0))
0222      TE=TTOT/(1.0+(GAM2-1.0)/2.0*XMOR**2)
0223      UE=SQRT(5.0E4*CVY*GAM2*(TTOT-TE))
0224      TREF=(TE+TSAMP(1))/2.0+4.4E-6*UE**2/ CVY/GAM2
0225      VIS=7.0E-7*TREF**1.5/(TREF+198.0)
0226      RHOREF=PS/(BETA2*PS+R2*TREF)
0227      QFLUX=0.052*(RHOREF*UE)**0.8*VIS**0.2*CVY*GAM2*(TTOT-TSAMP(1))
0228      IF(TSAMP(1).GT.3100.0) QFLUX=QFLUX*(TTOT-3100.0)/(TTOT-TSAMP(1))
0229      QFLUX = QFLUX*FACTOR
0230      TZIP=QFLUX*2.0*DELX(1)/XK+TSAMP(2)
0231      DTEMP(1)=ALPHA/(DELX(1)**2)*(TZIP-2.0*TSAMP(1)+TSAMP(2))
0232      DO 56 K=2, KTEMP
0233      DTEMP(K)=CONST1/(DELX(K-1)**2)*(TSAMP(K-1)-CONST2*TSAMP(K)+
      * CONST3*TSAMP(K+1))
0234      56 CONTINUE
0235      DO 57 K=1, KTEMP
0236      TSAMP(K)=TSAMP(K)+DTEMP(K)*DELT
0237      57 CONTINUE
0238      TSAMP(KTEMP+1)=TSAMP(KTEMP-1)
0239      QTOT=QTOT+QFLUX*DELT
0240      IF(P20.GT.P1) UE=-UE
0241      GO TO 60
0242      58 CONTINUE
C
0243      VOL=VOL1+VOL2
0244      XMTOT=M1+M2
0245      ESUM=E1+E2+P1*A2*DXP/778.0 +WORK
0246      M1=XMTOT*VOL1/VOL
0247      M2=XMTOT*VOL2/VOL
0248      E1=ESUM*VOL1/VOL
0249      E2=ESUM*VOL2/VOL
0250      T1=ESUM/ CVY/XMTOT
0251      T2=T1
0252      VVT=VOL/XMTOT
0253      P1=(R2*T1)/(VVT-BETA2)+ALFA2/VVT**2
0254      P2=P1
0255      RHO1=M1/VOL1
0256      RHO2=M2/VOL2
0257      VV1=1.0/RHO1
0258      VV2=1.0/RHO2
0259      60 CONTINUE
0260      IF (VOL1.GT.0.2*VMAX) GO TO 80
0261      IF(VOL1.LE.0.2*VMAX)DELT=0.1*DELTO
0262      IF(VOL1.LE.0.2*VMAX.AND.KK.EQ.1) GO TO 62
0263      IF(VOL1.LE.0.02*VMAX)DELT=0.01*DELTO
0264      IF(VOL1.LE.0.02*VMAX.AND.KK.EQ.2) GO TO 62
0265      GO TO 80
C
C  REVISE GRID SIZE DUE TO CHANGE IN TIME STEP.
0266      62 DELX0=SQRT(ALPHA*DELT/0.25)
0267      SUMX=DELX0
0268      DXNEW(1)=DELX0

```

```

0269      DO 64 I=2,40
0270      DXNEW(I)=DXNEW(I-1)*F
0271      IF(SUMX.GE.DEPTH) GO TO 64
0272      SUMX=SUMX+DXNEW(I)
0273      KNMAX = I
0274      64 CONTINUE
0275      XKOLD=DELX(1)
0276      XKNEW=0.0
0277      K=1
0278      KNEW=1
0279      A=(TZIP-TSAMP(2))/(2.0*DELX(K))
0280      B=(TSAMP(1)-TSAMP(2)-A*DELX(K))/DELX(K)**2
0281      TNEW(1)=TSAMP(1)
0282      66 KNEW=KNEW+1
0283      XKNEW=XKNEW+DXNEW(KNEW-1)
0284      TNEW(KNEW)=TSAMP(1)-(A*XKNEW+B*XKNEW**2)
0285      IF(XKNEW.LT.XKOLD)GO TO 66
0286      67 K=K+1
0287      XKOLD=XKOLD+DELX(K)
0288      A=(TSAMP(K-1)-TSAMP(K+1))/((F+1.0)*DELX(K-1))
0289      B=(TSAMP(K)-TSAMP(K+1)-A*DELX(K))/DELX(K)**2
0290      68 KNEW=KNEW+1
0291      XKNEW=XKNEW+DXNEW(KNEW-1)
0292      XDEL=XKNEW-XKOLD+DELX(K)
0293      TNEW(KNEW)=TSAMP(K)-(A*XDEL+B*XDEL**2)
0294      IF(XKNEW.LT.XKOLD.AND.KNEW+1.LE.KNMAX) GO TO 68
0295      IF(K+1.LE.KTEMP.AND.KNEW+1.LE.KNMAX) GO TO 67
0296      DO 70 I=1,KNMAX
0297      DELX(I)=DXNEW(I)
0298      TSAMP(I)=TNEW(I)
0299      TNEW(I)=T0
0300      70 CONTINUE
0301      KTEMP=KNMAX
0302      KK = KK+1
0303      80 CONTINUE

C
C PRINT OUT COMPUTED RESULTS.
0304      IF (JJ.EQ.1) GO TO 88
0305      87 NN=1
0306      PARTIM=PARTIM+DELT
0307      IF(TIME.GT.TFO) GO TO 99
0308      IF(IPRINT.LT.IPRC) GO TO 90
0309      GO TO 89

C
0310      88 WRITE (6,187)
0311      WRITE (6,188)
0312      JJ=JJ+1
0313      89 PCHP=PCH/144.
0314      P1P=P1/144.0
0315      P2P=P2/144.
0316      TIME=TIME+PARTIM
0317      PARTIM = 0.
0318      WRITE(6,190) TIME,P1P,T1,M1,VOL1,VELP,VPROJ,WORK,QFLUX,PCHP,P2P,T2
      +,M2,VOL2,XP,XPROJ,UE,QTOT,(TSAMP(I),I=1,9)
0319      IF(NN.EQ.0) GO TO 87
0320      IPRINT = 0
0321      90 IPRINT=IPRINT+1
0322      GO TO 10

```

```

0323      C      99 CONTINUE
0324      C
0325      100 FORMAT (8F10.5)
0326      101 FORMAT (I1)
0327      102 FORMAT (F5.2,5A3,6E10.3)
0328      103 FORMAT (12H1 INPUT DATA,T48,'TEST NO.',T59,I1)
0329      104 FORMAT (////T6,'TEST GAS MIXTURE BY MOLE FRACTION'//)
0330      105 FORMAT (/T6,F6.3,T17,SA3)
0331      110 FORMAT (////T6,'INITIAL CONDITIONS FOR TEST')
0331      120 FORMAT (////T6,'P20 =',T17,F13.6,T31,'PSI',T48,'PCH =',T59,F13.6,
+T73,'PSI',T90,'AT =',T101,F13.6,T115,'FT**2'//T6,'T20 =',T17,
+F13.6,T31,'DEGR',T48,'T0 =',T59,F13.6,T73,'DEGR',T90,'KPI =',T101,
+F13.6,T115,'LBF/FT'//T6,'R2 =',T17,F13.6,T31,'FT-LBF/LBM-DEGR',
+T48,'RDVR =',T59,F13.6,T73,'FT-LBF/LBM-DEGR',T90,'WSHELL =',T101,
+F13.6,T115,'LBM'//T6,'CV2 =',T17,F13.6,T31,'BTU/LBM-DEGR',T48,
+'CVDVR =',T59,F13.6,T73,'BTU/LBM-DEGR',T90,'SHELLRV =',T101,F13.6,
+T115,'LBM'//T6,'CVT2 =',T17,F13.6,T48,'VOL0 =',T59,F13.6,T73,
+'FT**3',T90,'XPMAX =',T101,F13.6,T115,'FT'//T6,'CVEXP =',T17,
+F13.6,T48,'PSTART =',T59,F13.6,T73,'PSI'//T6,'ALFA2 =',T17,F13.6,
+T90,'BARL =',T101,F13.6,T115,'FT'//T6,'BETA2 =',T17,F13.6,T48,
+'A2 =',T59,F13.6,T73,'FT**2',T90,'BORED =',T101,F13.6,T115,'IN'//
+T6,'GAM2 =',T17,F13.6,T48,'DOR12 =',T59,F13.6,T73,'IN'//
+/T48,'CD2 =',T59,F13.6,T90,'RES0 =',T101,F13.6,T115,'LBM'//T6,
+'DELT =',T17,F13.6,T31,'SEC',T48,'VOL1F =',T59,F13.6,T73,'FT**3',
+T90,'RESS =',T101,F13.6,T115,'LBM/FT'//T6,'PRCI =',T17,F13.6,T48,
+'VOL20 =',T59,F13.6,T73,'FT**3',T90,'RESC =',T101,F13.6,T115,'LBM'
+//T6,'TFO =',T17,F13.6,T31,'SEC',T90,'WPROJ =',T101,F13.6,T115,
+'LBM'/////))
0332      187 FORMAT (18H1 TABULATED OUTPUT)
0333      188 FORMAT(////T6,'TIME',T20,'P1',T34,'T1',T48,'M1',T62,'VOL1',T76,'VEL
+P',T90,'VPROJ',T104,'WORK',T118,'QFLUX'//T6,'PCH',T20,'P2',T34,'T2'
+,T48,'M2',T62,'VOL2',T76,'XP',T90,'XPROJ',T104,'UE',T118,'QTOT'//
+T4,'TSAMP(1)',T18,'TSAMP(2)',T32,'TSAMP(3)',T46,'TSAMP(4)',
+T60,'TSAMP(5)',T74,'TSAMP(6)',T88,'TSAMP(7)',T102,'TSAMP(8)',
+T116,'TSAMP(9)'//)
0334      190 FORMAT(9E14.6/9E14.6/9E14.6/)
0335      C      STOP
0336      END

```

INPUT DATA

TEST NO. 1

TEST GAS MIXTURE BY MOLE FRACTION

0.140 CARBON MONOXIDE
 0.025 CARBON DIOXIDE
 0.290 NITROGEN
 0.545 ARGON

INITIAL CONDITIONS FOR TEST

P20 = 14.699998 PSI PCH = 600.000000 PSI AT = 0.306800 FT**2
 T20 = 530.000000 DEGR T0 = 535.000000 DEGR KP1 = 6.000000 LBF/FT
 R2 = 45.673965 FT-LBF/LBM-DEGR RDVR = 55.199997 FT-LBF/LBM-DEGR VSHLL = 150.000000 LBM
 CV2 = 0.121402 BTU/LBM-DEGR CVDVR = 0.176000 BTU/LBM-DEGR SHELAV = 150.000000 LBM
 CVT2 = 0.002123 VOL0 = 31.500000 FT**3 XPMAX = 81.000000 FT
 CVEKP = 1.000000 PSTART = 1000.000000 PSI
 ALFA2 = 700.583008 BARL = 15.000000 FT
 BETA2 = 0.017071 BORED = 1.180999 IN
 GAM2 = 1.537455 DOR12 = 0.500000 IN
 DELT = 0.001000 SEC CD2 = 0.750000 RES0 = 7200.00000 LBM
 PRC1 = 10.000000 VOL1F = 0.082000 FT**3 RESS = 4320.00000 LBM/FT
 TFO = 0.250000 SEC VOL20 = 0.082000 FT**3 RESC = 7200.00000 LBM
 WPROJ = 0.250000 LBM

TABULATED OUTPUT

| TIME PCH TSAMP(1) | P1 P2 TSAMP(2) | T1 T2 TSAMP(3) | M1 M2 TSAMP(4) | VOL1 VOL2 TSAMP(5) | VELP XP TSAMP(6) | VPROJ XPROJ TSAMP(7) | WORK UE TSAMP(8) | QFLUX OTOT TSAMP(9) |
|-------------------------|----------------------|----------------------|----------------------|--------------------------|------------------------|----------------------------|------------------------|---------------------------|
| 0.0 | 0.147791E+02 | 0.530664E+03 | 0.218025E+01 | 0.249302E+02 | 0.554569E+01 | 0.0 | 0.0 | 0.0 |
| 0.597192E+03 | 0.147791E+02 | 0.530664E+03 | 0.717122E-02 | 0.820000E-01 | 0.809917E+02 | 0.0 | 0.0 | 0.0 |
| 0.535000E+03 | 0.535000E+03 | 0.535000E+03 | 0.535000E+03 | 0.535000E+03 | 0.535000E+03 | 0.535000E+03 | 0.535000E+03 | 0.535000E+03 |
| 0.110000E-01 | 0.148804E+02 | 0.531774E+03 | 0.218021E+01 | 0.248122E+02 | 0.602501E+02 | 0.0 | 0.0 | 0.0 |
| 0.594360E+03 | 0.148804E+02 | 0.531774E+03 | 0.720520E-02 | 0.820000E-01 | 0.806071E+02 | 0.0 | 0.0 | 0.0 |
| 0.535000E+03 | 0.535000E+03 | 0.535000E+03 | 0.535000E+03 | 0.535000E+03 | 0.535000E+03 | 0.535000E+03 | 0.535000E+03 | 0.535000E+03 |
| 0.210000E-01 | 0.151310E+02 | 0.534546E+03 | 0.218013E+01 | 0.245285E+02 | 0.113278E+03 | 0.0 | 0.0 | 0.0 |
| 0.587227E+03 | 0.151310E+02 | 0.534546E+03 | 0.728828E-02 | 0.820000E-01 | 0.796822E+02 | 0.0 | 0.0 | 0.0 |
| 0.535000E+03 | 0.535000E+03 | 0.535000E+03 | 0.535000E+03 | 0.535000E+03 | 0.535000E+03 | 0.535000E+03 | 0.535000E+03 | 0.535000E+03 |
| 0.310000E-01 | 0.155385E+02 | 0.538982E+03 | 0.217999E+01 | 0.240832E+02 | 0.165767E+03 | 0.0 | 0.0 | 0.0 |
| 0.576149E+03 | 0.155385E+02 | 0.538982E+03 | 0.742257E-02 | 0.820000E-01 | 0.782309E+02 | 0.0 | 0.0 | 0.0 |
| 0.535000E+03 | 0.535000E+03 | 0.535000E+03 | 0.535000E+03 | 0.535000E+03 | 0.535000E+03 | 0.535000E+03 | 0.535000E+03 | 0.535000E+03 |
| 0.409999E-01 | 0.161188E+02 | 0.545158E+03 | 0.217981E+01 | 0.234819E+02 | 0.215842E+03 | 0.0 | 0.0 | 0.0 |
| 0.561637E+03 | 0.161188E+02 | 0.545158E+03 | 0.761199E-02 | 0.820000E-01 | 0.762711E+02 | 0.0 | 0.0 | 0.0 |
| 0.535000E+03 | 0.535000E+03 | 0.535000E+03 | 0.535000E+03 | 0.535000E+03 | 0.535000E+03 | 0.535000E+03 | 0.535000E+03 | 0.535000E+03 |
| 0.509999E-01 | 0.168964E+02 | 0.553193E+03 | 0.217956E+01 | 0.227310E+02 | 0.263721E+03 | 0.0 | 0.0 | 0.0 |
| 0.544279E+03 | 0.168964E+02 | 0.553193E+03 | 0.786255E-02 | 0.820000E-01 | 0.738234E+02 | 0.0 | 0.0 | 0.0 |
| 0.535000E+03 | 0.535000E+03 | 0.535000E+03 | 0.535000E+03 | 0.535000E+03 | 0.535000E+03 | 0.535000E+03 | 0.535000E+03 | 0.535000E+03 |
| 0.609999E-01 | 0.179073E+02 | 0.563257E+03 | 0.217923E+01 | 0.218376E+02 | 0.309172E+03 | 0.0 | 0.0 | 0.0 |
| 0.524774E+03 | 0.179073E+02 | 0.563257E+03 | 0.818302E-02 | 0.820000E-01 | 0.709113E+02 | 0.0 | 0.0 | 0.0 |
| 0.535000E+03 | 0.535000E+03 | 0.535000E+03 | 0.535000E+03 | 0.535000E+03 | 0.535000E+03 | 0.535000E+03 | 0.535000E+03 | 0.535000E+03 |
| 0.709999E-01 | 0.192028E+02 | 0.575586E+03 | 0.217883E+01 | 0.208095E+02 | 0.352025E+03 | 0.0 | 0.0 | 0.0 |
| 0.503707E+03 | 0.192028E+02 | 0.575586E+03 | 0.898573E-02 | 0.820000E-01 | 0.675602E+02 | 0.0 | 0.0 | 0.0 |
| 0.535000E+03 | 0.535000E+03 | 0.535000E+03 | 0.535000E+03 | 0.535000E+03 | 0.535000E+03 | 0.535000E+03 | 0.535000E+03 | 0.535000E+03 |
| 0.809999E-01 | 0.208570E+02 | 0.590501E+03 | 0.217834E+01 | 0.196548E+02 | 0.392165E+03 | 0.0 | 0.0 | 0.0 |
| 0.481687E+03 | 0.208570E+02 | 0.590501E+03 | 0.908802E-02 | 0.820000E-01 | 0.637968E+02 | 0.0 | 0.0 | 0.0 |
| 0.535000E+03 | 0.535000E+03 | 0.535000E+03 | 0.535000E+03 | 0.535000E+03 | 0.535000E+03 | 0.535000E+03 | 0.535000E+03 | 0.535000E+03 |
| 0.909997E-01 | 0.229775E+02 | 0.608446E+03 | 0.217771E+01 | 0.183822E+02 | 0.429519E+03 | 0.0 | 0.0 | 0.0 |
| 0.459236E+03 | 0.229775E+02 | 0.608446E+03 | 0.971443E-02 | 0.820000E-01 | 0.596487E+02 | 0.0 | 0.0 | 0.0 |
| 0.535000E+03 | 0.535000E+03 | 0.535000E+03 | 0.535000E+03 | 0.535000E+03 | 0.535000E+03 | 0.535000E+03 | 0.535000E+03 | 0.535000E+03 |
| 0.101000E+00 | 0.257251E+02 | 0.630028E+03 | 0.217693E+01 | 0.170001E+02 | 0.464053E+03 | 0.0 | 0.0 | 0.0 |
| 0.436732E+03 | 0.257251E+02 | 0.630028E+03 | 0.105004E-01 | 0.820000E-01 | 0.551439E+02 | 0.0 | 0.0 | 0.0 |
| 0.535000E+03 | 0.535000E+03 | 0.535000E+03 | 0.535000E+03 | 0.535000E+03 | 0.535000E+03 | 0.535000E+03 | 0.535000E+03 | 0.535000E+03 |
| 0.111000E+00 | 0.293472E+02 | 0.656106E+03 | 0.217593E+01 | 0.155173E+02 | 0.495750E+03 | 0.0 | 0.0 | 0.0 |
| 0.414710E+03 | 0.293472E+02 | 0.656106E+03 | 0.114985E-01 | 0.820000E-01 | 0.503107E+02 | 0.0 | 0.0 | 0.0 |
| 0.535000E+03 | 0.535000E+03 | 0.535000E+03 | 0.535000E+03 | 0.535000E+03 | 0.535000E+03 | 0.535000E+03 | 0.535000E+03 | 0.535000E+03 |
| 0.121000E+00 | 0.342411E+02 | 0.687918E+03 | 0.217462E+01 | 0.139425E+02 | 0.524595E+03 | 0.0 | 0.0 | 0.0 |
| 0.393261E+03 | 0.342411E+02 | 0.687918E+03 | 0.127896E-01 | 0.820000E-01 | 0.451777E+02 | 0.0 | 0.0 | 0.0 |
| 0.535000E+03 | 0.535000E+03 | 0.535000E+03 | 0.535000E+03 | 0.535000E+03 | 0.535000E+03 | 0.535000E+03 | 0.535000E+03 | 0.535000E+03 |
| 0.130999E+00 | 0.410810E+02 | 0.727327E+03 | 0.217289E+01 | 0.122845E+02 | 0.550549E+03 | 0.0 | 0.0 | 0.0 |
| 0.372845E+03 | 0.410810E+02 | 0.727327E+03 | 0.145042E-01 | 0.820000E-01 | 0.397736E+02 | 0.0 | 0.0 | 0.0 |
| 0.535000E+03 | 0.535000E+03 | 0.535000E+03 | 0.535000E+03 | 0.535000E+03 | 0.535000E+03 | 0.535000E+03 | 0.535000E+03 | 0.535000E+03 |

| | | | | | | | | | |
|--------------|--------------|--------------|--------------|--------------|--------------|--------------|--------------|--------------|--------------|
| 0.140999E+00 | 0.510935E+02 | 0.777261E+03 | 0.217052E+01 | 0.105524E+02 | 0.573502E+03 | 0.0 | 0.0 | 0.0 | 0.0 |
| 0.353000E+03 | 0.510935E+02 | 0.777261E+03 | 0.168665E-01 | 0.810000E-01 | 0.341277E+02 | 0.0 | 0.0 | 0.0 | 0.0 |
| 0.535000E+03 | 0.535000E+03 | 0.535000E+03 | 0.535000E+03 | 0.535000E+03 | 0.535000E+03 | 0.535000E+03 | 0.535000E+03 | 0.535000E+03 | 0.535000E+03 |
| 0.150999E+00 | 0.667293E+02 | 0.842650E+03 | 0.216168E+01 | 0.815574E+01 | 0.593200E+03 | 0.0 | 0.0 | 0.0 | 0.0 |
| 0.334420E+03 | 0.667293E+02 | 0.842650E+03 | 0.202952E-01 | 0.810000E-01 | 0.282716E+02 | 0.0 | 0.0 | 0.0 | 0.0 |
| 0.535000E+03 | 0.535000E+03 | 0.535000E+03 | 0.535000E+03 | 0.535000E+03 | 0.535000E+03 | 0.535000E+03 | 0.535000E+03 | 0.535000E+03 | 0.535000E+03 |
| 0.160999E+00 | 0.935705E+02 | 0.932589E+03 | 0.216168E+01 | 0.610549E+01 | 0.609060E+03 | 0.0 | 0.0 | 0.0 | 0.0 |
| 0.316964E+03 | 0.935705E+02 | 0.932589E+03 | 0.256691E-01 | 0.815500E-01 | 0.222408E+02 | 0.0 | 0.0 | 0.0 | 0.0 |
| 0.535000E+03 | 0.535000E+03 | 0.535000E+03 | 0.535000E+03 | 0.535000E+03 | 0.535000E+03 | 0.535000E+03 | 0.535000E+03 | 0.535000E+03 | 0.535000E+03 |
| 0.170999E+00 | 0.147085E+03 | 0.106629E+04 | 0.215216E+01 | 0.51572E+01 | 0.619658E+03 | 0.0 | 0.0 | 0.0 | 0.0 |
| 0.300677E+03 | 0.147085E+03 | 0.106629E+04 | 0.331847E-01 | 0.810000E-01 | 0.160812E+02 | 0.0 | 0.0 | 0.0 | 0.0 |
| 0.535000E+03 | 0.535000E+03 | 0.535000E+03 | 0.535000E+03 | 0.535000E+03 | 0.535000E+03 | 0.535000E+03 | 0.535000E+03 | 0.535000E+03 | 0.535000E+03 |
| 0.171999E+00 | 0.163314E+03 | 0.109901E+04 | 0.214946E+01 | 0.405394E+01 | 0.620780E+03 | 0.0 | 0.0 | 0.0 | 0.0 |
| 0.296730E+03 | 0.163314E+03 | 0.109901E+04 | 0.378723E-01 | 0.810000E-01 | 0.149020E+02 | 0.0 | 0.0 | 0.0 | 0.0 |
| 0.535000E+03 | 0.535000E+03 | 0.535000E+03 | 0.535000E+03 | 0.535000E+03 | 0.535000E+03 | 0.535000E+03 | 0.535000E+03 | 0.535000E+03 | 0.535000E+03 |
| 0.172999E+00 | 0.173255E+03 | 0.111847E+04 | 0.214786E+01 | 0.445341E+01 | 0.621196E+03 | 0.0 | 0.0 | 0.0 | 0.0 |
| 0.295203E+03 | 0.173255E+03 | 0.111847E+04 | 0.394597E-01 | 0.810000E-01 | 0.142810E+02 | 0.0 | 0.0 | 0.0 | 0.0 |
| 0.535000E+03 | 0.535000E+03 | 0.535000E+03 | 0.535000E+03 | 0.535000E+03 | 0.535000E+03 | 0.535000E+03 | 0.535000E+03 | 0.535000E+03 | 0.535000E+03 |
| 0.173999E+00 | 0.184270E+03 | 0.113909E+04 | 0.214613E+01 | 0.427276E+01 | 0.621498E+03 | 0.0 | 0.0 | 0.0 | 0.0 |
| 0.293699E+03 | 0.184270E+03 | 0.113909E+04 | 0.411870E-01 | 0.810000E-01 | 0.136596E+02 | 0.0 | 0.0 | 0.0 | 0.0 |
| 0.535000E+03 | 0.535000E+03 | 0.535000E+03 | 0.535000E+03 | 0.535000E+03 | 0.535000E+03 | 0.535000E+03 | 0.535000E+03 | 0.535000E+03 | 0.535000E+03 |
| 0.174999E+00 | 0.196528E+03 | 0.116101E+04 | 0.214423E+01 | 0.408205E+01 | 0.621676E+03 | 0.0 | 0.0 | 0.0 | 0.0 |
| 0.292187E+03 | 0.196528E+03 | 0.116101E+04 | 0.430732E-01 | 0.810000E-01 | 0.130380E+02 | 0.0 | 0.0 | 0.0 | 0.0 |
| 0.535000E+03 | 0.535000E+03 | 0.535000E+03 | 0.535000E+03 | 0.535000E+03 | 0.535000E+03 | 0.535000E+03 | 0.535000E+03 | 0.535000E+03 | 0.535000E+03 |
| 0.175999E+00 | 0.210235E+03 | 0.118437E+04 | 0.214215E+01 | 0.389131E+01 | 0.621717E+03 | 0.0 | 0.0 | 0.0 | 0.0 |
| 0.290697E+03 | 0.210235E+03 | 0.118437E+04 | 0.451408E-01 | 0.810000E-01 | 0.124163E+02 | 0.0 | 0.0 | 0.0 | 0.0 |
| 0.535000E+03 | 0.535000E+03 | 0.535000E+03 | 0.535000E+03 | 0.535000E+03 | 0.535000E+03 | 0.535000E+03 | 0.535000E+03 | 0.535000E+03 | 0.535000E+03 |
| 0.176999E+00 | 0.225639E+03 | 0.120932E+04 | 0.213987E+01 | 0.310058E+01 | 0.621608E+03 | 0.0 | 0.0 | 0.0 | 0.0 |
| 0.289221E+03 | 0.225639E+03 | 0.120932E+04 | 0.474167E-01 | 0.810000E-01 | 0.117946E+02 | 0.0 | 0.0 | 0.0 | 0.0 |
| 0.535000E+03 | 0.535000E+03 | 0.535000E+03 | 0.535000E+03 | 0.535000E+03 | 0.535000E+03 | 0.535000E+03 | 0.535000E+03 | 0.535000E+03 | 0.535000E+03 |
| 0.177999E+00 | 0.243049E+03 | 0.123605E+04 | 0.213734E+01 | 0.350991E+01 | 0.621331E+03 | 0.0 | 0.0 | 0.0 | 0.0 |
| 0.287758E+03 | 0.243049E+03 | 0.123605E+04 | 0.499334E-01 | 0.810000E-01 | 0.111731E+02 | 0.0 | 0.0 | 0.0 | 0.0 |
| 0.535000E+03 | 0.535000E+03 | 0.535000E+03 | 0.535000E+03 | 0.535000E+03 | 0.535000E+03 | 0.535000E+03 | 0.535000E+03 | 0.535000E+03 | 0.535000E+03 |
| 0.178999E+00 | 0.262846E+03 | 0.126479E+04 | 0.213454E+01 | 0.311937E+01 | 0.620866E+03 | 0.0 | 0.0 | 0.0 | 0.0 |
| 0.286309E+03 | 0.262846E+03 | 0.126479E+04 | 0.527305E-01 | 0.810000E-01 | 0.105521E+02 | 0.0 | 0.0 | 0.0 | 0.0 |
| 0.535000E+03 | 0.535000E+03 | 0.535000E+03 | 0.535000E+03 | 0.535000E+03 | 0.535000E+03 | 0.535000E+03 | 0.535000E+03 | 0.535000E+03 | 0.535000E+03 |
| 0.179999E+00 | 0.285514E+03 | 0.129579E+04 | 0.213140E+01 | 0.312901E+01 | 0.620188E+03 | 0.0 | 0.0 | 0.0 | 0.0 |
| 0.284874E+03 | 0.285514E+03 | 0.129579E+04 | 0.558564E-01 | 0.810000E-01 | 0.993157E+01 | 0.0 | 0.0 | 0.0 | 0.0 |
| 0.535000E+03 | 0.535000E+03 | 0.535000E+03 | 0.535000E+03 | 0.535000E+03 | 0.535000E+03 | 0.535000E+03 | 0.535000E+03 | 0.535000E+03 | 0.535000E+03 |
| 0.180999E+00 | 0.311665E+03 | 0.132938E+04 | 0.212787E+01 | 0.293889E+01 | 0.619269E+03 | 0.0 | 0.0 | 0.0 | 0.0 |
| 0.283452E+03 | 0.311665E+03 | 0.132938E+04 | 0.593712E-01 | 0.810000E-01 | 0.931191E+01 | 0.0 | 0.0 | 0.0 | 0.0 |
| 0.535000E+03 | 0.535000E+03 | 0.535000E+03 | 0.535000E+03 | 0.535000E+03 | 0.535000E+03 | 0.535000E+03 | 0.535000E+03 | 0.535000E+03 | 0.535000E+03 |
| 0.181999E+00 | 0.342090E+03 | 0.136593E+04 | 0.212389E+01 | 0.214911E+01 | 0.618073E+03 | 0.0 | 0.0 | 0.0 | 0.0 |
| 0.282045E+03 | 0.342090E+03 | 0.136593E+04 | 0.633508E-01 | 0.810000E-01 | 0.869333E+01 | 0.0 | 0.0 | 0.0 | 0.0 |
| 0.535000E+03 | 0.535000E+03 | 0.535000E+03 | 0.535000E+03 | 0.535000E+03 | 0.535000E+03 | 0.535000E+03 | 0.535000E+03 | 0.535000E+03 | 0.535000E+03 |
| 0.182999E+00 | 0.377826E+03 | 0.140539E+04 | 0.211934E+01 | 0.215976E+01 | 0.616555E+03 | 0.0 | 0.0 | 0.0 | 0.0 |
| 0.280654E+03 | 0.377826E+03 | 0.140539E+04 | 0.678914E-01 | 0.810000E-01 | 0.807614E+01 | 0.0 | 0.0 | 0.0 | 0.0 |
| 0.535000E+03 | 0.535000E+03 | 0.535000E+03 | 0.535000E+03 | 0.535000E+03 | 0.535000E+03 | 0.535000E+03 | 0.535000E+03 | 0.535000E+03 | 0.535000E+03 |

| | | | | | | | | |
|--------------|--------------|--------------|--------------|--------------|--------------|--------------|---------------|--------------|
| 0.14999E+00 | 0.420254E+03 | 0.144985E+04 | 0.211410E+01 | 0.217094E+01 | 0.614660E+03 | 0.0 | 0.0 | 0.0 |
| 0.27477E+03 | 0.420254E+03 | 0.144985E+04 | 0.731172E+01 | 0.810000E+01 | 0.746068E+01 | 0.0 | 0.0 | 0.0 |
| 0.535000E+03 | 0.535000E+03 | 0.535000E+03 | 0.535000E+03 | 0.535000E+03 | 0.535000E+03 | 0.535000E+03 | 0.535000E+03 | 0.535000E+03 |
| 0.184999E+00 | 0.471246E+03 | 0.149850E+04 | 0.210802E+01 | 0.218278E+01 | 0.612318E+03 | 0.0 | 0.0 | 0.0 |
| 0.277917E+03 | 0.471246E+03 | 0.149850E+04 | 0.791915E+01 | 0.820000E+01 | 0.684738E+01 | 0.0 | 0.0 | 0.0 |
| 0.535000E+03 | 0.535000E+03 | 0.535000E+03 | 0.535000E+03 | 0.535000E+03 | 0.535000E+03 | 0.535000E+03 | 0.535000E+03 | 0.535000E+03 |
| 0.185999E+00 | 0.533402E+03 | 0.155273E+04 | 0.210086E+01 | 0.195433E+01 | 0.609437E+03 | 0.0 | 0.0 | 0.0 |
| 0.276574E+03 | 0.533402E+03 | 0.155273E+04 | 0.863327E+01 | 0.820000E+01 | 0.623674E+01 | 0.0 | 0.0 | 0.0 |
| 0.535000E+03 | 0.535000E+03 | 0.535000E+03 | 0.535000E+03 | 0.535000E+03 | 0.535000E+03 | 0.535000E+03 | 0.535000E+03 | 0.535000E+03 |
| 0.186999E+00 | 0.610413E+03 | 0.161372E+04 | 0.209235E+01 | 0.100909E+01 | 0.605900E+03 | 0.0 | 0.0 | 0.0 |
| 0.275249E+03 | 0.610413E+03 | 0.161372E+04 | 0.948392E+01 | 0.820000E+01 | 0.562936E+01 | 0.0 | 0.0 | 0.0 |
| 0.535000E+03 | 0.535000E+03 | 0.535000E+03 | 0.535000E+03 | 0.535000E+03 | 0.535000E+03 | 0.535000E+03 | 0.535000E+03 | 0.535000E+03 |
| 0.187999E+00 | 0.707687E+03 | 0.168297E+04 | 0.208205E+01 | 0.12397E+01 | 0.601544E+03 | 0.0 | 0.0 | 0.0 |
| 0.273943E+03 | 0.707687E+03 | 0.168297E+04 | 0.105130E+01 | 0.820000E+01 | 0.502600E+01 | 0.0 | 0.0 | 0.0 |
| 0.535000E+03 | 0.535000E+03 | 0.535000E+03 | 0.535000E+03 | 0.535000E+03 | 0.535000E+03 | 0.535000E+03 | 0.535000E+03 | 0.535000E+03 |
| 0.188999E+00 | 0.833398E+03 | 0.176254E+04 | 0.206936E+01 | 0.14038E+01 | 0.596147E+03 | 0.0 | 0.0 | 0.0 |
| 0.272659E+03 | 0.833398E+03 | 0.176254E+04 | 0.117807E+01 | 0.820000E+01 | 0.442759E+01 | 0.0 | 0.0 | 0.0 |
| 0.535000E+03 | 0.535000E+03 | 0.535000E+03 | 0.535000E+03 | 0.535000E+03 | 0.535000E+03 | 0.535000E+03 | 0.535000E+03 | 0.535000E+03 |
| 0.189999E+00 | 0.100042E+04 | 0.185525E+04 | 0.205338E+01 | 0.125869E+01 | 0.589391E+03 | 0.0 | 0.0 | 0.0 |
| 0.271397E+03 | 0.100042E+04 | 0.185525E+04 | 0.133772E+01 | 0.820000E+01 | 0.383536E+01 | 0.0 | 0.0 | 0.0 |
| 0.535000E+03 | 0.535000E+03 | 0.535000E+03 | 0.535000E+03 | 0.535000E+03 | 0.535000E+03 | 0.535000E+03 | 0.535000E+03 | 0.535000E+03 |
| 0.190999E+00 | 0.123574E+04 | 0.196814E+04 | 0.203875E+01 | 0.117939E+01 | 0.580801E+03 | 0.146275E+03 | -0.236648E-01 | 0.970879E+03 |
| 0.270162E+03 | 0.123574E+04 | 0.196814E+04 | 0.148395E+01 | 0.820000E+01 | 0.325094E+01 | 0.710303E+01 | 0.647891E+03 | 0.226852E+03 |
| 0.562860E+03 | 0.540305E+03 | 0.535255E+03 | 0.535000E+03 | 0.535000E+03 | 0.535000E+03 | 0.535000E+03 | 0.535000E+03 | 0.535000E+03 |
| 0.191999E+00 | 0.159645E+04 | 0.211332E+04 | 0.203575E+01 | 0.93397E+01 | 0.569483E+03 | 0.300090E+03 | -0.523783E-01 | 0.195027E+04 |
| 0.268957E+03 | 0.159645E+04 | 0.211332E+04 | 0.151389E+01 | 0.820000E+01 | 0.276663E+01 | 0.294326E+00 | 0.150721E+04 | 0.178944E+03 |
| 0.647885E+03 | 0.592057E+03 | 0.555093E+03 | 0.535093E+03 | 0.535093E+03 | 0.535016E+03 | 0.535000E+03 | 0.535000E+03 | 0.535000E+03 |
| 0.192999E+00 | 0.216255E+04 | 0.229867E+04 | 0.203018E+01 | 0.71201E+01 | 0.553976E+03 | 0.452680E+03 | -0.840886E-01 | 0.271626E+04 |
| 0.267789E+03 | 0.216255E+04 | 0.229867E+04 | 0.158961E+01 | 0.81002E+01 | 0.211604E+01 | 0.670787E+00 | 0.213590E+04 | 0.415867E+01 |
| 0.737601E+03 | 0.656249E+03 | 0.592532E+03 | 0.553961E+03 | 0.53675E+03 | 0.535366E+03 | 0.535016E+03 | 0.535000E+03 | 0.535000E+03 |
| 0.193999E+00 | 0.314056E+04 | 0.254489E+04 | 0.202340E+01 | 0.551133E+01 | 0.531605E+03 | 0.604263E+03 | -0.118523E+00 | 0.382837E+04 |
| 0.266669E+03 | 0.314056E+04 | 0.254489E+04 | 0.163738E+01 | 0.911199E+01 | 0.157475E+01 | 0.119946E+01 | 0.241676E+04 | 0.742315E+01 |
| 0.850391E+03 | 0.735128E+03 | 0.64147E+03 | 0.57844E+03 | 0.53663E+03 | 0.536787E+03 | 0.535139E+03 | 0.535004E+03 | 0.535000E+03 |
| 0.194459E+00 | 0.401462E+04 | 0.271591E+04 | 0.201897E+01 | 0.477287E+01 | 0.514486E+03 | 0.686447E+03 | -0.139871E-01 | 0.483308E+04 |
| 0.266010E+03 | 0.119143E+04 | 0.200487E+04 | 0.169164E+01 | 0.933189E+01 | 0.128842E+01 | 0.155443E+01 | 0.251061E+04 | 0.983139E+01 |
| 0.937004E+03 | 0.885143E+03 | 0.826536E+03 | 0.763216E+03 | 0.70990E+03 | 0.644629E+03 | 0.594918E+03 | 0.560569E+03 | 0.553045E+03 |
| 0.194559E+00 | 0.421627E+04 | 0.275139E+04 | 0.201805E+01 | 0.41569E+01 | 0.510782E+03 | 0.701324E+03 | -0.143797E-01 | 0.505848E+04 |
| 0.265905E+03 | 0.421627E+04 | 0.275139E+04 | 0.169081E+01 | 0.93464E+01 | 0.123719E+01 | 0.162381E+01 | 0.252948E+04 | 0.103270E+02 |
| 0.954666E+03 | 0.900529E+03 | 0.839788E+03 | 0.774701E+03 | 0.709551E+03 | 0.649759E+03 | 0.598626E+03 | 0.563191E+03 | 0.553050E+03 |
| 0.194659E+00 | 0.443427E+04 | 0.278830E+04 | 0.21708E+01 | 0.415968E+01 | 0.506881E+03 | 0.716197E+03 | -0.147824E-01 | 0.529829E+04 |
| 0.265801E+03 | 0.443427E+04 | 0.278830E+04 | 0.170038E+01 | 0.934853E+01 | 0.118634E+01 | 0.169468E+01 | 0.254902E+04 | 0.108459E+02 |
| 0.973777E+03 | 0.917158E+03 | 0.853858E+03 | 0.786211E+03 | 0.713259E+03 | 0.655417E+03 | 0.602448E+03 | 0.565741E+03 | 0.553199E+03 |
| 0.194759E+00 | 0.467042E+04 | 0.282671E+04 | 0.201608E+01 | 0.470491E+01 | 0.502766E+03 | 0.731073E+03 | -0.151964E-01 | 0.555484E+04 |
| 0.265697E+03 | 0.120284E+04 | 0.202462E+04 | 0.171038E+01 | 0.934354E+01 | 0.113589E+01 | 0.176704E+01 | 0.256927E+04 | 0.113897E+02 |
| 0.994170E+03 | 0.934864E+03 | 0.868699E+03 | 0.798128E+03 | 0.77226E+03 | 0.661467E+03 | 0.606415E+03 | 0.568252E+03 | 0.553478E+03 |
| 0.194859E+00 | 0.492676E+04 | 0.286672E+04 | 0.201503E+01 | 0.470444E+01 | 0.498419E+03 | 0.745957E+03 | -0.156232E-01 | 0.583024E+04 |
| 0.265594E+03 | 0.120781E+04 | 0.203260E+04 | 0.172085E+01 | 0.939970E+01 | 0.108587E+01 | 0.184089E+01 | 0.259027E+04 | 0.119601E+02 |
| 0.101584E+04 | 0.953634E+03 | 0.884355E+03 | 0.810590E+03 | 0.70549E+03 | 0.667850E+03 | 0.610537E+03 | 0.57750E+03 | 0.553871E+03 |

| | | | | | | | | |
|--------------|--------------|--------------|--------------|--------------|--------------|--------------|---------------|--------------|
| 0.194959E+00 | 0.520562E+04 | 0.290844E+04 | 0.201392E+01 | 0.311935E+00 | 0.493821E+03 | 0.760859E+03 | -0.160644E-01 | 0.612647E+04 |
| 0.265491E+03 | 0.121349E+04 | 0.204139E+04 | 0.173183E+00 | 0.901698E-01 | 0.103629E+01 | 0.191622E+01 | 0.261206E+04 | 0.125593E+02 |
| 0.103884E+04 | 0.973523E+03 | 0.900855E+03 | 0.823677E+03 | 0.740293E+03 | 0.674550E+03 | 0.614822E+03 | 0.573258E+03 | 0.554369E+03 |
| 0.195059E+00 | 0.550968E+04 | 0.295197E+04 | 0.201277E+01 | 0.311935E+00 | 0.488948E+03 | 0.775787E+03 | -0.165221E-01 | 0.644568E+04 |
| 0.265391E+03 | 0.121995E+04 | 0.205109E+04 | 0.174335E+00 | 0.901698E-01 | 0.987199E+00 | 0.199305E+01 | 0.263470E+04 | 0.131893E+02 |
| 0.106330E+04 | 0.994616E+03 | 0.918364E+03 | 0.837457E+03 | 0.716510E+03 | 0.681570E+03 | 0.619927E+03 | 0.575795E+03 | 0.554962E+03 |
| 0.195159E+00 | 0.584197E+04 | 0.299745E+04 | 0.201155E+01 | 0.311935E+00 | 0.483777E+03 | 0.790752E+03 | -0.169983E-01 | 0.679014E+04 |
| 0.265292E+03 | 0.122727E+04 | 0.206178E+04 | 0.175578E+00 | 0.901698E-01 | 0.938611E+00 | 0.207137E+01 | 0.265824E+04 | 0.138526E+02 |
| 0.108932E+04 | 0.101701E+04 | 0.936871E+03 | 0.851995E+03 | 0.716510E+03 | 0.638922E+03 | 0.623903E+03 | 0.578379E+03 | 0.555645E+03 |
| 0.195258E+00 | 0.620601E+04 | 0.304500E+04 | 0.201027E+01 | 0.311935E+00 | 0.478277E+03 | 0.805766E+03 | -0.174956E-01 | 0.716243E+04 |
| 0.265193E+03 | 0.123355E+04 | 0.207357E+04 | 0.176823E+00 | 0.901698E-01 | 0.890561E+00 | 0.215119E+01 | 0.268272E+04 | 0.145518E+02 |
| 0.111705E+04 | 0.104083E+04 | 0.956498E+03 | 0.867358E+03 | 0.716510E+03 | 0.696826E+03 | 0.628719E+03 | 0.581024E+03 | 0.556411E+03 |
| 0.195358E+00 | 0.660583E+04 | 0.309475E+04 | 0.200892E+01 | 0.311935E+00 | 0.472419E+03 | 0.820839E+03 | -0.180168E-01 | 0.756540E+04 |
| 0.265095E+03 | 0.124492E+04 | 0.208658E+04 | 0.178169E+00 | 0.901698E-01 | 0.843081E+00 | 0.223252E+01 | 0.270822E+04 | 0.152899E+02 |
| 0.114665E+04 | 0.106621E+04 | 0.977345E+03 | 0.883619E+03 | 0.716510E+03 | 0.704707E+03 | 0.633731E+03 | 0.583741E+03 | 0.557258E+03 |
| 0.195458E+00 | 0.704607E+04 | 0.314686E+04 | 0.200749E+01 | 0.311935E+00 | 0.466165E+03 | 0.835989E+03 | -0.185651E-01 | 0.800217E+04 |
| 0.264999E+03 | 0.125548E+04 | 0.210094E+04 | 0.179592E+00 | 0.901698E-01 | 0.796211E+00 | 0.231535E+01 | 0.273479E+04 | 0.160702E+02 |
| 0.117930E+04 | 0.109328E+04 | 0.999528E+03 | 0.900859E+03 | 0.813011E+03 | 0.713191E+03 | 0.638957E+03 | 0.586544E+03 | 0.558183E+03 |
| 0.195558E+00 | 0.753211E+04 | 0.320149E+04 | 0.200598E+01 | 0.311935E+00 | 0.459476E+03 | 0.851230E+03 | -0.191443E-01 | 0.847627E+04 |
| 0.264905E+03 | 0.126740E+04 | 0.211680E+04 | 0.181098E+00 | 0.901698E-01 | 0.749997E+00 | 0.239971E+01 | 0.276250E+04 | 0.168961E+02 |
| 0.121220E+04 | 0.112221E+04 | 0.102317E+04 | 0.919165E+03 | 0.816293E+03 | 0.722110E+03 | 0.644409E+03 | 0.589443E+03 | 0.559182E+03 |
| 0.195558E+00 | 0.807014E+04 | 0.325881E+04 | 0.200438E+01 | 0.311935E+00 | 0.452305E+03 | 0.866581E+03 | -0.197585E-01 | 0.899151E+04 |
| 0.264812E+03 | 0.128082E+04 | 0.213433E+04 | 0.182695E+00 | 0.901698E-01 | 0.704470E+00 | 0.248559E+01 | 0.279142E+04 | 0.177716E+02 |
| 0.124856E+04 | 0.115317E+04 | 0.104840E+04 | 0.938633E+03 | 0.813011E+03 | 0.731497E+03 | 0.650106E+03 | 0.592448E+03 | 0.560257E+03 |
| 0.195758E+00 | 0.866728E+04 | 0.331898E+04 | 0.200268E+01 | 0.311935E+00 | 0.444601E+03 | 0.882063E+03 | -0.204129E-01 | 0.955211E+04 |
| 0.264717E+03 | 0.129594E+04 | 0.215372E+04 | 0.184394E+00 | 0.901698E-01 | 0.659696E+00 | 0.257302E+01 | 0.282161E+04 | 0.187011E+02 |
| 0.128762E+04 | 0.118637E+04 | 0.107537E+04 | 0.959372E+03 | 0.813011E+03 | 0.741392E+03 | 0.656069E+03 | 0.595571E+03 | 0.561406E+03 |
| 0.195858E+00 | 0.933184E+04 | 0.338221E+04 | 0.200086E+01 | 0.311935E+00 | 0.436304E+03 | 0.897698E+03 | -0.211132E-01 | 0.101626E+05 |
| 0.264630E+03 | 0.131297E+04 | 0.217517E+04 | 0.186204E+00 | 0.901698E-01 | 0.615729E+00 | 0.266200E+01 | 0.285316E+04 | 0.196894E+02 |
| 0.132965E+04 | 0.122201E+04 | 0.110426E+04 | 0.981500E+03 | 0.813011E+03 | 0.751637E+03 | 0.662316E+03 | 0.598822E+03 | 0.562630E+03 |
| 0.195958E+00 | 0.100733E+05 | 0.344866E+04 | 0.199893E+01 | 0.311935E+00 | 0.427347E+03 | 0.913515E+03 | -0.218659E-01 | 0.108280E+05 |
| 0.264541E+03 | 0.133214E+04 | 0.219892E+04 | 0.188136E+00 | 0.901698E-01 | 0.572630E+00 | 0.275255E+01 | 0.288614E+04 | 0.207417E+02 |
| 0.137493E+04 | 0.126034E+04 | 0.113524E+04 | 0.100515E+04 | 0.817939E+03 | 0.762879E+03 | 0.668874E+03 | 0.602212E+03 | 0.563929E+03 |
| 0.196058E+00 | 0.109026E+05 | 0.351853E+04 | 0.199885E+01 | 0.311935E+00 | 0.417651E+03 | 0.929542E+03 | -0.226789E-01 | 0.115533E+05 |
| 0.264455E+03 | 0.135375E+04 | 0.222525E+04 | 0.190204E+00 | 0.901698E-01 | 0.530470E+00 | 0.284470E+01 | 0.292060E+04 | 0.218638E+02 |
| 0.142378E+04 | 0.130162E+04 | 0.116851E+04 | 0.103046E+04 | 0.819579E+03 | 0.774572E+03 | 0.675765E+03 | 0.605753E+03 | 0.565305E+03 |
| 0.196158E+00 | 0.118321E+05 | 0.359199E+04 | 0.199463E+01 | 0.311935E+00 | 0.407129E+03 | 0.945812E+03 | -0.235611E-01 | 0.123439E+05 |
| 0.264371E+03 | 0.137810E+04 | 0.225445E+04 | 0.192432E+00 | 0.901698E-01 | 0.489329E+00 | 0.293846E+01 | 0.295663E+04 | 0.230620E+02 |
| 0.147654E+04 | 0.134611E+04 | 0.120430E+04 | 0.105759E+04 | 0.915022E+03 | 0.786973E+03 | 0.683021E+03 | 0.609457E+03 | 0.566761E+03 |
| 0.196258E+00 | 0.128760E+05 | 0.366918E+04 | 0.199224E+01 | 0.311935E+00 | 0.395681E+03 | 0.962355E+03 | -0.245231E-01 | 0.132049E+05 |
| 0.264289E+03 | 0.140557E+04 | 0.228685E+04 | 0.194809E+00 | 0.901698E-01 | 0.449294E+00 | 0.303386E+01 | 0.299426E+04 | 0.243431E+02 |
| 0.153355E+04 | 0.139413E+04 | 0.124233E+04 | 0.108671E+04 | 0.915478E+03 | 0.800145E+03 | 0.690672E+03 | 0.613337E+03 | 0.568298E+03 |
| 0.196358E+00 | 0.140499E+05 | 0.375022E+04 | 0.198966E+01 | 0.311935E+00 | 0.383190E+03 | 0.979244E+03 | -0.255771E-01 | 0.141412E+05 |
| 0.264209E+03 | 0.143657E+04 | 0.232284E+04 | 0.197381E+00 | 0.901698E-01 | 0.410466E+00 | 0.313093E+01 | 0.303352E+04 | 0.257143E+02 |
| 0.159518E+04 | 0.144598E+04 | 0.128436E+04 | 0.111801E+04 | 0.917370E+03 | 0.814159E+03 | 0.698753E+03 | 0.617407E+03 | 0.569921E+03 |
| 0.196458E+00 | 0.153707E+05 | 0.383516E+04 | 0.198688E+01 | 0.311935E+00 | 0.369528E+03 | 0.996500E+03 | -0.267374E-01 | 0.151562E+05 |
| 0.264133E+03 | 0.147157E+04 | 0.236279E+04 | 0.200161E+00 | 0.901698E-01 | 0.372975E+00 | 0.322971E+01 | 0.307443E+04 | 0.271835E+02 |
| 0.166178E+04 | 0.150198E+04 | 0.132916E+04 | 0.115168E+04 | 0.919830E+03 | 0.829092E+03 | 0.707299E+03 | 0.621682E+03 | 0.571631E+03 |

| | | | | | | | | |
|--------------|--------------|--------------|--------------|--------------|---------------|--------------|---------------|--------------|
| 0.196558E+00 | 0.168561E+05 | 0.392395E+04 | 0.198386E+01 | 0.135358E+00 | 0.354547E+03 | 0.101419E+04 | -0.280203E-01 | 0.162517E+05 |
| 0.264059E+03 | 0.151112E+04 | 0.240717E+04 | 0.203771E+00 | 0.107321E+00 | 0.336891E+00 | 0.333024E+03 | 0.311692E+04 | 0.287587E+02 |
| 0.173371E+04 | 0.156244E+04 | 0.137748E+04 | 0.118793E+00 | 0.107600E+04 | 0.845027E+03 | 0.716354E+03 | 0.626180E+03 | 0.573434E+02 |
| 0.196658E+00 | 0.185233E+05 | 0.401640E+04 | 0.198059E+01 | 0.174780E+00 | 0.338084E+03 | 0.103237E+04 | -0.294447E-01 | 0.174265E+05 |
| 0.263389E+03 | 0.155579E+04 | 0.245640E+04 | 0.206438E+00 | 0.103099E+00 | 0.302411E+00 | 0.343256E+01 | 0.316089E+04 | 0.304477E+02 |
| 0.181123E+04 | 0.162765E+04 | 0.142959E+04 | 0.122698E+04 | 0.103303E+04 | 0.862084E+03 | 0.725962E+03 | 0.630918E+03 | 0.575335E+03 |
| 0.196758E+00 | 0.203869E+05 | 0.411211E+04 | 0.197704E+01 | 0.154736E+00 | 0.319961E+03 | 0.105112E+04 | -0.310323E-01 | 0.185743E+05 |
| 0.263921E+03 | 0.160623E+04 | 0.251076E+04 | 0.209989E+00 | 0.103891E+00 | 0.269675E+00 | 0.353672E+01 | 0.320614E+04 | 0.322584E+02 |
| 0.189451E+04 | 0.169781E+04 | 0.148572E+04 | 0.126902E+04 | 0.103208E+04 | 0.880271E+03 | 0.736172E+03 | 0.635916E+03 | 0.577338E+03 |
| 0.196858E+00 | 0.224560E+05 | 0.421040E+04 | 0.197371E+01 | 0.153283E+00 | 0.299987E+03 | 0.107052E+04 | -0.328068E-01 | 0.199820E+05 |
| 0.263958E+03 | 0.166313E+04 | 0.257126E+04 | 0.213854E+00 | 0.103698E+00 | 0.238861E+03 | 0.364279E+01 | 0.325233E+04 | 0.341972E+02 |
| 0.198355E+04 | 0.177304E+04 | 0.154603E+04 | 0.131425E+04 | 0.103303E+04 | 0.899780E+03 | 0.747036E+03 | 0.641196E+03 | 0.579451E+03 |
| 0.196958E+00 | 0.247286E+05 | 0.431023E+04 | 0.196896E+01 | 0.148479E+00 | 0.277968E+03 | 0.109065E+04 | -0.347942E-01 | 0.213267E+05 |
| 0.263800E+03 | 0.172715E+04 | 0.263764E+04 | 0.218061E+00 | 0.103519E+00 | 0.210166E+00 | 0.375084E+01 | 0.329897E+04 | 0.362691E+02 |
| 0.207809E+04 | 0.185329E+04 | 0.161063E+04 | 0.136282E+04 | 0.103683E+04 | 0.920685E+03 | 0.758613E+03 | 0.646779E+03 | 0.581679E+03 |
| 0.197058E+00 | 0.271850E+05 | 0.441005E+04 | 0.196438E+01 | 0.138391E+00 | 0.253718E+03 | 0.111164E+04 | -0.370211E-01 | 0.226727E+05 |
| 0.263745E+03 | 0.179890E+04 | 0.271030E+04 | 0.222637E+00 | 0.103556E+00 | 0.183804E+00 | 0.386094E+01 | 0.334535E+04 | 0.384759E+02 |
| 0.217746E+04 | 0.193822E+04 | 0.167944E+04 | 0.141481E+04 | 0.103682E+04 | 0.943090E+03 | 0.770960E+03 | 0.652593E+03 | 0.584030E+03 |
| 0.197158E+00 | 0.297788E+05 | 0.450776E+04 | 0.195941E+01 | 0.131091E+00 | 0.227081E+03 | 0.113355E+04 | -0.395135E-01 | 0.239690E+05 |
| 0.263696E+03 | 0.187885E+04 | 0.278921E+04 | 0.227603E+00 | 0.103519E+00 | 0.160010E+00 | 0.397319E+01 | 0.339052E+04 | 0.408151E+02 |
| 0.228053E+04 | 0.202721E+04 | 0.175219E+04 | 0.147021E+04 | 0.103134E+04 | 0.967095E+03 | 0.784142E+03 | 0.658965E+03 | 0.585512E+03 |
| 0.197258E+00 | 0.324275E+05 | 0.460057E+04 | 0.195404E+01 | 0.103654E+00 | 0.197959E+03 | 0.115652E+04 | -0.422930E-01 | 0.251476E+05 |
| 0.263653E+03 | 0.196714E+04 | 0.287397E+04 | 0.232971E+00 | 0.103808E+00 | 0.139028E+00 | 0.408768E+01 | 0.34323E+04 | 0.432780E+02 |
| 0.238557E+04 | 0.211910E+04 | 0.182833E+04 | 0.152883E+04 | 0.104243E+04 | 0.992786E+03 | 0.798221E+03 | 0.665623E+03 | 0.589135E+03 |
| 0.197358E+00 | 0.350058E+05 | 0.468508E+04 | 0.194827E+01 | 0.103715E+00 | 0.166349E+03 | 0.118065E+04 | -0.453733E-01 | 0.261255E+05 |
| 0.263615E+03 | 0.206352E+04 | 0.296372E+04 | 0.238736E+00 | 0.103696E+00 | 0.211109E+00 | 0.420453E+01 | 0.347199E+04 | 0.458485E+02 |
| 0.248997E+04 | 0.221227E+04 | 0.190693E+04 | 0.159032E+04 | 0.103605E+04 | 0.102022E+04 | 0.813258E+03 | 0.672697E+03 | 0.591907E+03 |
| 0.197458E+00 | 0.373461E+05 | 0.475742E+04 | 0.194213E+01 | 0.104672E+00 | 0.132388E+03 | 0.120604E+04 | -0.487544E-01 | 0.268119E+05 |
| 0.263585E+03 | 0.216708E+04 | 0.305706E+04 | 0.244874E+00 | 0.104876E+00 | 0.106493E+00 | 0.432385E+01 | 0.350508E+04 | 0.485016E+02 |
| 0.259075E+04 | 0.230452E+04 | 0.198667E+04 | 0.165404E+04 | 0.103201E+04 | 0.104943E+04 | 0.829308E+03 | 0.680219E+03 | 0.594840E+03 |
| 0.197558E+00 | 0.392525E+05 | 0.481357E+04 | 0.193567E+01 | 0.104688E+00 | 0.963827E+02 | 0.123276E+04 | -0.524185E-01 | 0.271203E+05 |
| 0.263562E+03 | 0.227622E+04 | 0.315203E+04 | 0.251330E+00 | 0.104803E+00 | 0.953989E-01 | 0.444577E+01 | 0.353075E+04 | 0.512030E+02 |
| 0.268427E+04 | 0.239314E+04 | 0.206580E+04 | 0.171909E+04 | 0.103999E+04 | 0.108039E+04 | 0.846417E+03 | 0.688223E+03 | 0.597943E+03 |
| 0.197657E+00 | 0.405317E+05 | 0.484990E+04 | 0.192896E+01 | 0.104999E+00 | 0.588292E+02 | 0.126089E+04 | -0.563255E-01 | 0.269863E+05 |
| 0.26345E+03 | 0.238854E+04 | 0.324622E+04 | 0.258026E+00 | 0.104751E+00 | 0.880033E-01 | 0.457044E+01 | 0.354741E+04 | 0.539115E+02 |
| 0.276584E+04 | 0.247518E+04 | 0.214224E+04 | 0.178429E+04 | 0.104295E+04 | 0.111238E+04 | 0.864614E+03 | 0.696738E+03 | 0.601235E+03 |
| 0.197757E+00 | 0.410349E+05 | 0.486380E+04 | 0.192213E+01 | 0.104901E+00 | 0.203907E+02 | 0.129042E+04 | -0.604140E-01 | 0.263851E+05 |
| 0.263537E+03 | 0.250106E+04 | 0.333698E+04 | 0.264856E+00 | 0.104721E+00 | 0.844222E-01 | 0.469799E+01 | 0.355391E+04 | 0.565807E+02 |
| 0.283316E+04 | 0.254773E+04 | 0.221373E+04 | 0.184819E+04 | 0.104990E+04 | 0.114704E+04 | 0.883906E+03 | 0.705794E+03 | 0.60421E+03 |
| 0.197857E+00 | 0.406976E+05 | 0.485416E+04 | 0.191528E+01 | 0.104985E+00 | -0.181631E+02 | 0.132133E+04 | -0.646059E-01 | 0.253414E+05 |
| 0.263536E+03 | 0.261047E+04 | 0.342179E+04 | 0.271699E+00 | 0.104713E+00 | 0.846983E-01 | 0.482856E+01 | 0.354974E+04 | 0.591653E+02 |
| 0.268691E+04 | 0.260835E+04 | 0.227814E+04 | 0.190925E+04 | 0.104302E+04 | 0.118228E+04 | 0.904269E+03 | 0.715416E+03 | 0.608416E+03 |
| 0.197957E+00 | 0.395587E+05 | 0.482163E+04 | 0.190854E+01 | 0.104243E+00 | -0.560517E+02 | 0.135355E+04 | -0.688152E-01 | 0.239272E+05 |
| 0.263543E+03 | 0.271359E+04 | 0.349861E+04 | 0.270433E+00 | 0.104730E+00 | 0.887962E-01 | 0.496222E+01 | 0.353518E+04 | 0.616241E+02 |
| 0.292107E+04 | 0.265545E+04 | 0.233366E+04 | 0.196597E+04 | 0.104798E+04 | 0.121834E+04 | 0.925641E+03 | 0.725622E+03 | 0.612338E+03 |
| 0.198057E+00 | 0.377492E+05 | 0.476847E+04 | 0.190203E+01 | 0.104399E+00 | -0.925671E+02 | 0.138696E+04 | -0.729584E-01 | 0.222471E+05 |
| 0.263558E+03 | 0.280775E+04 | 0.356607E+04 | 0.284947E+00 | 0.104772E+00 | 0.866059E-01 | 0.509930E+01 | 0.35119E+04 | 0.639261E+02 |
| 0.2806E+04 | 0.268842E+04 | 0.237909E+04 | 0.201702E+04 | 0.104751E+04 | 0.125476E+04 | 0.947923E+03 | 0.75421E+03 | 0.616495E+03 |

| | | | | | | | | |
|--------------|--------------|--------------|--------------|--------------|---------------|--------------|---------------|--------------|
| 0.198157E+00 | 0.354561E+05 | 0.469810E+04 | 0.189581E+01 | 0.115121E+00 | -0.127150E+03 | 0.142140E+04 | -0.769636E-01 | 0.204173E+05 |
| 0.263579E+03 | 0.289107E+04 | 0.362355E+04 | 0.291154E+00 | 0.11839E+00 | 0.107955E+00 | 0.523970E+01 | 0.347926E+04 | 0.660508E+02 |
| 0.293326E+04 | 0.270771E+04 | 0.241396E+04 | 0.206145E+04 | 0.167242E+04 | 0.129105E+00 | 0.970970E+03 | 0.747812E+03 | 0.620901E+03 |
| 0.198257E+00 | 0.328798E+05 | 0.461450E+04 | 0.188997E+01 | 0.119622E+00 | -0.159430E+03 | 0.145672E+04 | -0.807760E-01 | 0.185445E+05 |
| 0.263608E+03 | 0.296252E+04 | 0.367116E+04 | 0.296995E+00 | 0.12934E+00 | 0.12627E+00 | 0.538360E+01 | 0.344111E+04 | 0.679894E+02 |
| 0.292714E+04 | 0.271451E+04 | 0.243842E+04 | 0.209870E+04 | 0.171382E+04 | 0.132659E+04 | 0.994608E+03 | 0.759780E+03 | 0.625566E+03 |
| 0.198357E+00 | 0.301985E+05 | 0.452161E+04 | 0.188452E+01 | 0.115068E+00 | -0.189214E+03 | 0.149273E+04 | -0.843590E-01 | 0.167141E+05 |
| 0.263643E+03 | 0.302186E+04 | 0.370947E+04 | 0.302435E+00 | 0.114055E+00 | 0.140377E+00 | 0.553106E+01 | 0.339850E+04 | 0.697425E+02 |
| 0.290430E+04 | 0.271055E+04 | 0.245322E+04 | 0.212866E+04 | 0.173114E+04 | 0.136119E+04 | 0.101862E+04 | 0.772298E+03 | 0.630499E+03 |
| 0.198457E+00 | 0.275498E+05 | 0.442300E+04 | 0.187948E+01 | 0.131381E+00 | -0.216457E+03 | 0.152926E+04 | -0.876921E-01 | 0.149855E+05 |
| 0.263683E+03 | 0.306945E+04 | 0.373939E+04 | 0.307468E+00 | 0.12203E+00 | 0.160954E+00 | 0.568215E+01 | 0.335300E+04 | 0.713179E+02 |
| 0.287334E+04 | 0.269777E+04 | 0.245942E+04 | 0.215154E+04 | 0.178405E+04 | 0.139411E+04 | 0.104279E+04 | 0.785324E+03 | 0.635707E+03 |
| 0.198557E+00 | 0.250274E+05 | 0.432164E+04 | 0.187485E+01 | 0.138484E+00 | -0.241262E+03 | 0.156615E+04 | -0.907676E-01 | 0.133935E+05 |
| 0.263728E+03 | 0.310604E+04 | 0.376192E+04 | 0.312101E+00 | 0.125380E+00 | 0.184108E+00 | 0.583692E+01 | 0.330594E+04 | 0.727273E+02 |
| 0.283660E+04 | 0.267805E+04 | 0.245829E+04 | 0.216786E+04 | 0.171242E+04 | 0.142508E+04 | 0.106689E+04 | 0.798801E+03 | 0.641192E+03 |
| 0.19857E+00 | 0.226859E+05 | 0.421982E+04 | 0.187059E+01 | 0.145306E+00 | -0.263744E+03 | 0.160323E+04 | -0.935870E-01 | 0.119535E+05 |
| 0.263833E+03 | 0.31261E+04 | 0.377811E+04 | 0.316355E+00 | 0.127585E+00 | 0.209602E+00 | 0.59538E+01 | 0.325838E+04 | 0.739836E+02 |
| 0.279604E+04 | 0.265314E+04 | 0.245109E+04 | 0.217827E+04 | 0.153632E+04 | 0.145385E+04 | 0.109068E+04 | 0.812664E+03 | 0.646957E+03 |
| 0.198757E+00 | 0.205506E+05 | 0.411925E+04 | 0.186668E+01 | 0.154777E+00 | -0.284095E+03 | 0.164037E+04 | -0.961581E-01 | 0.106674E+05 |
| 0.263833E+03 | 0.315022E+04 | 0.378891E+04 | 0.320256E+00 | 0.123818E+00 | 0.237213E+00 | 0.615755E+01 | 0.321109E+04 | 0.751095E+02 |
| 0.275324E+04 | 0.262449E+04 | 0.243904E+04 | 0.218332E+04 | 0.165594E+04 | 0.148023E+04 | 0.111396E+04 | 0.826837E+03 | 0.652999E+03 |
| 0.198857E+00 | 0.186266E+05 | 0.402109E+04 | 0.186310E+01 | 0.163837E+00 | -0.302517E+03 | 0.167745E+04 | -0.984912E-01 | 0.952854E+04 |
| 0.263892E+03 | 0.315992E+04 | 0.379519E+04 | 0.323833E+00 | 0.130079E+00 | 0.266743E+00 | 0.632344E+01 | 0.316465E+04 | 0.761124E+02 |
| 0.270938E+04 | 0.259332E+04 | 0.242321E+04 | 0.218435E+04 | 0.187157E+04 | 0.150416E+04 | 0.113655E+04 | 0.841238E+03 | 0.659301E+03 |
| 0.198957E+00 | 0.169063E+05 | 0.392612E+04 | 0.185981E+01 | 0.174429E+00 | -0.319205E+03 | 0.171436E+04 | -0.100599E+00 | 0.852541E+04 |
| 0.263954E+03 | 0.316272E+04 | 0.379767E+04 | 0.321116E+00 | 0.131369E+00 | 0.298009E+00 | 0.649303E+01 | 0.311942E+04 | 0.770909E+02 |
| 0.266534E+04 | 0.256060E+04 | 0.240453E+04 | 0.218148E+04 | 0.188358E+04 | 0.152560E+04 | 0.115829E+04 | 0.855784E+03 | 0.665864E+03 |
| 0.199057E+00 | 0.153754E+05 | 0.383483E+04 | 0.185679E+01 | 0.183505E+00 | -0.334347E+03 | 0.175101E+04 | -0.102495E+00 | 0.764445E+04 |
| 0.264019E+03 | 0.315952E+04 | 0.379700E+04 | 0.330135E+00 | 0.132686E+00 | 0.330850E+00 | 0.666630E+01 | 0.307566E+04 | 0.778121E+02 |
| 0.262176E+04 | 0.252706E+04 | 0.238376E+04 | 0.217556E+04 | 0.189232E+04 | 0.154462E+04 | 0.117906E+04 | 0.870391E+03 | 0.672669E+03 |
| 0.199157E+00 | 0.140164E+05 | 0.374743E+04 | 0.185401E+01 | 0.194019E+00 | -0.348115E+03 | 0.178732E+04 | -0.104193E+00 | 0.687171E+04 |
| 0.264088E+03 | 0.315114E+04 | 0.379369E+04 | 0.332915E+00 | 0.114031E+00 | 0.365121E+00 | 0.684321E+01 | 0.303349E+04 | 0.785331E+02 |
| 0.257907E+04 | 0.249327E+04 | 0.236152E+04 | 0.216717E+04 | 0.119820E+04 | 0.156132E+04 | 0.119878E+04 | 0.884978E+03 | 0.679701E+03 |
| 0.199257E+00 | 0.128110E+05 | 0.366402E+04 | 0.185144E+01 | 0.204933E+00 | -0.360665E+03 | 0.182332E+04 | -0.105704E+00 | 0.619388E+04 |
| 0.264159E+03 | 0.313831E+04 | 0.378818E+04 | 0.335482E+00 | 0.115404E+00 | 0.400695E+00 | 0.702374E+01 | 0.299299E+04 | 0.791822E+02 |
| 0.253756E+04 | 0.245963E+04 | 0.233832E+04 | 0.215680E+04 | 0.190155E+04 | 0.157580E+04 | 0.121737E+04 | 0.899467E+03 | 0.686938E+03 |
| 0.199357E+00 | 0.117414E+05 | 0.358457E+04 | 0.184906E+01 | 0.216212E+00 | -0.372132E+03 | 0.185865E+04 | -0.107041E+00 | 0.559873E+04 |
| 0.264232E+03 | 0.312165E+04 | 0.378083E+04 | 0.337858E+00 | 0.115804E+00 | 0.437458E+00 | 0.720783E+01 | 0.295418E+04 | 0.797682E+02 |
| 0.249741E+04 | 0.242645E+04 | 0.231456E+04 | 0.214488E+04 | 0.190273E+04 | 0.158823E+04 | 0.123480E+04 | 0.913788E+03 | 0.694360E+03 |
| 0.199457E+00 | 0.107911E+05 | 0.350898E+04 | 0.184685E+01 | 0.277825E+00 | -0.382640E+03 | 0.189357E+04 | -0.108216E+00 | 0.507527E+04 |
| 0.264308E+03 | 0.310171E+04 | 0.377195E+04 | 0.340081E+00 | 0.116230E+00 | 0.475309E+00 | 0.739544E+01 | 0.291701E+04 | 0.802986E+02 |
| 0.245872E+04 | 0.239394E+04 | 0.229053E+04 | 0.213176E+04 | 0.190204E+04 | 0.159876E+04 | 0.125107E+04 | 0.927676E+03 | 0.701942E+03 |
| 0.199557E+00 | 0.994544E+04 | 0.343709E+04 | 0.184479E+01 | 0.279744E+00 | -0.392294E+03 | 0.192793E+04 | -0.109238E+00 | 0.461391E+04 |
| 0.264386E+03 | 0.307898E+04 | 0.376178E+04 | 0.342111E+00 | 0.119683E+00 | 0.514158E+00 | 0.758651E+01 | 0.288146E+04 | 0.807802E+02 |
| 0.242153E+04 | 0.236223E+04 | 0.226648E+04 | 0.211774E+04 | 0.199976E+04 | 0.160755E+04 | 0.126617E+04 | 0.941677E+03 | 0.709663E+03 |
| 0.199657E+00 | 0.919116E+04 | 0.336875E+04 | 0.184288E+01 | 0.271945E+00 | -0.401188E+03 | 0.196169E+04 | -0.110119E+00 | 0.420626E+04 |
| 0.264466E+03 | 0.305387E+04 | 0.375052E+04 | 0.344022E+00 | 0.141162E+00 | 0.553927E+00 | 0.778099E+01 | 0.284745E+04 | 0.812187E+02 |
| 0.238584E+04 | 0.233143E+04 | 0.224425E+04 | 0.210306E+04 | 0.17613E+04 | 0.161475E+04 | 0.128013E+04 | 0.955142E+03 | 0.717496E+03 |

| | | | | | | | | |
|--------------|--------------|--------------|--------------|--------------|---------------|--------------|---------------|--------------|
| 0.199757E+00 | 0.851676E+04 | 0.330375E+04 | 0.184109E+01 | 0.244406E+00 | -0.409404E+03 | 0.199483E+04 | -0.110867E+00 | 0.384514E+04 |
| 0.264547E+03 | 0.302675E+04 | 0.373836E+04 | 0.345808E+00 | 0.112666E+00 | 0.594544E+00 | 0.797882E+01 | 0.281492E+04 | 0.816190E+02 |
| 0.235164E+04 | 0.230158E+04 | 0.221897E+04 | 0.208792E+04 | 0.189137E+04 | 0.162052E+04 | 0.129239E+04 | 0.968234E+03 | 0.725416E+03 |
| 0.199857E+00 | 0.791223E+04 | 0.324132E+04 | 0.183941E+01 | 0.277108E+00 | -0.417012E+03 | 0.202733E+04 | -0.111491E+00 | 0.352435E+04 |
| 0.264630E+03 | 0.299791E+04 | 0.372543E+04 | 0.347481E+00 | 0.144195E+00 | 0.635945E+00 | 0.179939E+01 | 0.278379E+04 | 0.819855E+02 |
| 0.231888E+04 | 0.227271E+04 | 0.219575E+04 | 0.207248E+04 | 0.188566E+04 | 0.162500E+04 | 0.130477E+04 | 0.980919E+03 | 0.733399E+03 |
| 0.199958E+00 | 0.736885E+04 | 0.318307E+04 | 0.183783E+01 | 0.290033E+00 | -0.424075E+03 | 0.205916E+04 | -0.112000E+00 | 0.323889E+04 |
| 0.264715E+03 | 0.296766E+04 | 0.371186E+04 | 0.349051E+00 | 0.147499E+00 | 0.678074E+00 | 0.838426E+01 | 0.275401E+04 | 0.823219E+02 |
| 0.228750E+04 | 0.224482E+04 | 0.217299E+04 | 0.205687E+04 | 0.187916E+04 | 0.162832E+04 | 0.131553E+04 | 0.993172E+03 | 0.741422E+03 |
| 0.200058E+00 | 0.687911E+04 | 0.312701E+04 | 0.183635E+01 | 0.303156E+00 | -0.430647E+03 | 0.209031E+04 | -0.112401E+00 | 0.298328E+04 |
| 0.264801E+03 | 0.293622E+04 | 0.369774E+04 | 0.350529E+00 | 0.147326E+00 | 0.720879E+00 | 0.859173E+01 | 0.272547E+04 | 0.826314E+02 |
| 0.225746E+04 | 0.221792E+04 | 0.215073E+04 | 0.204119E+04 | 0.187202E+04 | 0.163060E+04 | 0.132552E+04 | 0.100498E+04 | 0.749462E+03 |
| 0.200158E+00 | 0.643502E+04 | 0.307335E+04 | 0.183468E+01 | 0.315492E+00 | -0.436776E+03 | 0.212078E+04 | -0.112795E+00 | 0.276504E+04 |
| 0.264888E+03 | 0.290588E+04 | 0.368374E+04 | 0.352192E+00 | 0.148927E+00 | 0.764315E+00 | 0.880229E+01 | 0.264748E+04 | 0.829172E+02 |
| 0.222880E+04 | 0.219199E+04 | 0.212902E+04 | 0.202554E+04 | 0.186435E+04 | 0.163196E+04 | 0.133420E+04 | 0.101632E+04 | 0.757495E+03 |
| 0.200258E+00 | 0.603162E+04 | 0.302201E+04 | 0.183289E+01 | 0.329998E+00 | -0.442503E+03 | 0.215060E+04 | -0.113196E+00 | 0.257263E+04 |
| 0.264976E+03 | 0.287803E+04 | 0.366966E+04 | 0.353979E+00 | 0.150551E+00 | 0.809339E+00 | 0.901586E+01 | 0.251140E+04 | 0.831830E+02 |
| 0.220158E+04 | 0.216717E+04 | 0.210734E+04 | 0.200999E+04 | 0.185626E+04 | 0.163250E+04 | 0.134221E+04 | 0.102719E+04 | 0.765504E+03 |
| 0.200358E+00 | 0.565561E+04 | 0.297303E+04 | 0.183125E+01 | 0.343674E+00 | -0.447864E+03 | 0.217976E+04 | -0.113474E+00 | 0.238961E+04 |
| 0.265067E+03 | 0.284781E+04 | 0.365593E+04 | 0.356108E+00 | 0.152197E+00 | 0.852913E+00 | 0.923238E+01 | 0.237667E+04 | 0.834301E+02 |
| 0.217539E+04 | 0.214327E+04 | 0.208749E+04 | 0.199462E+04 | 0.184784E+04 | 0.163231E+04 | 0.134942E+04 | 0.103758E+04 | 0.773468E+03 |
| 0.200458E+00 | 0.532644E+04 | 0.292627E+04 | 0.182976E+01 | 0.357508E+00 | -0.452893E+03 | 0.220825E+04 | -0.113637E+00 | 0.221546E+04 |
| 0.265158E+03 | 0.281619E+04 | 0.363994E+04 | 0.357096E+00 | 0.153865E+00 | 0.898004E+00 | 0.945178E+01 | 0.224282E+04 | 0.836593E+02 |
| 0.215014E+04 | 0.212016E+04 | 0.206760E+04 | 0.197946E+04 | 0.183918E+04 | 0.163148E+04 | 0.135587E+04 | 0.104751E+04 | 0.781369E+03 |
| 0.200558E+00 | 0.502895E+04 | 0.289158E+04 | 0.182441E+01 | 0.371490E+00 | -0.457620E+03 | 0.223605E+04 | -0.113694E+00 | 0.204945E+04 |
| 0.265258E+03 | 0.278338E+04 | 0.362448E+04 | 0.358448E+00 | 0.155555E+00 | 0.943579E+00 | 0.967400E+01 | 0.210934E+04 | 0.838716E+02 |
| 0.212556E+04 | 0.209775E+04 | 0.204832E+04 | 0.196451E+04 | 0.183033E+04 | 0.163009E+04 | 0.136162E+04 | 0.105697E+04 | 0.789192E+03 |
| 0.200658E+00 | 0.475128E+04 | 0.283884E+04 | 0.182718E+01 | 0.385612E+00 | -0.462071E+03 | 0.226316E+04 | -0.113655E+00 | 0.189070E+04 |
| 0.265342E+03 | 0.274960E+04 | 0.360872E+04 | 0.359674E+00 | 0.157265E+00 | 0.989610E+00 | 0.989896E+01 | 0.197565E+04 | 0.840676E+02 |
| 0.210197E+04 | 0.207595E+04 | 0.202929E+04 | 0.194975E+04 | 0.182133E+04 | 0.162820E+04 | 0.136671E+04 | 0.106597E+04 | 0.796923E+03 |
| 0.200758E+00 | 0.449680E+04 | 0.279791E+04 | 0.182606E+01 | 0.399886E+00 | -0.466270E+03 | 0.228956E+04 | -0.113522E+00 | 0.173825E+04 |
| 0.265436E+03 | 0.271501E+04 | 0.359271E+04 | 0.360783E+00 | 0.157995E+00 | 0.103607E+01 | 0.101266E+02 | 0.184102E+04 | 0.842482E+02 |
| 0.207889E+04 | 0.205473E+04 | 0.201079E+04 | 0.193519E+04 | 0.182221E+04 | 0.162587E+04 | 0.137120E+04 | 0.107452E+04 | 0.804549E+03 |
| 0.200858E+00 | 0.426304E+04 | 0.275870E+04 | 0.182506E+01 | 0.414243E+00 | -0.470236E+03 | 0.231525E+04 | -0.113306E+00 | 0.159101E+04 |
| 0.265531E+03 | 0.267976E+04 | 0.357652E+04 | 0.361780E+00 | 0.160747E+00 | 0.108293E+01 | 0.103568E+02 | 0.170462E+04 | 0.844138E+02 |
| 0.205639E+04 | 0.203401E+04 | 0.199257E+04 | 0.192081E+04 | 0.199300E+04 | 0.162315E+04 | 0.137513E+04 | 0.108263E+04 | 0.812057E+03 |
| 0.200958E+00 | 0.404784E+04 | 0.272108E+04 | 0.182417E+01 | 0.428738E+00 | -0.473990E+03 | 0.234023E+04 | -0.113013E+00 | 0.144772E+04 |
| 0.265627E+03 | 0.264398E+04 | 0.356017E+04 | 0.362671E+00 | 0.162517E+00 | 0.113017E+01 | 0.105896E+02 | 0.156534E+04 | 0.845648E+02 |
| 0.203440E+04 | 0.201374E+04 | 0.197439E+04 | 0.196660E+04 | 0.179372E+04 | 0.162009E+04 | 0.137853E+04 | 0.109031E+04 | 0.819437E+03 |
| 0.201058E+00 | 0.384930E+04 | 0.268438E+04 | 0.182337E+01 | 0.445344E+00 | -0.477548E+03 | 0.236450E+04 | -0.112648E+00 | 0.159685E+04 |
| 0.265724E+03 | 0.260779E+04 | 0.354372E+04 | 0.363461E+00 | 0.164305E+00 | 0.117778E+01 | 0.108248E+02 | 0.142170E+04 | 0.847018E+02 |
| 0.201285E+04 | 0.199387E+04 | 0.195743E+04 | 0.182555E+04 | 0.171438E+04 | 0.161670E+04 | 0.138144E+04 | 0.109757E+04 | 0.826686E+03 |
| 0.201158E+00 | 0.366575E+04 | 0.265078E+04 | 0.182268E+01 | 0.43056E+00 | -0.480924E+03 | 0.238806E+04 | -0.112215E+00 | 0.116632E+04 |
| 0.265821E+03 | 0.257127E+04 | 0.352718E+04 | 0.364152E+00 | 0.166112E+00 | 0.122574E+01 | 0.110625E+02 | 0.127156E+04 | 0.848247E+02 |
| 0.199168E+04 | 0.197434E+04 | 0.194023E+04 | 0.187866E+04 | 0.177499E+04 | 0.161304E+04 | 0.138391E+04 | 0.110444E+04 | 0.843759E+03 |
| 0.201258E+00 | 0.349577E+04 | 0.261692E+04 | 0.182208E+01 | 0.42869E+00 | -0.484133E+03 | 0.241091E+04 | -0.111720E+00 | 0.102377E+04 |
| 0.265918E+03 | 0.253450E+04 | 0.351060E+04 | 0.364746E+00 | 0.167937E+00 | 0.127402E+01 | 0.113024E+02 | 0.111169E+04 | 0.849335E+02 |
| 0.201307E+04 | 0.195507E+04 | 0.192377E+04 | 0.186488E+04 | 0.176555E+04 | 0.160911E+04 | 0.138596E+04 | 0.11192E+04 | 0.840746E+03 |

APPENDIX B

ISENTROPIC EQUILIBRIUM COMBUSTION CODE

APPENDIX B

ISENTROPIC EQUILIBRIUM COMBUSTION CODE

Adiabatic Compression Program

An existing equilibrium combustion program has been modified to calculate the properties of an STG test gas mixture at various points along an isentrope. The computer code uses an internal listing of constituents and their thermal properties to dictate the instantaneous composition and thermal properties of the STG test gas at any specified pressure.

Input

Input consists of an initial temperature and pressure, along with 25 other pressure values. The pressure schedule ranges from atmospheric to 500 MPa in 20 MPa steps but the input pressures must be specified in atmospheres. Also, for every constituent in the STG test mixture, a "reactant" card must be submitted that gives the program its initial composition and mole fraction. "Omit" cards may also be submitted which exclude the indicated species from consideration in any reaction processes. Solid carbon, or C(s) is routinely omitted from STG runs because of the high C(s) concentration already present in the specimen surface which would inhibit any further formation.

Operation

The initial mixture and mixture ratios are analyzed to determine which chemical elements are present. The number of gram atoms of each initial constituent is calculated along with the total molecular weight and enthalpy of the mixture.

The taped thermal data is searched and the names and thermal properties of possible compounds which could be formed from the available atoms are extracted. This list is then compared to the "omit" cards and the net list of species to be considered is printed.

The initial composition is then varied in an attempt to minimize the Gibbs free energy of the mixture. Species with mole fractions of less than 10^{-7} at any iteration, are dropped from consideration. The initial number of atoms of each element present must, of course, remain the same.

The program calculates the entropy of the initial composition, which is then held constant. For the next value in the pressure schedule, a corresponding temperature is estimated. Based on this estimated temperature a new equilibrium composition and mixture entropy are calculated. If the new entropy and the fixed entropy agree, the program advances to the next pressure value and the procedure is repeated. If the entropies do not agree, the temperature estimate and the equilibrium calculation are iterated until the entropies do agree.

After the first 13 pressure values have been used by the program, their corresponding equilibrium and thermal values for the STG test gas mixture will be output. Then the remaining 13 groups of data will be calculated and printed. Upon completion of the pressure schedule, the program will look for a new test gas mixture in the input.

PT C O N AR
1 47.509 -117.819 -12.135 -19.217 16.000

THE TEMPERATURE= 0.2981E+03 IS OUT OF RANGE FOR POINT 1

2 -10.079 -18.106 -11.095 -15.341 15.000
3 -10.162 -17.950 -11.097 -15.319 2.000
4 -10.238 -17.807 -11.099 -15.299 2.000
5 -10.309 -17.674 -11.101 -15.280 2.000
6 -10.372 -17.552 -11.103 -15.262 2.000
7 -10.431 -17.438 -11.105 -15.245 2.000
8 -10.486 -17.332 -11.106 -15.228 2.000
9 -10.537 -17.233 -11.108 -15.212 2.000
10 -10.584 -17.140 -11.110 -15.197 2.000
11 -10.628 -17.053 -11.111 -15.183 2.000
12 -10.669 -16.971 -11.113 -15.169 2.000
13 -10.708 -16.894 -11.114 -15.155 2.000

THERMODYNAMIC EQUILIBRIUM PROPERTIES AT ASSIGNED

ENTROPY AND PRESSURE

CASE NO. 1

CHEMICAL FORMULA

FUEL C 1.00000 O 1.00000
FUEL C 1.00000 O 2.00000
FUEL N 2.00000
FUEL AR 1.00000

O/F= 0.0 PERCENT FUEL=100.0000 EQUIVALENCE RATIO= 1.7368 REACTANT DENSITY= 0.0

MOLES ENERGY STATE TEMP DENSITY
CAL/MOL DEG K G/CC
0.14000 -26416.152 G 298.15 0.0
0.02500 -94048.312 G 298.15 0.0
0.29000 0.0 G 298.15 0.0
0.54500 0.0 G 298.15 0.0

THERMODYNAMIC PROPERTIES

P, ATM 0.999 1579.10 1677.79 1776.48 1875.18 1973.87 2072.56 2171.26 2269.95 2368.64 2467.34 2566.03 2664.72

T, DEG K 298 2958 3010 3059 3107 3153 3197 3240 3281 3321 3359 3397 3435

RHO, G/CC 1.4271-3 2.2717-1 2.3720-1 2.4707-1 2.5679-1 2.6637-1 2.7582-1 2.8515-1 2.9437-1 3.0348-1 3.1249-1 3.2140-1 3.3023-1

H, CAL/G -173.2 328.0 338.3 348.2 357.7 366.8 375.6 384.2 392.4 400.4 408.2 415.7 423.0

S, CAL/(G)(K) 1.2434 1.2434 1.2434 1.2434 1.2434 1.2434 1.2434 1.2434 1.2434 1.2434 1.2434 1.2434 1.2434

M, MOL VT 34.917 34.916 34.915 34.914 34.914 34.914 34.913 34.912 34.912 34.911 34.910 34.909 34.908

(DLV/DLP)T -1.00000 -1.00002 -1.00003 -1.00004 -1.00005 -1.00006 -1.00007 -1.00008 -1.00009 -1.00011 -1.00013 -1.00014 -1.00015

(DLV/DLP)P 1.00000 1.00007 1.00013 1.00010 1.00012 1.00015 1.00017 1.00020 1.00023 1.00026 1.00030 1.00034 1.00038

CP, CAL/(G)(K) 0.1696 0.1984 0.1987 0.1990 0.1994 0.1998 0.2002 0.2007 0.2011 0.2016 0.2021 0.2026 0.2031

GAMMA (S) 1.5049 1.4031 1.4023 1.4015 1.4007 1.3998 1.3989 1.3980 1.3971 1.3961 1.3951 1.3942 1.3931

SOM VEL,M/SEC 326.9 994.1 1002.5 1010.5 1018.0 1025.2 1032.0 1038.6 1044.8 1050.8 1056.5 1062.0 1067.3

MOLE FRACTIONS

AR 0.54500 0.54498 0.54497 0.54496 0.54495 0.54495 0.54493 0.54492 0.54491 0.54490 0.54488 0.54497 0.54485

CO 0.14000 0.14008 0.14010 0.14012 0.14015 0.14018 0.14021 0.14025 0.14029 0.14033 0.14038 0.14043 0.14048

CO2 0.02500 0.02491 0.02489 0.02487 0.02484 0.02480 0.02477 0.02473 0.02468 0.02464 0.02458 0.02453 0.02447

NO 0.0 0.00008 0.00010 0.00012 0.00015 0.00017 0.00020 0.00024 0.00028 0.00031 0.00036 0.00040 0.00045

N2 0.29000 0.28995 0.28993 0.28992 0.28990 0.28988 0.28986 0.28984 0.28981 0.28979 0.28976 0.28973 0.28969

O 0.0 0.00000 0.00000 0.00001 0.00001 0.00001 0.00001 0.00001 0.00001 0.00002 0.00003 0.00003 0.00003

O2 0.0 0.00000 0.00000 0.00000 0.00000 0.00000 0.00001 0.00001 0.00001 0.00001 0.00001 0.00002 0.00002

ADDITIONAL PRODUCTS WHICH WERE CONSIDERED BUT WHOSE MOLE FRACTIONS WERE LESS THAN 0.50000E-05 FOR ALL ASSIGNED CONDITIONS

C CN CNM CN2 C2 C2N C2H2 C2O C3 C302 C302
C4 C5 C5 N N3
O3

[illegible]

2.000

ENTROPY AND PRESSURE

[illegible]

REACTANT DENSITY= 0.0

THE THERMODYNAMIC PROPERTIES

[illegible]

MOLE FRACTIONS

[illegible][illegible][illegible]

DISTRIBUTION LIST

| <u>No. of Copies</u> | <u>Organization</u> | <u>No. of Copies</u> | <u>Organization</u> |
|--------------------------|---|--------------------------|---|
| 12 | Administrator Defense Technical Info Center ATTN: DTIC-DDA Cameron Station Alexandria, VA 22314 | 5 | Commander US Army Armament Research & Development Command ATTN: DRDAR-LC, J. Frasier J. Lannon A. Bracuti A. Moss R. Walker Dover, NJ 07801 |
| 1 | Director of Defense Research and Engineering ATTN: R. Thorkildsen The Pentagon Arlington Va 20301 | 3 | Commander US Army Armament Research & Development Command ATTN: DRDAR-LC E. Barrieres R. Corn K. Rubin Dover, NJ 07801 |
| 1 | Defense Advanced Research Projects Agency Director, Materials Division 1400 Wilson Boulevard Arlington, VA 22209 | 2 | Commander US Army Armament Research & Development Command ATTN; DRDAR-LC K. Russell D. Downs Dover, NJ 07801 |
| 3 | HDQA (DAMA-ARZ, DAMA-CSM, DAMA-WSW) Washington, DC 20301 | 1 | Commander US Army Armament Research & Development Command ATTN: DRDAR-QA, J. Rutkowski Dover, NJ 07801 |
| 1 | Commander US Army Material Development and Readiness Command ATTN: DRCDMD-ST 5001 Eisenhower Avenue Alexandria, VA 22333 | 1 | Commander US Army Armament Material Readiness Command ATTN: DRSAR-LEP-L, Tech Lib Rock Island, IL 61299 |
| 2 | Commander US Army Armament Research & Development Command ATTN: DRDAR-TSS Dover, NJ 07801 | 3 | Commander US Army Armament Materials Readiness Command ATTN: DRSAR-ASR DRSAR-LEA DRSAR-QAL Rock Island, IL 61299 |
| 4 | Commander US Army Armament Research & Development Command ATTN: DRDAR-SC Dr. T. Hung H. Kaln B. Brodman S. Cytron Dover, NJ 07801 | | |
| 1 | Commander US Army Armament Research and Development Command ATTN: DRDAR-TDC Dover, NJ 07801 | | |

DISTRIBUTION LIST

| <u>No. of</u> <u>Copies</u> | <u>Organization</u> | <u>No. of</u> <u>Copies</u> | <u>Organization</u> |
|--------------------------------|---|--------------------------------|--|
| 6 | Commander US Army Armament Research & Development Command Benet' Laboratory ATTN: I. Ahmad T. Davidson G. Friar P. Greco M. Kamdar J. Zweig Watervliet, NY 12189 | 1 | Commander US Army Electronics Research & Development Command Technical Support Activity ATTN: DELSD-L Fort Monmouth, NJ 07703 |
| 6 | Commander US Army Research & Development Command Benet' Laboratory ATTN: J. Busuttil W. Austin R. Montgomery R. Billington J. Santini DRDAR-LCB-TL Watervliet, NY 12189 | 1 | Commander US Army Missile Command ATTN: DRSMI-R Redstone Arsenal. AL 35898 |
| 1 | Commander US Army Aviation Research & Development Command ATTN: DRDAV-E 4300 Goodfellow Blvd. St. Louis, MO 63120 | 1 | Commander US Army Missile Command ATTN: DRSMI-YDL Redstone Arsenal, AL 35898 |
| 1 | Director US Army Air Mobility Research and Development Laboratory Ames Research Center Moffett Field, CA 94035 | 1 | Commander US Army Tank Automotive Rsch and Development Command ATTN: DRDTA-UL Warren, MI 48090 |
| 1 | Director US Army Research & Technology Laboratories ATTN: R.A. Langsworthy FT. Eustis, VA 23604 | 1 | President US Army Armor & Engineer Bd Ft. Knox, KY 40121 |
| 1 | Commander US Army Communications Rsch and Development Command ATTN: DRDCO-PPA-SA Fort Monmouth, NJ 07703 | 1 | Project Manager, M6C Tanks US Army Tank & Automotive Cmd Warren, MI 48090 |
| | | 3 | Project Manager Cannon Artillery Weapons Systems ATTN: DRCPM-CAWS US Army Armament Research & Development Command Dover, NJ 07801 |
| | | 2 | Project Manager ATTN: J. Turkeltaub S. Smith Rock Island, IL 61299 |
| | | 1 | Program Manager - Abrams Tank System US Army Tank Automotive Development Command ATTN: DRCPM-GCM-S Warren, MI 48090 |

DISTRIBUTION LIST

| <u>No. of Copies</u> | <u>Organization</u> | <u>No. of Copies</u> | <u>Organization</u> |
|--------------------------|--|--------------------------|--|
| 1 | Project Manager Tank Main Armament ATTN: A. Albright Dover, NJ 07801 | 1 | Commander US Army Field Artillery School Ft. Sill, OK 73503 |
| 1 | Project Manager, ARGADS Dover, NJ 07801 | 5 | Commander Naval Surface Wpns Center ATTN: M. Shamblen J. O'Brasky C. Smith L. Russell T.W. Smith Dahlgren, VA 22448 |
| 3 | Director US Army Research Office ATTN: P. Parish E. Saibel D. Squire P.O. Box 12211 Rsch Triangle Park, NC 27709 | 2 | Commander Naval Ordnance Station, Louisville ATTN: F. Blume Louisville, KY 40202 |
| 2 | Director US Army Materials & Mechanics Research Center ATTN: J.W. Johnson K. Sheppard Watertown, MA 02172 | 2 | AFATL (D. Uhrig, O. Heiney) Eglin AFB, FL 32542 |
| 1 | Commander US Army DARCOM Material Readiness Support Activity ATTN: DRXMD-ED Lexington, KY 40511 | 1 | National Bureau of Standards Materials Division ATTN: A.W. Ruff Washington, DC 20234 |
| 1 | Director US Army TRADOC Systems Analysis Activity ATTN: ATAA-SL, Tech Lib White Sands Missile Range, NM 88002 | 1 | National Science Foundation Materials Division Washington, DC 20550 |
| 1 | Commander US Army Air Defense Center ATTN: ATSA-SM-L Ft. Bliss, TX 79916 | 1 | Battelle Columbus Institute ATTN: G. Wolken Columbus, OH 43201 |
| 1 | Commander US Army Armor Center ATTN: ATZK-XMI Ft. Knox, KY 40121 | 1 | Lawrence Livermore Laboratory ATTN: J. Kury Livermore, CA 94550 |
| | | 2 | Calspan Corporation ATTN: G. Sterbutzel F. Vassallo P.O. Box 400 Buffalo, NY 14225 |

DISTRIBUTION LIST

| <u>No. of</u> <u>Copies</u> | <u>Organization</u> | <u>No. of</u> <u>Copies</u> | <u>Organization</u> |
|--------------------------------|---|--------------------------------|--|
| 1 | Director Materials Engineering and Technology G.P.D. P&WA Group, UTC P.O. Box 2691 West Palm Beach, FL 33402 | 1 | University of Illinois Dept of Mechanical Engineering ATTN: H. Krier 144 MEB, 1206 W. Green St. Urbana, IL 61801 |
| 1 | Director Chemical Propulsion Info Agency Johns Hopkins University ATTN: T. Christian Johns Hopkins Road Laurel, MD 20810 | | <u>Aberdeen Proving Ground</u> Dir, USAMTD ATTN: H. Graves, Bldg 400 R. Moody, Bldg. 525 L. Barnhart, Bldg 400 K. Jones, Bldg 400 R. Moody, Bldg 525 |
| 2 | Princeton University Forrestal Campus Library ATTN: Tech Lib B. Royce P.O. Box 710 Princeton, NJ 08540 | | Cdr, TECOM ATTN: DRSTE-FA DRSTE-AR DRSTE-AD DRSTE-TO-F |
| 1 | Purdue University School of Mechanical Engineering ATTN: J.R. Osborn W. Lafayette, IN 47909 | | Dir, USAMSAA ATTN: DRXSY-D DRXSY-MP, H. Cohen D. Barnhart, RAM Div G. Alexander, RAM Div Air Warfare Div Ground Warfare Div RAM Division |
| 1 | SRI International Materials Research Center 333 Ravenswood Avenue Menlo Park, AC 94025 | | Dir, USACSL, Bldg E3516, EA ATTN: DRDAR-CLB-PA |

USER EVALUATION OF REPORT

Please take a few minutes to answer the questions below; tear out this sheet, fold as indicated, staple or tape closed, and place in the mail. Your comments will provide us with information for improving future reports.

1. BRL Report Number _____

2. Does this report satisfy a need? (Comment on purpose, related project, or other area of interest for which report will be used.)

3. How, specifically, is the report being used? (Information source, design data or procedure, management procedure, source of ideas, etc.) _____

4. Has the information in this report led to any quantitative savings as far as man-hours/contract dollars saved, operating costs avoided, efficiencies achieved, etc.? If so, please elaborate.

5. General Comments (Indicate what you think should be changed to make this report and future reports of this type more responsive to your needs, more usable, improve readability, etc.) _____

6. If you would like to be contacted by the personnel who prepared this report to raise specific questions or discuss the topic, please fill in the following information.

Name: _____

Telephone Number: _____

Organization Address: _____

----- FOLD HERE -----

Director
US Army Ballistic Research Laboratory
Aberdeen Proving Ground, MD 21005

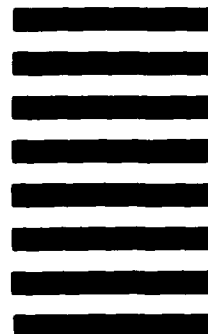


NO POSTAGE
NECESSARY
IF MAILED
IN THE
UNITED STATES

OFFICIAL BUSINESS
PENALTY FOR PRIVATE USE, \$300

BUSINESS REPLY MAIL
FIRST CLASS PERMIT NO 12062 WASHINGTON, DC
POSTAGE WILL BE PAID BY DEPARTMENT OF THE ARMY

Director
US Army Ballistic Research Laboratory
ATTN: DRDAR-TSB
Aberdeen Proving Ground, MD 21005



----- FOLD HERE -----